

**The triplet state of chlorophyll-a
in whole algal cells**

III

CENTRALE LANDBOUWCATALOGUS



0000 0086 5408

III

BIBLIOTHEEK L.H.

0 3 MAART 1982

ONTV. TIJDSCHR. ADM.

Promotor : dr. T. J. Schaafsma,
hoogleraar in de moleculaire fysica

Co-promotor : dr. W. J. Vredenberg,
hoogleraar in de plantenfysiologie met bijzondere aandacht voor de fysische aspecten

Co-referent : dr. ir. J. J. S. van Rensen,
wetenschappelijk hoofdmedewerker

G. H. van Brakel

The triplet state of chlorophyll-a in whole algal cells

Proefschrift

ter verkrijging van de graad van
doctor in de landbouwwetenschappen,
op gezag van de rector magnificus,
dr. C. C. Oosterlee,
hoogleraar in de veeteeltwetenschap,
in het openbaar te verdedigen
op woensdag 17 maart 1982
des namiddags te vier uur in de aula
van de Landbouwhogeschool te Wageningen.

LANDBOUWHOGESCHOOL
WAGENINGEN

ISBN= 157405-03

STELLINGEN

1. Het beschrijven van de overgang tussen de laagste triplet en de grondtoestand van zink-chlorofyl, uitsluitend met behulp van $\pi\pi^*$ toestanden, is onjuist.

S.S.Dvornikov, V.N.Knyukshto, K.N.Solov'ev en
M.P.Tsvirko (1979) Opt.Spektrosk. 46:689-695.

D.S.McMlure (1951) J.Chem.Phys. 20:682-686.

2. Bij de bepaling van de kinetische konstanten van de triplettoestand van chlorofyldimeren wordt door Clarke *et al.* ten onrechte geen rekening gehouden met triplet-triplet absorptie.

R.H.Clarke, D.R.Hobart en W.R.Leenstra (1979)
J.Am.Chem.Soc. 101:2416-2423.

3. De solubiliserende eigenschappen van ethyleenglycol worden door Frank *et al.* onderschat.

H.A.Frank, M.B.Mclean en K.Sauer (1979)
Proc.Natl.Acad.Sci.USA 76:5124-5128.

J.de Kok, S.E.Braslavsky en C.J.P.Spruit (1981)
Photochem.Photobiol. 34:705-710.

4. De nauwkeurigheid van de warmtepulsmethode, die gebruikt wordt om vloeistofstroming te meten in biologische systemen, is niet vastgesteld.

K.Schurer, H.Griffioen, J.G.Kornet en G.J.W.Visscher
(1979) Neth.J.agric.Sci. 27:136-141.

5. Ten onrechte beweren Hemminga en de Jager in de door hen beschreven gepulste NMR methode om vloeistofstroming te meten, dat het effect van verlenging van de meetspoel op het NMR signaal hetzelfde is als het verhogen van de lineaire magneetveldgradient.

M.A.Hemminga en P.A.de Jager (1980)
J.Magn.Res. 37:1-16.

6. Voor een goede beschrijving van het ladingsscheidingsproces in reactie centra van fotosynthetiserende bacteriën met behulp van het radikaal paar mechanisme, is het noodzakelijk tenminste de eerste twee electronenacceptoren in de beschouwing te betrekken.

R.E.Blankenship (1981) Acc.Chem.Res. 14:163-170

R.Haberkorn, M.E.Michel-Beyerle en R.A.Marcus
(1979) Proc.Natl.Acad.Sci.USA 76:4185-4188.

7. De eenzijdigheid in de relatie, die er in de Rooms Katholieke Kerk bestaan heeft, en deels nog bestaat, tussen de geestelijkheid en de leken, wordt niet slechts door het optreden van de geestelijken, maar mede door de leken in stand gehouden.
8. Aan het begrip inwonerequivalent, zoals gebruikt door waterzuiveringsdeskundigen, moet in derde wereldlanden een andere waarde worden toegekend, dan in meer ontwikkelde landen.
9. Een berekening van de trefkansen van de verschillende straten bij het monopolyspel, tesamen met een kosten-baten analyse, laat zien, dat beleggingen in onroerend goed in Utrecht en Arnhem relatief gunstig zijn. Investerings in Rotterdam zijn daarentegen relatief bijzonder ongunstig.

Aan mijn moeder

VOORWOORD

Dankbaar grijp ik deze gelegenheid aan om uit te drukken, dat dit boekje niet het gevolg is van de inspanningen van een enkel persoon, maar als het resultaat van "teamwork" gezien moet worden.

In de eerste plaats gaat mijn dank uit naar Tjeerd Schaafsma, onder wiens dagelijkse leiding het werk, in de volgende pagina's beschreven, is geschied. Behalve dat hij de voortgang van het werk bevorderde door onmisbare besprekingen en adviezen, slaagde hij er steeds weer in mij te verbazen door de persoonlijke inzet, die hij ten toon spreidde.

De medewerkers van de vakgroep Plantenfysiologisch Onderzoek, die nauw bij het werk betrokken zijn geweest, Wim Vredenberg, Jacques van Rensen, Jan Wesselijs en dhr. Hobé, zeg ik dank voor het feit, dat ze te allen tijde bereid waren om van gedachten te wisselen met een theoretisch chemicus, die zich volledig onthand geplaatst zag temidden van de levende natuur, en me met raad en daad bijgestaan hebben om de preparaten te bereiden. Met name Jacques van Rensen slaagde erin om de algenkweek steeds sneller klaar te hebben dan ik verwachtte.

Hans Kleinen Hamans, van de vakgroep Biofysica der Rijksuniversiteit te Utrecht, zeg ik dank voor zijn hulp met het isoleren van chlorofyl-eiwit complexen.

Mevr. I. Diraoui, die het leeuwendeel van deze tekst getypt heeft, en de andere medewerkers van de afdeling Tekstverwerking dank ik voor het feit, dat ze verdragen hebben, dat ik op een onmogelijk tijdstip met het manuscript aan kwam zetten.

Dhr. Hoogeveen heeft op voortreffelijke wijze de tekeningen verzorgd, gelijk U kunt constateren.

De firma Ponsen en Looyen te Wageningen heeft op bijzondere wijze haar medewerking verleend bij het verzorgen van het drukwerk.

De medewerkers van de vakgroep Moleculaire Fysica, die in deze jaren goede vrienden zijn geworden, dank ik ieder voor hun bijdragen, klein of groot. De beide studenten Wim Vermaas en Hans Hudales hebben een aandeel geleverd aan het onderzoek. Hun werk is in dit boekje terug te vinden.

Zoals steeds, zijn er ook nu weer mensen, zonder wie dit boekje er niet zou zijn gekomen. In dit geval zijn dit de beide technici van de vakgroep Moleculaire Fysica, Adrie de Jager en Arie van Hoek, die me bijstonden met technische zaken, maar bovenal mij wisten te bemoedigen met hun aanwezigheid.

CONTENTS

List of abbreviations and symbols

Chapter 1 Introduction	1
1.1 General	1
1.2 Introduction to photosynthesis	3
1.2.1 Structure and function of the photosynthetic apparatus	3
1.2.2 Properties of the algae	7
1.3 The rôle of the triplet state of chlorophyll-a in photosynthesis research	9
1.3.1 The use of the triplet state as a probe in photosynthetic systems	9
1.3.2 The rôle of the triplet state in photochemistry	12
1.4 The electronic structure of chlorophyll-a	13
1.5 Radiationless transitions in chlorophyll-a	21
1.6 References	34
Chapter 2 Materials and methods	40
2.1 Introduction	40
2.2 The cultivation of the algae	40
2.3 Isolation of chlorophyll-protein complexes	43
2.4 Electron spin resonance	44
2.5 Absorption difference spectroscopy	45
2.6 Optically detected magnetic resonance	47
2.7 References	51
Chapter 3 Theory of ODMR	53
3.1 Introduction	53
3.2 Amplitude and shape of signals	53
3.2.1 Amplitude	53
3.2.2 The shape of ODMR resonance transitions	62
3.3 The sign of ODMR signals	63
3.3.1 Introduction	63
3.3.2 The radical pair mechanism	64
3.3.3 Site effects	67
3.3.4 Fluorescence detected magnetic resonance (FDMR) of whole algae and the <i>Anacystis nidulans</i> CP-I complex	70

3.3.5 Conclusion	98
3.4 References	99
Chapter 4 ODMR of algae and chlorophyll-protein complexes	102
4.1 Introduction	102
4.2 Chlorophyll triplets and energy transfer in isolated PSI chlorophyll proteins from blue-green algae	105
4.3 ODMR of algae	121
4.4 Kinetics	128
4.4.1 Theory	128
4.4.2 Results	132
4.5 Discussion	134
4.6 Conclusions	140
4.7 References	141
Chapter 5 The effect of metal ions and oxygen on the low temperature triplet yield of chlorophyll-a in algae	142
5.1 Introduction	142
5.2 The effect of metal ions and oxygen on the low temperature triplet yield of chlorophyll-a in algae	145
5.3 Conclusions	151
5.4 References	151
Summary	
Samenvatting	
Curriculum vitae	

LIST OF ABBREVIATIONS AND SYMBOLS

A	In chemical structure of reaction centers: arbitrary electron acceptor
A	In Hamiltonian: spin-orbit coupling constant
A ₁	primary electron acceptor of PSI
A ₂	secondary electron acceptor of PSI
asc	sodium isoascorbate
ATP	adenosine triphosphate
BChl-(a,b)	bacteriochlorophyll-(a,b)
BO	Born-Oppenheimer
B-states	Soret absorption states
c	velocity of light
c	concentration of solute molecules (in mol.l ⁻¹)
CAT	computer for the averaging of transients
CF _{0,1}	cofactors 0,1 for proton channel across thylakoid membrane
Chl-(a,b)	chlorophyll-(a,b)
CP-I	chlorophyll-protein complex with PSI activity
cyt	cytochrome
D	zero-field splitting parameter
DBMB	2,5-dibromo-3-methyl-6-isopropyl-p-benzoquinone
DCMU	3-(3,4-dichlorophenyl)-1,1-dimethylurea
DCPIP	2,6-dichlorophenolindophenol
DPA	diphenylamine
E	zero-field splitting parameter
ΔE	difference in energy
ESR	electron spin resonance
Et Chl-a	ethyl chlorophyllide-a
Fd	ferredoxin
FDMR	fluorescence detected magnetic resonance
FeCy	ferricyanide
FF	fluorescence fading
g	g-factor of free electron
H	zero-field spin Hamiltonian
H ⁽⁰⁾	zeroth-order Hamiltonian
H _{so}	spin-orbit coupling Hamiltonian
h	Planck's constant divided by 2π

HT	Herzberg-Teller
I	excitation intensity (dimensionless)
$ i\rangle$	triplet sublevel in general i = x, y, z in zero-field i = -1, 0, 1 in high magnetic field
I_0	excitation light intensity (in $\text{photons.cm}^{-2}.\text{s}^{-1}$)
I_A	absorbed photons (in $\text{photons.cm}^{-3}.\text{s}^{-1}$)
I_f	fluorescence intensity (in $\text{Einstein.l}^{-1}.\text{s}^{-1}$)
$I_f(t)$	time dependent fluorescence intensity
ΔI_f	change of fluorescence intensity
δI_f	relative change of fluorescence intensity
ISC	intersystem crossing
k_1	rate constant for energy transfer from antenna to trap (in s^{-1})
k_2	rate constant for energy transfer from trap to antenna (in s^{-1})
k_d	(decay) rate constant for radiationless decay (in s^{-1})
k_{ex}	rate constant for excitation; contains excitation light intensity (in s^{-1})
k_f	rate constant for fluorescence (in s^{-1})
k_i	decay rate constant of triplet sublevel $ i\rangle$ (in s^{-1})
k_{ic}	rate constant for internal conversion (in s^{-1})
k_{isc}	rate constant for intersystem crossing (in s^{-1})
$k_{\text{isc}}^{(i)}$	population rate constant for sublevel $ i\rangle$ (in s^{-1})
k_j	decay rate constant of sublevel $ j\rangle$ (in s^{-1})
k_T	mean decay rate constant of $T_0 \rightarrow S_0$ (in s^{-1})
$k_{x,y,z}$	decay rate constant of the denoted sublevel (in s^{-1})
l	angular momentum operator
LHC	light-harvesting complex
M	water-splitting enzym
MIRF	microwave induced response of fluorescence
MIHF	3-methyltetrahydrofuran
MV	methylviologen
N	total amount of molecules subjected to the experiment
[N]	chlorophyll concentration (in mol.l^{-1})
n	character of MO
N_{AV}	Avogadro's number
NADPH	nicotine adenosine diphosphate
N_b	total amount of molecules in the bath

$[N_i]$	concentration of molecules in denoted sublevel (in mol.l^{-1})
$[N_i^0]$	steady state concentration of molecules in denoted sublevel (in mol.l^{-1})
N_{tr}	total amounts of traps
$N_{x,y,z}$	steady state population of denoted sublevel
$N(\text{open})$	fraction of bacterial reaction centers open for energy transfer
$N(S_0)$	steady state number of molecules in S_0
$N(T_0)$	steady state number of molecules in T_0
$\Delta N(T_0)$	change of steady state number of molecules in T_0
NMR	nuclear magnetic resonance
$n_1(t)$	population of S_0
$n_2(t)$	population of S_1
$n_3(t)$	population of T_0
$n_{i,j,k,x,y,z}^0$	steady state population of denoted sublevel
OCSOI	one-center spin-orbit integral
ODMR	optically detected magnetic resonance
P	total population rate of ($S_1 \rightarrow$) T_0 (in $\text{mol.l}^{-1}.\text{s}^{-1}$)
P680	reaction center of PSII
P700	reaction center of PSI
P870	reaction center of photosynthetic bacteria
PAGE	polyacrylamide gel electrophoresis
PC	plastocyanin
PD	primary donor
Pheo-(a,b)	pheophytin-(a,b)
P_i	population rate of denoted sublevel (in $\text{mol.l}^{-1}.\text{s}^{-1}$)
P_i	relative population rate of denoted sublevel (dimensionless)
Pi	inorganic phosphate
PQ	plastoquinone
PSI,II	photosystem I,II
PIFE	polytetrafluoroethylene
Q	acceptor of PSII
Q-states	Q_x and Q_y states of chlorophyll
$\{Q\}$	full set of nuclear coordinates
$\{q\}$	full set of electronic coordinates
Q_p	normal coordinate
R	secondary acceptor of PSII
RC	reaction center

RPM	radical pair mechanism
\underline{S}^2	spin operator for total spin
S_0	ground state
$[S_0]$	concentration of molecules in ground state (in mol.l ⁻¹)
S_1	first excited singlet state
$[S_1]$	concentration of molecules in S_1 (in mol.l ⁻¹)
S_n	arbitrary singlet state
$\underline{S}_{x,y,z}$	cartesian components of spin operator
s	spin variable
SDS	sodium dodecylsulphate
S/N	signal to noise ratio
SOC	spin-orbit-coupling
T_0	lowest triplet state
$[T_0]$	concentration of molecules in T_0 (in mol.l ⁻¹)
$\Delta[T_0]$	change of concentration of molecules in T_0
T_0^i	triplet sublevel
TEMED	N,N,N',N'-tetramethylethylenediamine
TG	Tris-glycine
T_N	operator for nuclear kinetic energy
tr	(superscript) trap
Tris	N-trishydroxymethyl-amino-methane
V	perturbing operator
$V(r_{ik})$	potential energy of electron i w.r.t. nucleus k
v	set of vibrational quantum numbers
X,Y,Z	eigenvalues of zero-field spin Hamiltonian
x,y,z	coordinates w.r.t. molecular frame of reference
$ x\rangle, y\rangle, z\rangle$	triplet sublevels, in absence of magnetic field
y_m	amplitude of resonance line
$Z_{1,2}$	components of donor side of PSII
ZFS	zero-field splitting
α, β	spin functions
α, β	proportionality constants
γ	dimensionless parameter
ϵ	extinction coefficient (in l.mol ⁻¹ .cm ⁻¹)
ϵ	sign of permutation
ϵ_0	dielectric constant of vacuum
Λ	vibrational wave function

λ_d	wavelength of fluorescence detection (in nm)
λ_f	wavelength of fluorescence (in nm)
μ_B	electronic Bohr magneton
ν	frequency
$\Delta\nu_{1/2}$	fwhm of ODMR resonance line
π, π^*	character of MO
$\rho(E)$	density of states
σ, σ^*	character of MO
σ_S	singlet spin function
$\tau_{x,y,z}$	triplet spin function of denoted sublevel
ϕ	wave function
ϕ_f	fluorescence yield
ϕ_f^O	fluorescence yield of isolated molecule
ϕ_T	triplet yield
ψ	wave function

1 INTRODUCTION

1.1 GENERAL

A number of physical and chemical properties of the lowest triplet state of chlorophyll-a (Chl-a), detected in photosynthetic organisms, are treated in this Thesis.

This triplet state is demonstrated to occur at low temperature (4 K) in cells of unicellular algae, using optically detected magnetic resonance (ODMR), low temperature fluorescence, and the response of this fluorescence to an excitation step function.

Questions concerning the role of the Chl-a triplet state in photosynthetic systems under physiological conditions have been the subjects of debate in literature for some 25 years. The first issue to be solved, was to determine whether the triplet state indeed occurs under physiological conditions. This question can now be answered affirmatively.

Subsequently, one may ask whether the Chl-a triplet has a role in photosynthesis. Recently, this question has been put more specifically in the form: is the excited state of the reaction centre, immediately preceding charge-separation a singlet or a triplet state? This last question can be considered essential for our understanding of the primary processes of photosynthesis. In the last few years evidence has accumulated, that the initial electron charge separation originates from an excited singlet state. Immediately after charge separation, the resulting singlet radical pair intermediate can be partly converted into a triplet radical pair, as a precursor to the formation of a Chl-a triplet state trapped in the reaction centre. Our study demonstrates, that such trapped triplet states may also occur in other parts of the photosynthetic apparatus of algae.

Under physiological conditions these trapped triplet states of Chl-a are involved in dissipating excess excitation energy, thus protecting the contents of plant cells from photochemical damage.

In addition to the present and previous studies on the mechanis-

tic role of the Chl-a triplet state, this may also be used as a natural internal spin-probe, yielding detailed information about the structural and functional organization of the photosynthetic system.

Moreover, for the study of the photosynthetic pigments and their interaction in the photosynthetic apparatus, it is important to understand their physical and chemical properties. In this respect triplet state parameters of Chl-a are relevant in themselves.

The objective of this Thesis is to obtain information by various ODMR techniques, pertinent to some of the questions mentioned above by studying the presence and/or amount of triplet states in algal cells, for various species, culturing conditions, supply of metal ions, and photosynthetic inhibitors. We made use of algal mutants, with known deficiencies in the photosynthetic apparatus, to determine the localization of the triplets and to study photochemical breakdown of chlorophylls.

It should be realized, that whole algal cells represent a very complicated system to study by this physical technique, which was developed only recently and mostly applied to pure *in vitro* substances. In order to bridge the gap between the data on *in vitro* and *in vivo* chlorophylls, it is advantageous to make use of chlorophyll-protein complexes, isolated from the same algae as studied by ODMR. The photosynthetic pigments in cells are embedded in a protein environment, and this complex can be isolated in such a way that the native structure is largely retained. The properties of most of the chlorophyll complexes thus isolated can be regarded as identical to those of Chl-a in whole cells. Much more is known about the composition and properties of these isolated complexes than for the whole cells. Optical techniques have been applied to determine their constitution and function under the conditions of our ODMR experiments. We have explored the similarities and differences between the spectroscopic properties (mainly at very low temperature, ≤ 4 K) of these complexes and those of whole algae, in order to gain insight into the role and properties of the Chl-a triplets observed in whole algal cells.

1.2 INTRODUCTION TO PHOTOSYNTHESIS

1.2.1 *Structure and function of the photosynthetic apparatus*

An exhaustive review of photosynthesis is beyond the scope of this Thesis. Therefore, only those features which are of immediate relevance to our purposes will be discussed. The fundamentals of photosynthesis presented here are generally accepted, but there exist various opposing opinions on details of its mechanism. For more detailed presentations and discussions we refer to [1,2,3], containing many useful references. Very recent results can be found in [4]. The following resumé applies to higher plants as well as algae. Architectural differences are discussed in §1.2.2.

In plant cells the complete photosynthetic system is situated within chloroplasts. These are intracellular green organelles, which sometimes constitute more than half the cell volume. The pigments and proteins and other compounds constituting the photosynthetic system are embedded in a lamellar structure, where absorption of sunlight and the formation of ATP and NADPH takes place.

The steps immediately following light-absorption and production of unstable intermediates are called the 'primary steps'.

The lamellar structure is composed of phospholipid bilayers, called the thylakoid membrane. This membrane occurs as vesicles of two kinds: grana lamellae and stroma lamellae, which are present as more elongated vesicles between the grana. The grana lamellae are stacked in cylindrical piles, called grana stacks, interconnected by the stroma lamellae. This is schematically shown in Fig. 1.1.

The thylakoid membrane always has an inner space and an outside, the inside being the inside of the vesicle, the outside the stroma of the chloroplasts.

In all green parts of plants these structures are found, although the ratio of grana and stroma lamellae may differ widely between various species. In addition a plant may vary this ratio for adapting to external factors.

Most of the chlorophyll pigments, present as chlorophyll-protein complexes, have an antenna function, i.e. they collect sunlight and transfer it to a collection of specialized chlorophyll molecules, the reaction centre (RC). Presumably, there are relatively strong

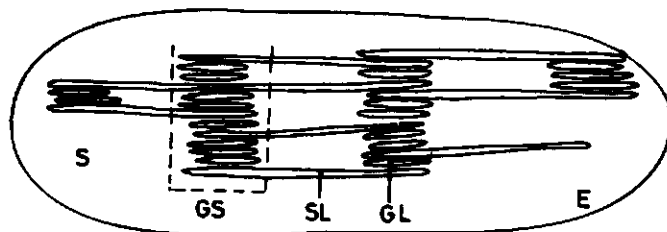


Figure 1.1 Schematic picture of the ordering of photosynthetic membrane in chloroplasts.

GS: grana stack; SL: stroma lamellae; GL: grana lamellae;

E: envelope of the chloroplast; S: stroma.

electronic interactions between the chlorophylls within this collection. There are two physically distinguishable kinds of RC, contained in photosystem I and II (PSI and PSII). Every RC has its own group of antenna pigments, although there is interaction between both groups, permitting energy transfer between both photosystems under certain conditions.

Part of the antenna chlorophyll delivers excitation energy arbitrarily to PSI or PSII, via the antenna chlorophyll specific for each photosystem. This part is called the light-harvesting complex (LHC).

The antenna pigments consist of a range of Chl-a molecules, in different environmental circumstances, and absorbing light of slightly different wavelengths. In algae and higher plants Chl-b is present as an antenna pigment.

In addition to chlorophylls, there are 'accessory pigments', which also collect light and deliver their excitation to the RC via the antenna system. Among these are carotenoids, xanthophylls and phycobilines.

All the pigments are embedded by non-covalent bonding in proteins. These proteins are different for every part of the antenna system [5]. Also between species there are differences in these proteins.

A vast amount of work has been done to determine the sequence of events following capture of light by the antenna system, eventually

resulting in the fixation of CO_2 in carbohydrates and other products, and many models have been proposed.

It has become usual to represent the order of succession of these factors schematically in the so-called Z-scheme. Since at present much more is known about the topography of the various substances within the thylakoid membrane, a more detailed visualization is now possible. Among these, one of the more complete is that of von Wettstein and co-workers, presented and discussed in [6]. Some of the features of this model are represented in Fig. 1.2.

The RC of PSII is called P680, after its maximum of absorption at 680 nm, and involves at least one Chl-a molecule. After excita-

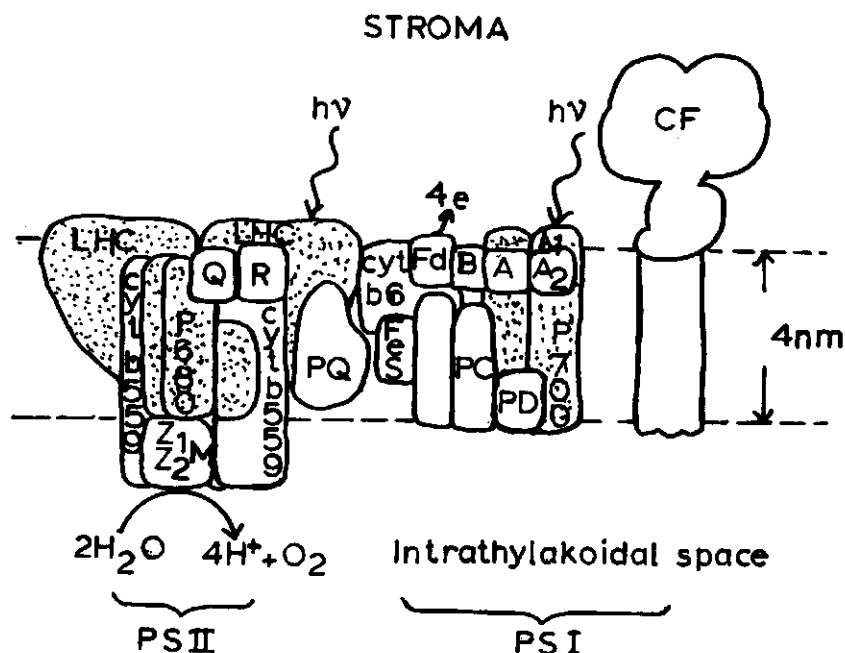


Figure 1.2 Model of the spatial ordering of the factors contributing to the primary steps of photosynthesis within the thylakoid membrane, adapted from von Wettstein et al. [6].

LHC: light-harvesting complex; Z₁, Z₂, M: factors involved in water splitting and subsequent electron transfer; PS I,II: photosystem I, II; Q: electron acceptor of PS II; R: secondary electron acceptor; FeS: Rieske's iron-sulphur protein; PC: plastocyanin; PD: primary donor; A₁: primary acceptor of PSI; A₂: secondary acceptor of PSI; A,B: factors involved in electron transfer; Fd: ferredoxin; CF: co-factor; dotted proteins contain antenna chlorophyll.

tion it transfers within a picosecond an electron to an intermediate acceptor. This intermediate acceptor is probably a pheophytin [7,8]. The oxidized P680 is neutralized by an electron, ultimately derived from the watersplitting reaction $2\text{H}_2\text{O} \rightarrow 4\text{H}^+ + \text{O}_2 + 4\text{e}^-$ at the donor side of PSII. Oxygen gas is set free, while the protons are delivered into the inner space of the membrane. Between the splitting of water and reduction of P680^+ three chemically different components are involved (Z_1 , Z_2 and M).

The photoinduced charge separation is a transmembrane process, P680 being located at the inner side of the membrane.

On the reducing side of PSII electrons are transported from pheophytin to the following acceptor Q. The primary acceptor Q quenches the PSII Chl-a fluorescence [9].

Q is a protein-bound quinone and a single electron carrier. It transfers its electrons to another bound quinone, the secondary acceptor R [10,11]. R is a two electron carrier, accumulating electrons in pairs before transferring them to the large plastoquinone pool (PQ).

The well-known inhibitor of photosynthesis, DCMU, inhibits very specifically electron flow between Q and R.

From the PQ pool electrons are transferred sequentially to the Rieske iron-sulphur protein, cytochrome f, plastocyanin (PC), the hypothetical primary donor (PD) for PSI, and finally to the RC of PSI: P700, with its maximum absorption at 700 nm.

After a further transmembrane photoinduced charge separation the electrons are further transferred to the primary acceptor A_1 , the iron-sulphur protein A_2 , and then to centres A and/or B. The transfer proceeds via ferredoxin (Fd) eventually to ferredoxin- NADP^+ reductase, NADPH being the first stable product of the process.

Cytochromes b_{559} and b_6 allow cyclic photophosphorylation by electron flow around PSII and PSI respectively.

As a result of this overall process a proton gradient is built up across the membrane. Protons are released by the watersplitting at the inner side. Furthermore protons are taken from the outer space as a result of the reduction of PQ, and released in the inner space when the reduced PQ is oxidized again. The coupling factors (CF_0 and CF_1) are responsible for converting the energy stored in this proton gradient into ATP. In this conversion a proton channel

across the membrane is involved transferring the protons from the inner space to the outside.

During these processes about 75% of the useful energy of the absorbed photons is temporarily stored in NADPH and 25% in ATP.

After these primary steps the NADPH and ATP are used to bind CO_2 in a process of about 60 chemical steps, of which the ultimate product is starch. In this sense the total process of photosynthesis can be summarized as $\text{H}_2\text{O} + \text{CO}_2 \xrightarrow{h\nu} \text{C}(\text{H}_2\text{O}) + \text{O}_2$.

1.2.2 Properties of the algae

In the experiments described in this Thesis two types of unicellular algae have been used: the cyanobacterium *Synechococcus leopoliensis* (1405/1; Cambridge), more commonly called *Anacystis nidulans*, and the green alga *Scenedesmus obtusiusculus*.

Formerly both organisms were classified as plants, but more recently it has been realized that there are large differences be-

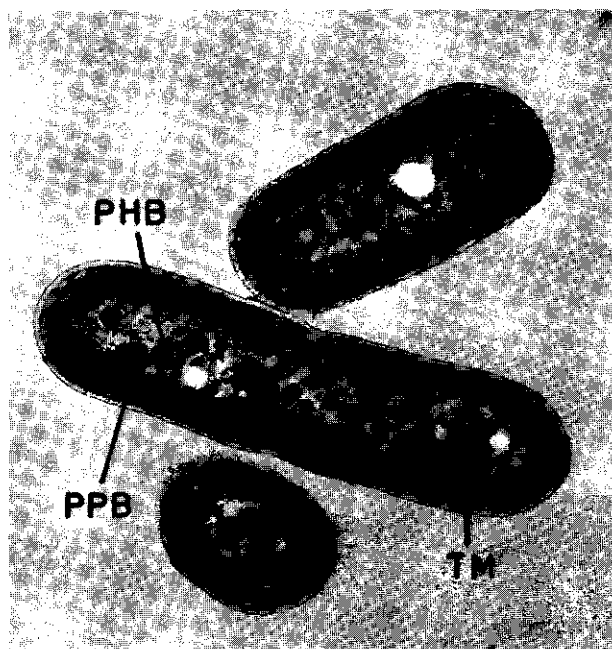


Figure 1.2a Electron micrograph (22750 \times) of wild type *Anacystis nidulans*.

PHB = polyhedral body; PPB = polyphosphate body; TM = thylakoid membrane. (By courtesy of A.C. van Aelst, Dept. of Plantcytology and Morphology, Agricultural University)

tween the two types of algae, which is expressed by the more recent designation of the blue-green algae as cyanobacteria.

The criteria for the primary classification are: differences in gross morphology, pigmentation, other biochemical characteristics and the structure of organelles. The most apparent distinction is that cyanobacteria have very little internal structure. Like bacteria, they lack a nucleus and mitochondria; the nuclear material appears to be embedded in a cytoplasmatic structure. This classifies them as procaryotes.

A distinct membrane-bound chloroplast is also lacking and the photosynthetic lamellae are distributed in the peripheral region of the cytoplasm.

The photosynthetic apparatus, however, is very similar to that of algae and other plants at the molecular level. It is composed of two photosystems, operating in series, just as described in §1.2.1. It starts with the splitting of water and ultimately results in the production of carbohydrate. Special features of the pigment system of cyanobacteria, distinguishing it from that of algae, are: the absence of Chl-b in the antenna pigment, a different amount of carotenoids as compared to green algae and higher plants, i.e. mainly β -carotene, zeaxanthin, isozeaxanthin and myxoxanthophyll. At the outer side of the photosynthetic membranes phycobilisomes are located. They contain the phycobiliproteins, phycocyanin, allophycocyanin and phycoerythrin. These phycobilisomes have a light-harvesting function [12,13].

The shape and colour of cyanobacteria may vary widely due to environmental factors [14]. The characteristic bluish-green colour is caused by the phycobiliproteins. When the cells are grown under limited nitrate supply, the phycobiliproteins are disrupted and the culture turns more green.

The cell walls of cyanobacteria lack cellulose and mainly consist of amino acids and aminosugars.

Taxonomically the cyanobacterium *Synechococcus leopoliensis* is classified as belonging to the division Cyanophyta, class Cyanophyceae, order Chroococcales, family Chroococcaceae. Only recently it has been generally recognized that this alga belongs to the genus *Synechococcus* [15], and not to *Anacystis*. Nevertheless, the name *Anacystis nidulans* is well-known in literature and will be used oc-

casionally in this Thesis. The taxonomy of cyanobacteria undergoes frequent alterations and the above-mentioned classification of *Synechococcus* cannot be regarded as final.

A recent review on cyanobacteria is given in [16].

The green algae (Chlorophyta) belong to the eucaryotes. They encompass a morphological range from unicellular organisms to quite complex multicellular plants. The pigments are characteristically those of higher plants: Chl-a, Chl-b and the carotenoids β -carotene, lutein, violaxanthin and neoxanthin. The cell wall is composed of cellulose and pectin, and other substances differing for various species.

The pigments are contained in the chloroplasts, in which the photosynthetic apparatus is situated in lamellar structures similar to those of cyanobacteria. The chloroplasts appear to have a tendency to move towards the light.

The species *Scenedesmus obtusiusculus* is classified as belonging to the division of the Chlorophyta (green algae), the class Chlorophyceae, the order Chlorococcales and the family Coelastraceae.

In §5.2.2 experiments will be described with mutants of the alga *Scenedesmus obliquus*. These are the mutants *Scenedesmus*#8 and *Scenedesmus* C-6E, classified according to the system of Bishop [17,18], who has described the preparation of mutants and the characterization of their properties in detail. These two mutants were chosen for our experiments because of their photosynthetic properties: in *Scenedesmus*#8 photosystem I is not functional and in *Scenedesmus* C-6E photosystem II is not functional.

The microbiology of algae has been reviewed in several textbooks, of which we only mention the book of Chapman and Chapman [19].

1.3 THE ROLE OF THE TRIPLET STATE OF CHLOROPHYLL-A IN PHOTOSYNTHESIS RESEARCH

1.3.1 The use of the triplet state as a probe in photosynthetic systems

The question whether the state, from which electron transfer proceeds in reaction centres of photosynthetic organisms, is a singlet or a triplet state, has been discussed for some 25 years

now. The development of picosecond techniques and application of magnetic resonance have firmly established the occurrence of the triplet state of photosynthetic pigments under physiological conditions.

The assumption that these triplet states do occur was at first based on the kinetics of changes of optical properties of these systems.

In the early seventies a trapped triplet state of BChl was detected by optical and magnetic resonance spectroscopy in isolated reaction centres of photosynthetic bacteria at cryogenic temperatures [20-25], and it appeared, that this triplet state could only be detected in systems where normal electron transport was blocked. In recent years the occurrence of triplets has been confirmed, for whole bacterial cells at low temperatures [26-28], as well as at room temperature in chemically blocked whole cells [29].

The precursor to the trapped triplet state has a radical pair character, and can also be present as a short-lived triplet state, after initial formation in the singlet configuration. This triplet intermediate has been proposed to explain the magnetic field effect on optical emission properties at room temperature in isolated RC and whole cells [26,30-33].

Triplets have also been detected in chlorophyll-proteins isolated from green algae and higher plants [34-38] (see also Ch.III, IV), in broken and whole chloroplasts [39-44] and whole algal cells [35,39,41,44-47] (see also Ch.V), at low and room temperatures, both in blocked as well as in unblocked organisms. In summary, there is no doubt left about the occurrence of the triplet state *in vivo*.

However, in a recent review [50] it is argued that the initial electron transfer occurs from an excited singlet state, in bacteria from the BChl dimer; the triplet state is considered to be on a sidepath away from the main course of photosynthesis.

This does not have to mean that the intermediate radical pair that is demonstrated to occur during the primary charge separation in photosynthetic organisms is of no importance. It is of interest to note, that the efficiency of the charge-recombination (back-reaction) depends on the spin-configuration of the radical-pair: a singlet pair recombines more easily than a triplet pair [48,49]. Any process converting the initially formed singlet pair into a

triplet pair therefore decreases the rate of the back-reaction and enhances further charge separation. In this sense the occurrence of a short-lived radical pair in the triplet configuration is of importance for the kinetics of forward electron transport in photosynthetic organisms.

Furthermore, the study of the triplet state of chlorophylls in model systems and organisms has yielded very detailed information about the structure of the RC's of the various organisms, the kinetics and the nature of the processes that take place. It may be expected that this use of the trapped triplet state as a probe will further expand our insight in these systems [50].

Much work on bacteria has recently been reviewed [51]. The work on model systems and isolated pigments must be considered essential for the progress of work on in vivo systems; the link between these two routes has been reviewed and emphasized [52,53].

Currently, from studies on model systems of chlorophyll, a vast amount of information has been gathered about its triplet state parameters, i.e.

- zero-field splittings
- kinetics of triplet sublevels
- ODMR linewidths

as well as its fluorescence spectra and -yields. In many cases a relation has been shown to exist between these parameters and the chemical and/or physical environment of the chlorophyll molecule. In this way, we may now detect various chemically different photosynthetic pigments in vivo, the presence of pigment aggregation, ligand interaction with Mg^{2+} and/or the ring V oxygens, and interaction with nearby paramagnetic perturbers. Finally, the mechanism of photochemical damage can be studied, when the chlorophyll triplet probe is involved in such a process, see Ch.VI.

The work described in this Thesis has many relations to the investigations mentioned above. Our aim has been to explore and expand the various possibilities of using the triplet state of Chl-a as an internal probe in the photosynthetic apparatus of whole algal cells and complexes. Emphasis has been laid on the question of where the triplet state of Chl-a, as found by ODMR in whole algal cells, is located in the photosynthetic apparatus. In addition, we have attempted to investigate the structure of the immediate surround-

ings, including the presence of paramagnetic ions, of the Chl-a triplet by studying its triplet state properties.

In this Thesis the kind of information which can be obtained from ODMR experiments on algae and chlorophyll-protein complexes is illustrated.

1.3.2 The role of the triplet state in the photochemistry of in vivo chlorophyll

The trapped triplet state of Chl-a (both in antenna and RC chlorophylls) can be formed under saturating light conditions, i.e. when the rate of deactivation of the excited singlet state of Chl-a in the antenna complex by energy transfer, or of Chl-a in the RC by charge-separation is not much larger than the rate of optical excitation. Since the triplet state of chlorophyll formed under these conditions is both reactive and relatively long-lived (~ 1 ms), it may easily result in photochemical damage to the photosynthetic apparatus. Usually, the photosynthetic organism is protected against this damage by the presence of large amounts of carotenoids, acting as effective quenchers of the chlorophyll triplet state, e.g. by triplet-triplet energy transfer [54,55].

In the presence of suitable electron-acceptors and light, Chl-a is known to be easily photooxidized, if no triplet quenchers are available. In vitro, the triplet state of chlorophyll has been demonstrated to be involved in photooxidation [56-59]. Plants, cultured in the shade, do not develop a mechanism to protect their chlorophyll content against irreversible photooxidation and thus are bleached, when exposed to bright sunlight. The photochemical damage is primarily done to chlorophyll itself, even though surrounding molecules may be involved in the process as well.

Ch.V describes experiments providing some clues to the questions, whether the Chl triplet state precedes its photooxidation, by which mechanism this process occurs, and - finally - which factors affect the concentration of Chl triplets.

1.4 THE ELECTRONIC STRUCTURE OF CHLOROPHYLL-A

The electronic structure of Chl-a can be approached by many dif-

ferent methods, ranging from purely qualitative to semi-empirical and *ab initio* calculations.

In this paragraph some of the results are presented, in order of increasing complexity of the calculations on which they are based. For more complete reviews we refer to [60-62] and, from a historical point of view, to [63].

For a start, Chl-a can be conceived to be derived from an unsubstituted porphyrin, containing a divalent metal ion. In these porphyrins (Fig. 1.3) the central metal atom is sp^2d hybridized, which implies that it has four orbitals in the plane of the porphyrin ring and two empty orbitals (p_z , d_{z^2}) perpendicular to the plane. The divalent metal atom provides two electrons for binding with four N atoms. The porphyrin ring is regarded as an inner 16-membered ring with 18 π -electrons, surrounded by four more or less isolated ethylenic bonds. This can be seen as follows: the inner ring consists of 12 sp^2 hybridized C atoms, each delivering 1 electron to the π -sys-

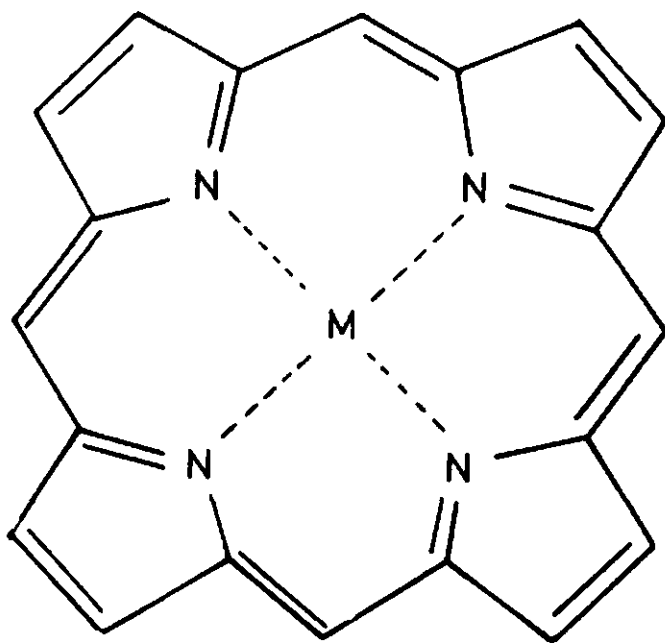


Figure 1.3 Molecular structure of metalloporphyrins; M = metal ion. For a detailed discussion of the conjugation pathway, see text.

tem, and 4 sp^2 hybridized N atoms. The N atoms together deliver 20 valence electrons; 8 form σ -orbitals with neighbouring C atoms, 6 are shared with the central metal atom, and 6 take part in the π -system of the ring, thus making up the number of 18 π -electrons. Each N atom provides $1\frac{1}{2}$ electron to the π -system via its p_z orbital.

The four ethylenic bonds are not completely isolated, nor completely conjugated with the inner ring. This fact can be argued in many ways from spectral data, e.g. as in [64]. This feature is not puzzling, however, since it is well known, that even in pyrrole the conjugation is incomplete [65,66].

The number of 18 π -electrons fulfills Hückel's rule for aromaticity [67,68], stating that the number of electrons required for aromaticity is given by $4n + 2$, where n is an integer. Also when the four ethylenic bonds are included, this rule is obeyed. In Chl-a (Fig. 1.4) many alterations with respect to unsubstituted porphyrin are made in the π -system via the outer four ethylenic bonds, each alteration having its own effect on the π -system of the inner ring, by way of the partial conjugation. The total of π -electrons in Chl-a amounts to 28, not an aromatic number. Aromaticity of the inner ring is still dominant, however, thanks to the partial conjugation with the outer ring.

To what extent conjugation really occurs can only be derived from a bond-order matrix. This matrix is defined [69] to have elements P_{ij} with

$$P_{ij} = \sum_{\substack{\text{all} \\ \text{electrons}}} c_i c_j \quad (1.1)$$

where the summation is over all electrons contributing to the bond between nuclei i and j and the c_i are the coefficients of the atomic orbitals in the MO at nucleus i . In this way electron densities are expressed as

$$P_{ii} = \sum_{\substack{\text{all} \\ \text{electrons}}} c_i^2 \quad (1.2)$$

Thus, the bond-order matrix can be found from the electron densities. For aromatic molecules bond-orders are equal for all bonds of

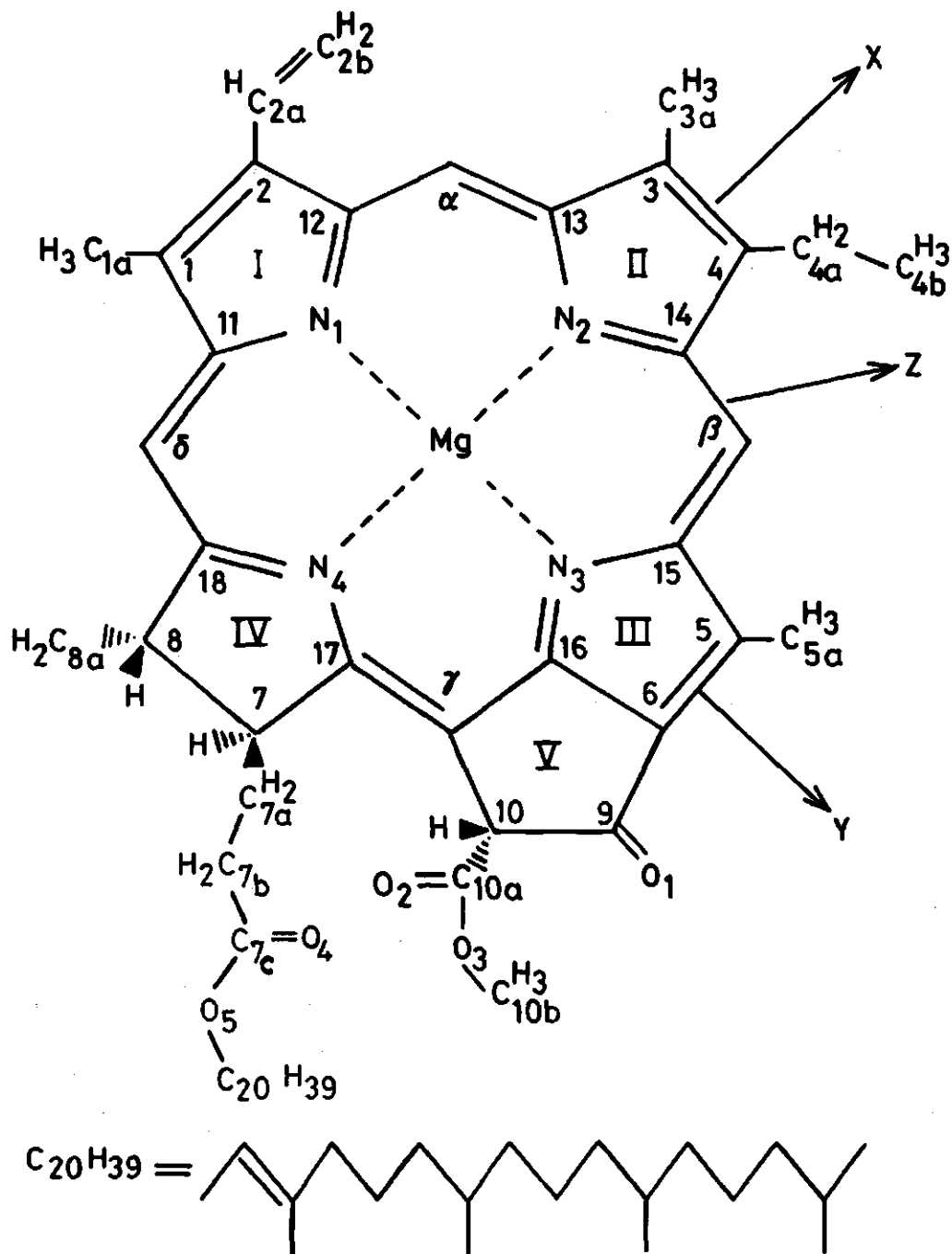


Figure 1.4 Molecular structure of Chl-*a*, systematic name: [3(D), 7(D), 11(D), 15(D)-tetramethyl-*trans*-2-hexadecenyl-9-ethenyl-14-ethyl-21-(methoxycarbonyl)-4,8,13,18 tetramethyl-20-oxo-phorbine-propanoato (2-)-N²³, N²⁴, N²⁵, N²⁶] magnesium. Numbering in the figure is taken from [74]. The axis system does not correspond to the conventional axis system used for the C_{2v} point group, but is widely used in chlorophyll-spectroscopy.

the aromatic ring. The electron densities and bond-orders have been calculated for model systems of Chl-a [70], showing that the conjugation is indeed only partial.

Another consequence of the partial conjugation of the outer ethylenic bonds with the inner ring is the fact that Chl-a can be regarded as a porphyrin, even though it is actually a dihydroporphyrin. Clearly the disturbance of the π -system by the hydrogenation is only small, so that a description of Chl-a as a porphyrin is still permitted and comparison with true porphyrins is meaningful, in particular with respect to the electron-distribution.

The simplest MO theory treats the unsubstituted metalloporphyrin using a particle-on-a-ring model [71]. The π -electrons are put in MO's ψ_k as

$$\psi_k = \exp(ik\phi) \quad (1.3)$$

with energies

$$E_k = \frac{\hbar^2 k^2}{2m_e R^2} \quad (1.4)$$

where $k = 0, \pm 1, \pm 2, \dots$ is the orbital ring quantum number, essentially the electronic angular momentum, ϕ is the angular coordinate, m_e is the electron mass and R is the radius of the ring. In the ground state the orbitals with $k = 0, \pm 1, \pm 2, \pm 3, \pm 4$ are occupied. Four degenerate transitions between orbitals with $k = \pm 4$ and $k = \pm 5$ are predicted, giving rise to four degenerate excited states with angular momenta $L_z = \pm 1$ and $L_z = \pm 9$. These states are then split in energy, transitions to $L_z = \pm 1$ being allowed for electric dipole transitions and to $L_z = \pm 9$ states dipole-forbidden. In this way the spectral properties of porphyrins can be accounted for.

The porphyrin ring has been treated in various ways as a cyclic polyene [63] and the Hückel MO method eventually has led to the development of Gouterman's four-orbital model [72,73]. The two highest occupied and two lowest unoccupied orbitals are considered to be effectively isolated from the remaining orbitals. The results of this calculation have been discussed and compared with calculations of different type and experiments in several papers, see [60,61,63]

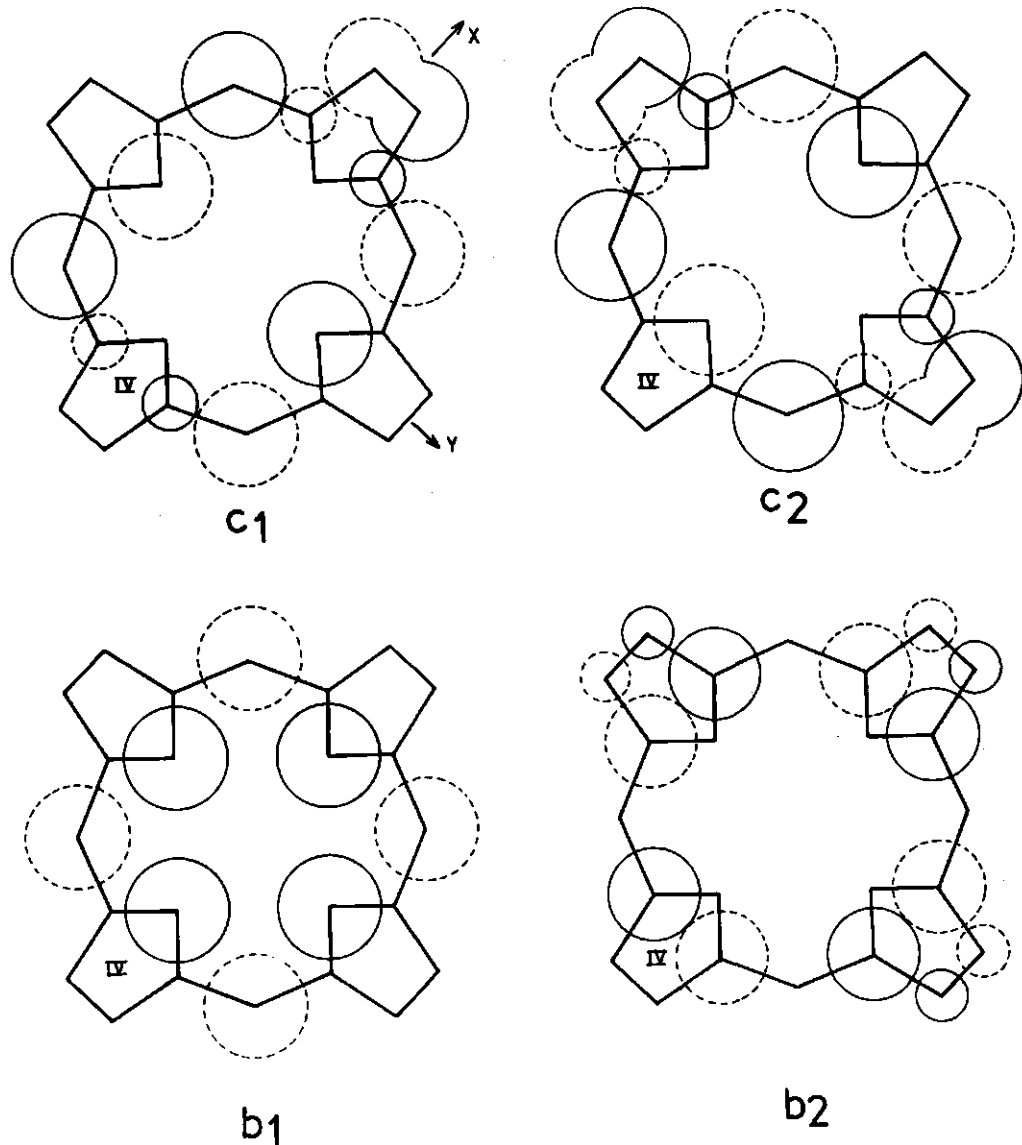


Figure 1.5 The four orbitals of Gouterman [72,73], representing the two highest occupied (c_1, c_2) and lowest unoccupied (b_1, b_2) orbitals of a metallodihydroporphyrin.

The AO coefficients are proportional to the size of the circles; solid and dashed circles indicate the sign of the wave function.

In D_{4h} symmetry, the symmetries of the four orbitals are: $b_1 = a_{2u}$, $b_2 = a_{1u}$, $c_1 = e_g$ and $c_2 = e_g$.

and references therein. The calculated AO coefficients are schematically shown in Fig. 1.5 for dihydroporphyrin.

Recently a detailed description of the electronic structure and properties of the ground state and excited singlet and triplet states of Et Chl-a has been published by Petke and co-workers [74]. As these results will be referred to in this Thesis, we reproduce here some of them and compare with those from the four-orbital model. Evidently the electronic structure and properties of Et Chl-a are highly comparable to those of Chl-a, since the only difference is the absence of the phytol-tail of Chl-a in Et Chl-a. This tail will certainly not have much influence on the electronic properties (energies and electron-distribution) of the porphyrin part of Chl-a.

The description of Petke et al. is based on ab initio calculations, as extensively outlined in [75] and references therein.

In order to reduce the basis set for Hartree-Fock SCF-MO calculations floating spherical gaussian orbitals (FSGO) are combined to form molecular fragments [76]. The molecular fragment method was first introduced in [77] and [78]. Another reduction of the basis set is obtained by combining the inner-shell electrons with the nuclei to form pseudopotentials [79]. The MO's of the molecular fragments are used as a basis set of functions for the SCF and subsequent CI calculation.

A discussion of the possibilities of this method is given in [75], and of the expected accuracy in [76]. The fragmentation of the molecule is a rather crude approximation, however, when the fragments influence each other, as in molecules with extensive conjugation. This drawback is only partially overcome by the CI calculation.

The calculated excitation energies yield a qualitatively correct prediction of the absorption spectra of Et Chl-a and pheophorbide-a. The energies can be compared to the experimental data by applying a linear equation:

$$\Delta E^{(\text{exp})} = 0.610 \Delta E^{(\text{calc})} - 441.0 \quad (1.5)$$

where $\Delta E^{(\text{exp})}$ and $\Delta E^{(\text{calc})}$ are the experimental and calculated transition energies, respectively, in units of cm^{-1} . It must be kept in mind that these $\Delta E^{(\text{calc})}$ are taken from a set of calculated

energies, which are much less accurate than the calculated transition energies $\Delta E^{(\text{calc})}$ [80]. Also, the calculated oscillator strengths only approximately agree with the experimental data [74].

A striking feature in the results of Petke et al. (see Fig. 1.6) is that the Soret band appears to be composed of ten states (S_3 - S_{12}) with primarily ($\pi\pi^*$) character, but the configurational composition is generally a complex mixture of excitations from both occupied macrocyclic π MO's and occupied MO's with electron density in the cyclopentanone ring (V in Fig. 1.4) and the carbomethoxy group (atoms C_{10a} , O_2 , O_3). The two lowest lying singlet states S_1 and S_2 have similar configurational compositions and can be qualitatively described by a four-orbital model. The calculated MO's do not differ much from those of Fig. 1.5. The two lowest triplet states T_0 and T_1 lie lower in energy than S_1 , while T_2 and S_1 are predicted to be approximately degenerate. The configurational compositions of T_0 - T_3 may be adequately described by a four-orbital model. Thus all four lowest triplet states are pure ($\pi\pi^*$) states, but only the triplet states T_0 and T_3 are composed of single ($\pi\pi^*$) configurations, i.e. exist of excitations of electrons from one MO only.

The higher lying triplet states cannot be described by the four-orbital model.

The calculations of Petke et al. throw new light on earlier discussions on properties of Chl-a and related compounds by Kleibeuker et al. [81,82]. These authors find a smaller ZFS (zero-field splitting) parameter D for Chl-a, and for dihydroporphyrins in general, than for corresponding porphyrins. One expects the D-value to be dependent on the extent of the electron distribution, resulting in a larger D-value for the porphyrins. Kleibeuker explains these results by assuming dihydroporphyrins to have approximately D_{4h} symmetry, using the four-orbital model. The observed D-values in photosynthetic pigments are accounted for by invoking CI involving the two highest occupied (HOMO's) and two lowest unoccupied (LUMO's) MO's. In order to understand the magnitude and variation of D for various photosynthetic pigments, including Chl-a, Kleibeuker has to assume that the lowest triplet state T_0 is not a single $\pi\pi^*$ configuration.

According to Petke et al., however, T_0 is calculated to have a single configurational composition, in evident contradiction with Kleibeuker's assumption.

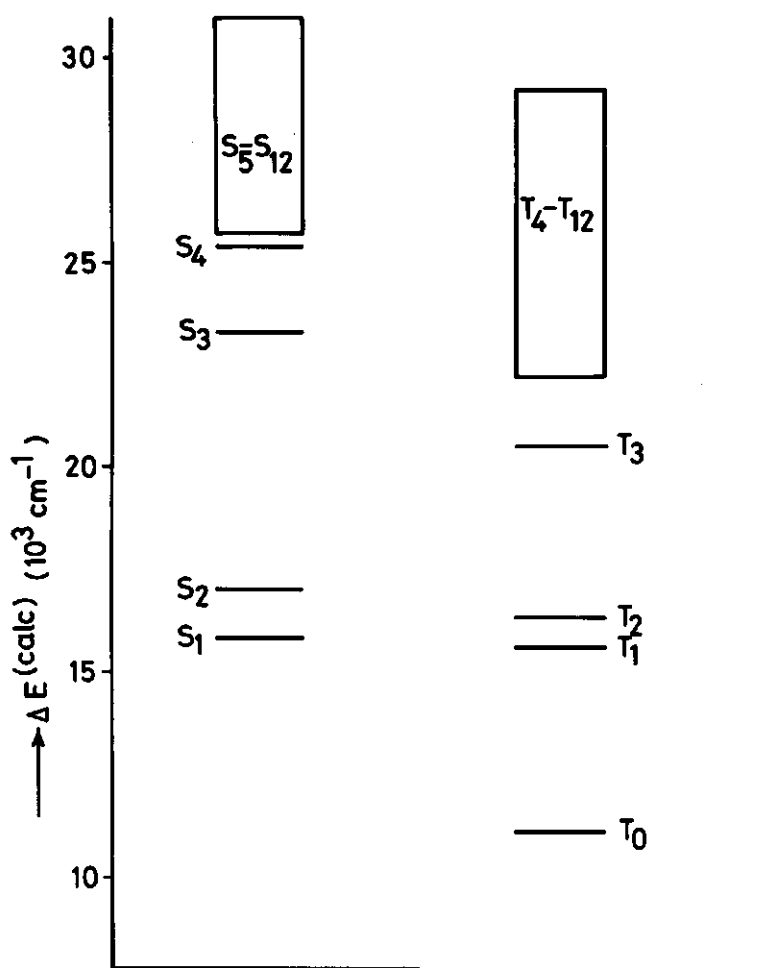


Figure 1.6 Calculated state diagram of the low-lying singlet and triplet states of Et Chl-a [74], relative to the ground state.

Both results may be reconciled, by noting the observation of Dvornikov et al. [83,84], who demonstrate from polarized phosphorescence experiments that the triplet states T_0 and T_1 of Chl-a may change their ordering by attaching of an additional ligand to the central Mg^{2+} ion. Then, the lowest triplet state does not have a single configurational composition any more.

The effects of ligation of H_2O to Mg^{2+} in Et Chl-a have been calculated [70]. Qualitatively, it has been found that ligation

does not produce an appreciable shift of T_0 , and only a small decrease (in the order of a few per cent) of the energies of T_1 through T_3 . Obviously, ligation does not result in switching of the ordering of T_0 and T_1 , within the framework of the calculations of Petke et al., although there is a decrease of the T_0 - T_1 distance upon ligation. In view of the approximations made in the CI calculations, one cannot draw firm conclusions with respect to the correctness of the explanation offered by Dvornikov et al.

More sophisticated calculations (PPP and CNDO with a larger basis set than used by Petke et al.) have been applied to different porphyrins [60,61], but as yet there are no essentially new data to add to the spectroscopist's view of Chl-a.

1.5 RADIATIONLESS TRANSITIONS IN CHLOROPHYLL-A

In this paragraph theories of radiationless transitions are applied to chlorophylls using the results obtained by Petke and co-workers [74] from calculations on the electronic properties of Et Chl-a (§1.4).

As will be shown, the predicted behaviour of individual sublevels in the populating and decay processes of the lowest excited triplet level T_0 of Chl-a qualitatively agrees with the results of the experiments of Chl-a *in vivo*, described in §4.2-4.3 and 5.2. We assume that the electronic structure of Et Chl-a, as studied by Petke et al., can be regarded as identical to that of Chl-a, apart from ligation, which certainly occurs *in vivo* [85]. Ligation on side-groups of Chl-a is not included in the calculations of Petke et al.

The framework of this paragraph will be to present the theory of radiationless transitions in an adequate formulation for our purposes; furthermore to use the results of Petke et al. as input for these calculations, and subsequently to relate the theoretical predictions for ISC with some experiments. A discussion related to our experimental results is given in §4.5.

Perturbation theory is used in a way first described by Siebrand and co-workers in a series of papers ([86-88] and earlier work) and subsequently applied and adapted to aromatic hydrocarbons by Metz et al. [89] and aza-aromatics by Anthéunis [90,91]. A review of the methods has been given in [92].

The intersystem crossing (ISC) rate constants can be written as

$$k_{isc}(T_O^i \rightarrow S_O) = \frac{2\pi}{\hbar} |\langle T_O^i | V | S_{O,v} \rangle|^2 \rho(E) \quad (1.5)$$

where V is the perturbing operator:

$$V = T_N + H_{SO} \quad (1.6)$$

T_N is the operator for nuclear kinetic energy and H_{SO} the hamiltonian for SOC.

Following the treatment of Metz et al. [89] and Antheunis [91], T_N , which takes into account the breakdown of the BO approximation, is neglected and the processes are described by taking $V = H_{SO}$ only.

$\rho(E)$ is the density of final states involved in ISC. The expression for populating the triplet level is readily written down by substituting the appropriate electronic states T_O^i and $S_{1,v}$.

In the following we discuss the matrix elements contributing to (1.5); we will not consider the role of $\rho(E)$.

The approach of Metz and Antheunis essentially consists of the choice of so-called pure-spin adiabatic BO states:

$$\begin{aligned} T_{O,o}^i &= {}^3\psi_{O,o}^i(q,s,Q) = T_O^i(q,s;Q) \wedge_{O,o}^3(Q) \\ S_{O,v} &= {}^1\psi_{O,v}(q,s,Q) = S_O(q,s;Q) \wedge_{O,v}^1(Q) \end{aligned} \quad (1.7)$$

for convenience abbreviated to

$$\begin{aligned} T_{O,o}^i &= T_O^i \wedge_{O,o}^3 \\ S_{O,v} &= S_O \wedge_{O,v}^1 \end{aligned}$$

$T_{O,o}^i$ and $S_{O,v}$ are eigenfunctions of the zeroth order hamiltonian $H_{(0)}$; Q and q represent the full sets of nuclear and electronic coordinates $\{Q\}$ and $\{q\}$; s labels the spin variable; \wedge is a vibrational wave function containing the nuclear coordinates only; v stands for the set of vibrational quantum numbers; s is a spin label, denoting the triplet state sublevels.

A full discussion of the implications of this choice of basis

set and operator is presented in [93].

The matrixelement $\langle T_O^i | H_{so} | S_{O,v} \rangle$ must be integrated over vibronic space, which implies that first the integral over electronic coordinates is taken and subsequently the integral over nuclear coordinate space:

$$\langle T_O^i | H_{so} | S_{O,v} \rangle = \langle \Lambda_{O,O}^3 \langle T_O^i | H_{so} | S_O \rangle \Lambda_{O,v}^1 \rangle \quad (1.8)$$

Antheunis has shown [91], that the vibrational integral can be written as a Franck-Condon factor. This factor can be ignored for this qualitative discussion because it is contained in identical form in all terms of the following expansion [91].

Now the electron matrixelement can be expanded in a Herzberg-Teller series about a nuclear equilibrium conformation $\{Q\} = 0$, to obtain its dependence on the nuclear conformation. Retaining terms up to first order in Q_p , this expansion reads:

$$\begin{aligned} \langle T_O^i | H_{so} | S_j \rangle = & \\ \text{0th order:} & \quad [\langle T_O^i | H_{so} | S_j \rangle]_{Q_p=0} + \\ \text{1st order:} & \quad \sum_p \left[\sum_{m \neq j} \frac{\langle T_O^i | \frac{\partial H^{(0)}}{\partial Q_p} | T_m^i \rangle \langle T_m^i | H_{so} | S_j \rangle}{E_{T_O} - E_{T_m}} + \right. \\ & \quad \left. \sum_{m \neq j} \frac{\langle T_O^i | H_{so} | S_m \rangle \langle S_m | \frac{\partial H^{(0)}}{\partial Q_p} | S_j \rangle}{E_{S_j} - E_{S_m}} + \right. \\ & \quad \left. \langle T_O^i | \frac{\partial H_{so}}{\partial Q_p} | S_j \rangle \right]_{Q_p=0} Q_p + \\ & \quad \text{2nd and higher order terms} \end{aligned} \quad (1.9)$$

Q_p is the normal coordinate to be considered in the summation over p of all normal coordinates; m labels electronic states. Substituting $j=0$ gives the expression for decay of the T_O state; $j=1$ gives the expression for the populating process.

A convenient way to find the significant contributions in (1.9)

is to divide H_{so} in parts symmetrical and antisymmetrical with respect to spin exchange.

$$H_{so} = \frac{1}{4n} \sum_i^n \sum_j^n (A_i l_{xi} + A_j l_{xj})(S_{xi} + S_{xj}) + \\ \frac{1}{4n} \sum_i^n \sum_j^n (A_i l_{xi} - A_j l_{xj})(S_{xi} - S_{xj}) +$$

terms in y and z =

$$H_{so}^+(x) + H_{so}^-(x) + \text{terms in y and z} \quad (1.10)$$

$$\text{where } A_i = \sum_{k=1}^n \frac{1}{r_{ik}} \frac{\partial V(r_{ik})}{\partial r_{ik}} \frac{1}{2m_e^2 c^2} \quad (1.11)$$

N and n are the number of nuclei and electrons respectively, l_{xi} and s_{xi} are the x components of the orbital angular momentum and electron spin operators, r_{ik} is the distance between nucleus k and electron i, $V(r_{ik})$ is the potential energy of the electron i with respect to the nucleus k, m_e is the electronic mass and c the velocity of light.

For one pair of electrons (1.10) reduces to

$$H_{so} = (A_1 l_{x1} + A_2 l_{x2})(S_{x1} + S_{x2}) \\ + (A_1 l_{x1} - A_2 l_{x2})(S_{x1} - S_{x2}) \\ + \text{terms in y and z} \quad (1.12)$$

It is easily demonstrated, that the H_{so}^+ operator does not convert a singlet spinfunction σ_s into a triplet spinfunction τ_x , τ_y or τ_z and vice versa. Thus, matrixelements of the type

$$\langle \phi_e \sigma_s | H_{so}^+ | \phi_e \tau_i \rangle \quad (i = x, y, z)$$

are vanishing.

On the other hand, the antisymmetrical part of H_{so} has the following properties, apart from the factors A_i (see e.g. [94])

$$\begin{aligned}
H_{so}^-(i) |p_j p_k \sigma_s\rangle &= \varepsilon i \hbar^2 \{ |p_k p_k \tau_i\rangle + |p_j p_j \tau_i\rangle \} \\
H_{so}^-(i) |p_j p_j \sigma_s\rangle &= \varepsilon i \hbar^2 \{ |p_k p_j \tau_i\rangle - |p_j p_k \tau_i\rangle \} \\
H_{so}^-(i) |p_j p_i \sigma_s\rangle &= \varepsilon i \hbar^2 |p_k p_i \tau_i\rangle \\
H_{so}^-(i) |p_j p_k \tau_i\rangle &= \varepsilon i \hbar^2 \{ |p_k p_k \sigma\rangle + |p_j p_j \sigma\rangle \} \\
H_{so}^-(i) |p_j p_j \tau_i\rangle &= \varepsilon i \hbar^2 \{ |p_k p_j \sigma\rangle - |p_j p_k \sigma\rangle \} \\
H_{so}^-(i) |p_j p_i \tau_i\rangle &= \varepsilon i \hbar^2 |p_k p_i \sigma\rangle \\
H_{so}^-(i) | \dots \tau_{j,k} \rangle &= 0 \\
H_{so}^-(i) | p_i p_i \dots \rangle &= 0 \\
(i \neq j \neq k = x, y, z) &
\end{aligned} \tag{1.13}$$

ε is the sign of the permutation of i, j and k with respect to x, y and z . H_{so}^- is the antisymmetrical part from (1.10), to be retained for calculating the non-zero contributions. In the following H_{so} thus symbolizes in fact H_{so}^- .

These relations (1.13) can now be used to evaluate the non-zero matrixelements in the expression (1.9). The dominant contributions in (1.9) are the non-zero terms of lowest order. If a non-zero term of a certain order is found, all higher order terms are neglected, because higher order terms contain increasing powers of Q_p , which remain small, especially at the temperature of our experiments. Generally the first (zeroth order) term at the right hand side of (1.9) is at least two orders of magnitude larger than the following three (first order) terms, and the first order terms two orders of magnitude larger than the nine second order terms, etc. [95].

However, after substituting the terms of (1.9) in (1.5), where the square of the sum of all terms must be taken, cross-terms will arise. This point is mostly overlooked in literature, or it is silently assumed that these cross-terms remain small. For the moment we may do the same, and assume that they constitute about 10% of the first non-zero term in (1.9), but for a quantitative calculation they have to be taken into account.

Another point, brought forward by Metz [89], is, that after substituting the appropriate wavefunctions in the orbital parts of (1.9), only one-center integrals (OCSOI = one-center spin-orbit integral) have to be evaluated, i.e. those integrals where both orbital parts differ only in one AO type (e.g. p vs s , or p_x vs p_y),

centered at the same nucleus; all so-called multi-center integrals can be neglected. This approximation has never really been justified, but is generally accepted [91,92].

Eq. (1.5) can now be evaluated for Et Chl-a by inserting the electronic configurations given in Tables 4 and 5 of [74] into the orbital parts of (1.9). In these tables the configurational composition of singlet and triplet states are given, expressed in MO's contributing more than 5% to the electronic states. In addition, the character of these MO's (n , π , σ or combinations of these) is given, in such a way that for each excited state the character can be written as a combination of the contribution of pure π MO's and $n\pi\sigma$ MO's, as follows

$$|m_i\rangle = \sum_s c_{si} |\pi\rangle + \sum_t c_{ti} |n\pi\sigma\rangle \quad (1.14)$$

Here the c_{si} is the s^{th} coefficient of the i^{th} state. The sum is over all coefficients contributing to state $|m_i\rangle$, s is over all pure π MO's, t over all MO's of mixed $n\pi\sigma$ character. The coefficients c_{si} and c_{ti} can be obtained by re-orthonormalizing the MO's calculated by Petke et al. via the method first given by Löwdin [96], see also [97]. The exact magnitude of the coefficients is not important, however, because the dominant effects arise from the different orders of approximation in (1.9).

The excitation is almost exclusively from MO's with π character or from MO's with mixed $n\pi\sigma$ character towards MO's with π^* character.

In Table 1.1 we have listed the order of the lowest Herzberg-Teller term in (1.9), where the first OCSOI appear for populating and decay of the lowest triplet state T_0 of Et Chl-a for the sub-levels $|x\rangle$, $|y\rangle$ or $|z\rangle$ by radiationless transitions. The entries in Table 1.1 denote those SO matrixelements for Et Chl-a, which are non-zero in the order given by the headings (0), (1) or (2) of the columns, due to the application of the properties of H_{SO} , as given in (1.13).

It should be realized that up to second order of (1.9) all possible matrixelements between singlet and triplet levels are implicitly represented in this Table. In order to evaluate the matrix-

Table 1.1 Non-zero matrix elements for $S_1 \rightarrow T_0$ and $T_0 \rightarrow S_0$ ISC of Et Chl-a^{a)}.

Relative populating rates (p) and decay rate constants (k)

	(0)	(1)	(2)
$ x\rangle, y\rangle$	-	$\pi\pi^* \rightarrow (\pi\pi)\pi^*$ $(\pi\pi)\pi^* \rightarrow \pi\pi^*$... ^{b)}
$ z\rangle$	-	-	$(\pi\pi)\pi^* \rightarrow (\pi\pi)\pi^*$

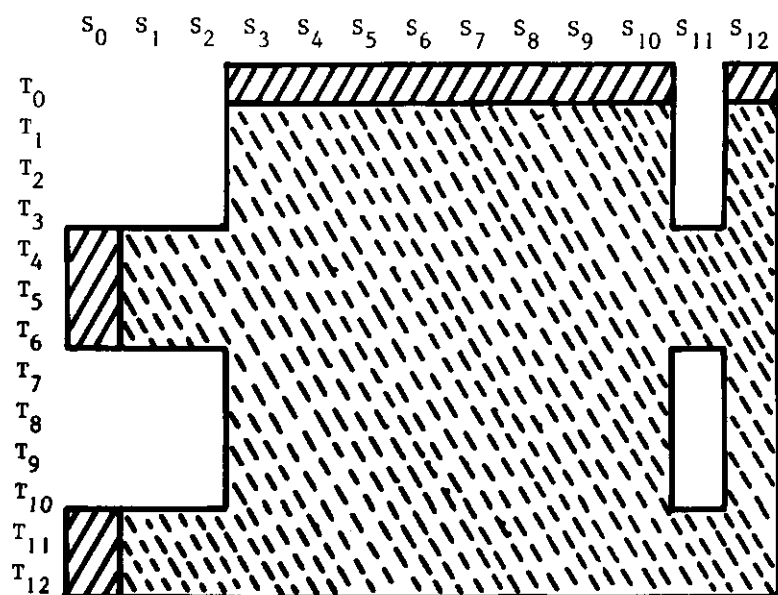
a) The order of the lowest HT term, where the first OCSOI's appear in expressions (1.9) for populating and decay of the lowest triplet state of Et Chl-a for the triplet sublevels $|x\rangle$, $|y\rangle$ and $|z\rangle$ by radiationless transitions. The character of the orbitals with the most important contributions is listed.

b) Neglected non-zero matrix elements.

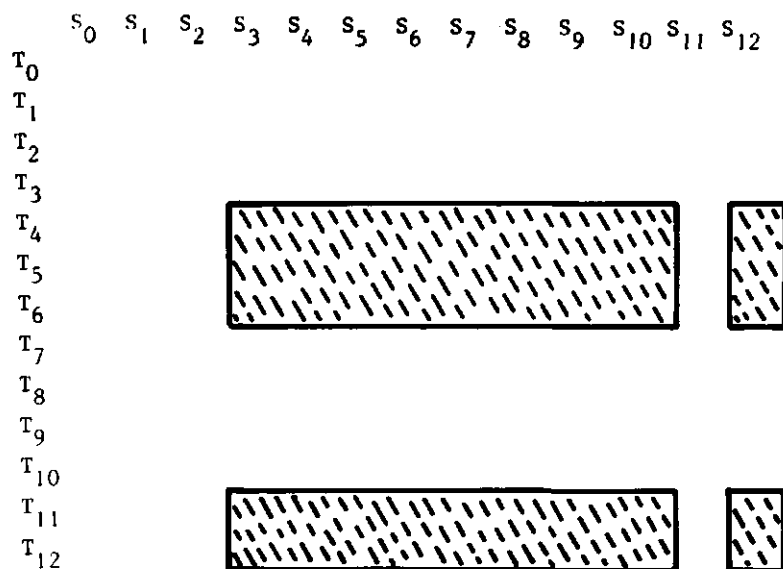
elements for the zeroth and first order contributions to the $S_1 \rightarrow T_0$ ISC process, we may limit ourselves to mixing of S_1 with nearby triplet states T_m and mixing of T_0 with nearby S_m states by H_{SO} for the $S_1 \rightarrow T_0$ ISC process. On the other hand, mixing of S_0 with nearby T_m triplet states, as well as mixing of T_0 with S_m states is important for the $T_0 \rightarrow S_0$ decay process. For both processes, mixing of higher S_m and T_m states occurs only in second or higher order, and is less important.

In Table 1.2 the lowest order HT contribution of each possible transition to a specific kinetic constant is given. The magnitude of these contributions depends a.o. on the magnitude of the matrix-elements of Table 1.1 itself and on the magnitude of the energy denominators in (1.9). Furthermore, the integrals contributing to a HT term are all burdened by multiplication with a different Franck-Condon factor. We may ignore these effects for a qualitative discussion of the various populating and decay routes; the effects due to these three causes remain small as compared to the differences between the HT terms of successive orders.

decay $T_0^{x,y} \rightarrow s_0$



decay $T_0^z \rightarrow s_0$



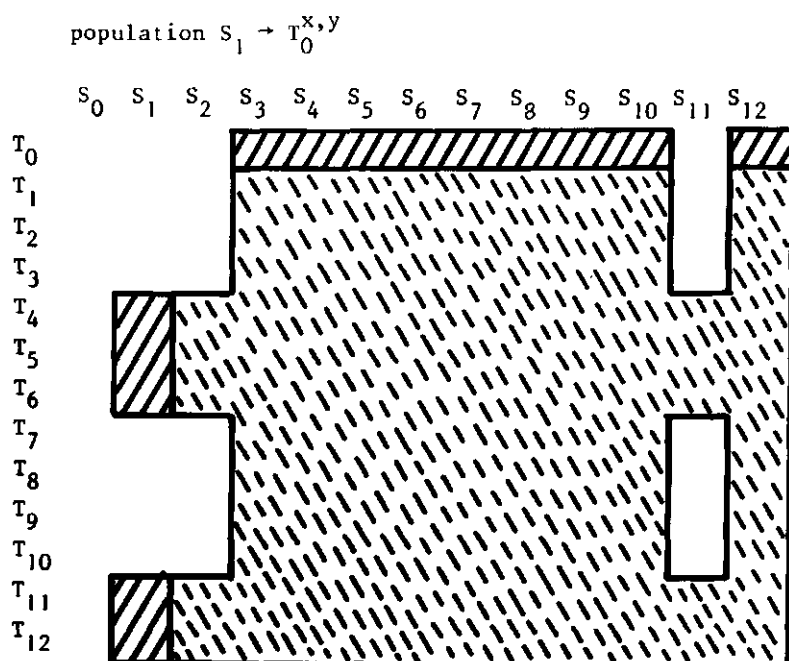




Table 1.2 Order of HT contributions

The order of the contributions in the HT expansion of all possible transitions between singlet and triplet states in Et Chl-a to the population and decay of the lowest triplet state.

The dominant contributions are denoted by

- : first order contributions
: second order contributions

Separate tables are given for populating and decay of each triplet sublevel $|x\rangle$, $|y\rangle$ and $|z\rangle$. Between $|x\rangle$ and $|y\rangle$ there is no difference in the order of the contributions only in the relative magnitude. The table for the populating of $|z\rangle$ is the same as for the decay of $|z\rangle$.

This discussion considers only the populating and decay processes of T_0 , and contributions to these processes by mixing S_1 and T_0 with other states. Transitions between higher singlet and triplet states $T_m \leftrightarrow S_n$ are also possible, however. After excitation into the Soret states, as in our experiments, decay to T_0 may occur not only by internal conversion to S_1 , and subsequently by ISC to T_0 , but also via higher lying triplet states, i.e. by $S_m \rightarrow T_n$ ISC transitions.

Transitions between these states should be considered, because of their partly n π o character, and because these transitions are governed by matrixelements appearing in zeroth order of the HT expansion; these matrixelements do not vanish by symmetry. $S_m \rightarrow T_n$ radiationless transitions may considerably participate in populating T_0 . Matrixelements $\langle S_m \sigma | H_{SO} | T_n \tau_i \rangle$ generally are different from $\langle S_1 \sigma | H_{SO} | T_0 \tau_i \rangle$. This results in a different populating pattern of molecules over $|x\rangle$, $|y\rangle$ and $|z\rangle$, as compared to that originating from S_1 only. These 'high crossings' are expected to exhibit increased population of the $|z\rangle$ sublevels of the involved triplet state.

The ratio of the rates of internal conversion $S_n \rightarrow S_1$ and ISC between higher levels $S_m \rightarrow T_n$ is unknown, and experiments are necessary to decide whether it is justified to neglect the $S_m \rightarrow T_n$ processes, as is usually done. Keller [98] has shown, that for a number of aromatics and aza-aromatics, the reverse process $T_n \rightarrow S_m$ is not an important pathway for de-excitation of excited triplet molecules. Also, non-bonding electrons do not appear to have a large effect on the ISC probability. Avarmaa could not measure $T_n \rightarrow S_m$ transitions for a number of chlorophylls by a similar procedure [99]. From these findings we derive that the $S_m \rightarrow T_n$ process generally cannot compete with $S_m \rightarrow S_1$ or $T_n \rightarrow T_0$ internal conversion processes.

For the processes where T_0 is involved, it has been shown for aromatic molecules, that a strong selection rule prevents contributions from zeroth order HT terms, to the populating and decay routes to occur, e.g. [92,84]. It follows from the work of Petke et al., that such a selection rule is also operative for Et Chl-a. These authors show [74], that the states S_0 through S_2 and T_0 through T_3 have $\pi\pi^*$ character, except for a small perturbation arising from the methoxycarbonylgroup attached to ring V (atoms C_{10a} and O_2 in Fig. 1.4).

After substituting only p_z orbitals in (1.9) and applying (1.13), it is evident, that in all HT-terms matrix elements between pure $\pi\pi^*$ states vanish. The perturbation from atoms C_{10a} and O_2 does not contribute to the zeroth order HT term, because there exist no matrix elements between states that both have this perturbation as part of their electronic configuration.

For the populating and decay processes of T_0 the most important contributions in the HT expansion appear in first order. For the populating process of T_0 these arise from the mixing of T_0 with singlet states higher than S_2 and mixing of S_1 with triplet states higher than T_3 (see Table 1.2). For the decay process, the contributions from mixing of T_0 with higher singlets are similar to those for the populating process, but the higher triplets now mix with S_0 instead of S_1 . This implies, that the energy denominator in the first order term is $E(S_0) - E(S_m)$, ($m \neq 0$) for the decay process, and $E(S_1) - E(S_n)$, ($n \neq 1$) for the populating process, the latter clearly being the smallest of the two.

Comparison of populating and decay of T_0 primarily has to deal with this difference in energy denominator. Consequently the populating rates are expected to be more affected by a change in electronic configuration than the decay rates. An example of this phenomenon will be presented in a following part of this paragraph.

The oxygen atoms O_1 , O_2 , O_3 are found to play an important role in the ISC transitions between singlet and triplet states. Very recently, Wasielewski and co-workers found [100], that when a chlorophyll-derivative is forced into the enol form involving the carbonyl group attached to ring V (O_1 and C_9 in Fig. 1.4), no triplets could be detected by ESR at 8K. This is not surprising since from the work of Petke et al. [74] it follows, that large OCSOI will appear in the HT expansion from the n electrons of oxygen atoms O_1 and O_2 .

The first order terms of Table 1.2 are only non-zero for populating and decay of the $|x\rangle$ and $|y\rangle$ sublevels, and not for $|z\rangle$. For the populating process this is due to the fact that this process results in a pure $\pi\pi^*$ triplet state, and the SOC operator is unable to populate a triplet sublevel $|p_z p_z \uparrow_z\rangle$ with the same character of the orbital and spin parts (see formulae (1.13)). An analogous argument holds for the decay process: the $|z\rangle$ sublevel only decays via second and higher order terms. It is well known, that in most

chlorophylls the $|x\rangle$ and $|y\rangle$ sublevels are the most active. In this sense chlorophylls behave like aromatic molecules [89,91,92].

Since the oxygen atoms O_1 and O_2 of Chl-a turn out to be important for the ISC process, however, the molecule lacks all symmetry-elements. Apart from the oxygen atoms O_1 and O_2 , there are more groups which perturb the C_{2v} symmetry of the Mg-dihydroporphin skeleton, which can be considered as the unperturbed basic structure of chlorophyll. It is therefore highly questionable whether the treatment of Dvornikov et al. [83,84] of ISC in chlorophylls and pheophytins on the basis of C_{2v} symmetry is correct.

Any deviation from fourfold symmetry of the molecule predicts a difference between the behaviour of the $|x\rangle$ and $|y\rangle$ T_0 sublevels for the populating as well as for the decay process. More precise calculations are necessary, in order to decide which of both would be the most active.

A discussion of experimental results with respect to ISC in chlorophylls is given in §4.5, in particular for the experimental data on Chl-a in CPI complexes. An example of the application of the previously developed theory is provided by a comparison of the data on Pheo-a with those on Chl-a, given in Table 1.3. The data have been taken from [81] and are confirmed by results of others [101], cf. also [102]. The comparison of populating rates and decay rate constants is obscured by the fact that the populating rates are given in percentages. After expressing the decay rate constants in percentages of the total decay of T_0 , there is no difference, within the limits of accuracy, between the populating rates and decay rate constants of Chl-a and Pheo-a, i.e. the variations in k_1 closely parallel those in p_1 on going from Chl-a to Pheo-a.

As found by Petke et al. [74], the n-orbitals of the $N_{2,4}$ atoms in Pheo-a are raised in energy if both protons in this compound are replaced by Mg^{2+} , resulting in Chl-a. As discussed before, the effects of this raise in energy are predicted to be larger for the populating rates than for the decay rate constants: the change in the first order HT terms in (1.9) in the energy is expected to be more important, when the energy denominator becomes smaller. For the populating rates, the energy denominator in (1.9) contains $E(S_1) - E(S_n)$, whereas for the decay rate constants $E(S_0) - E(S_n)$

Table 1.3 Kinetic triplet constants of Chl-a and Pheo-a

	sec ⁻¹			%		
	k _x	k _y	k _z	p _x	p _y	p _z
Chl-a	620±80 (33±4)	1120± 20 (60±1)	140± 40 (7±2)	31±3	60±3	11±3
Pheo-a	1040±50 (33±2)	1300±100 (41±3)	820±100 (26±3)	31±2	43±5	26±6

(numbers between parentheses are percentages)

k_i represent decay rate constants; p_i are the relative populating rates for triplet sublevels |i> (i = x,y,z). Data are taken from [82] and are measured with ESR at 100 K in MTHF.

appears. The other parts of the first order HT term remain approximately unaffected by changing from Chl-a to Pheo-a.

The data of Table 1.3 show that this effect does not apply for Chl-a vs Pheo-a, since the populating and decay processes are equally affected by substituting 2H⁺ by Mg²⁺.

The absence of the predicted effect can be simply explained by noting that a shift in the MO's containing non-bonding contributions from N_{2,4}, resulting from changing Pheo-a into Chl-a, is estimated to change the energy denominator for p_i by ~8% and for k_i by ~5%. This difference cannot be resolved by our experiments.

In conclusion, the relevant n-orbitals only participate in highly excited electronic states, which are too high in energy to have a different effect on k_i and p_i.

This behaviour is in sharp contrast to the effect of hydrogen-bonding to oxygen atoms at or close to ring V. The n-orbitals of these oxygen atoms participate in MO's which are lower in energy than those involving N_{2,4} n-orbitals. Therefore, we expect that hydrogen-bonding to ring V oxygens may have a detectably different effect on k_i vs p_i.

1.6 REFERENCES

1. A. Trebst and M. Avron, Eds. (1977). Encyclopedia of Plant Physiology, New Series, Volume V, Photosynthesis I. Springer, Berlin.
2. J. Barber, Ed. (1977). Topics in Photosynthesis, Vol II, Primary Processes of Photosynthesis. Elsevier, Amsterdam.
3. Govindjee, Ed. (1975). Bioenergetics of Photosynthesis. Academic Press, New York.
4. G. Akoyunoglou, Ed. (1981). Proc. Fifth Int. Congr. Photosynthesis. International Science Services Balaban, Rehovot, Israel (In press).
5. O. Machold, D.J. Simpson and B.L. Møller (1979). Carlsberg Res. Commun. 44: 235-254.
6. D. von Wettstein, B. Lindberg Møller, G. Høyer-Hansen and D. Simpson (1980). In: Origin of Chloroplasts. Eds.: J.A. Schiff and R.Y. Stanier. Elsevier, Amsterdam.
7. V.V. Klimov, A.V. Klevanik, V.A. Shuvalov and A.A. Krasnovsky (1977). FEBS Lett. 82: 183-186.
8. V.V. Klimov, E. Dolan and B. Ke (1980). FEBS Lett. 112: 97-100.
9. L.N.M. Duysens and H.E. Sweers (1963). In: Studies on Microalgae and Photosynthetic Bacteria, Special Issue of Plant Cell Physiol., Univ. of Tokyo Press, Tokyo, pp. 353-372.
10. B.R. Velthuys and J. Ames (1973). Biochim.Biophys.Acta 325: 126-137.
11. J. Ames, M.P.J. Pulles and B.R. Velthuys (1973). Biochim.Biophys.Acta 325: 472-482.
12. G. Porter, C.J. Tredwell, G.F.W. Searle and J. Barber (1978). Biochim.Biophys.Acta 501: 232-245.
13. G.F.W. Searle, J. Barber, G. Porter and C.J. Tredwell (1978). Biochim.Biophys.Acta 501: 246-256.
14. J.C. Goedheer (1976). Photosynthetica 10: 411-422.
15. T.D. Padmaja and T.V. Desikachary (1971). Phykos 7: 62-69.
16. R.Y. Stanier and G. Cohen-Bazire (1977). Ann.Rev.Microbiol. 31: 225-274.
17. N.I. Bishop (1971). In: Methods in Enzymology XXIII. Ed. A. San Pietro. Academic Press, New York, pp. 130-143.

18. N.I. Bishop (1973). In: Photophysiology, Vol VIII. Ed. A.C. Giese. Academic Press, New York, pp. 65-96.
19. V.J. Chapman and D.J. Chapman (1973). The Algae, Sec. Ed., Macmillan Press, London.
20. P.L. Dutton, J.S. Leigh and M. Seibert (1972). Biochem.Biophys. Res.Comm. 46: 406-413.
21. P.L. Dutton, J.S. Leigh Jr. and D.W. Reed (1973). Biochim.Biophys.Acta 292: 654-664.
22. J.S. Leigh Jr. and P.L. Dutton (1974). Biochim.Biophys.Acta 357: 67-77.
23. W.W. Parson, R.K. Clayton and R.J. Cogdell (1975). Biochim. Biophys.Acta 387: 265-278.
24. M.C. Thurnauer, J.J. Katz and J.R. Norris (1975). Proc.Natl. Acad.Sci.USA 72: 3270-3274.
25. R.A. Uphaus, J.R. Norris and J.J. Katz (1974). Biochem.Biophys. Res.Comm. 61: 1057-1063.
26. R. van Grondelle, N.G. Holmes, H. Rademaker and L.N.M. Duysens (1978). Biochim.Biophys.Acta 503: 10-25.
27. R.A. Mushlin, P. Gast and A.J. Hoff (1980). Chem.Phys.Lett. 76: 542-547.
28. H.A. Frank, R. Friesner, J.A. Nairn, G.C. Dismukes and K. Sauer (1979). Biochim.Biophys.Acta 547: 484-501.
29. V.I. Godik and A.I. Borisov (1979). Biochim.Biophys.Acta 548: 296-308.
30. V.M. Voznyak, E.I. Elfimova and I.I. Proskuryakov (1978). Dokl. Akad.Nauk USSR 242: 1200-1203.
31. V.M. Voznyak, E.I. Elfimov and V.K. Sukovatitzina (1980). Biochim.Biophys.Acta 592: 235-239.
32. H. Rademaker, A.J. Hoff and L.N.M. Duysens (1979). Biochim. Biophys.Acta 546: 248-255.
33. V.I. Godik and A.Y. Borisov (1980). Biochim.Biophys.Acta 590: 182-193.
34. G.F.W. Searle, G.H. van Brakel, W.F.J. Vermaas, A. van Hoek and T.J. Schaafsma (1981). Proc. Fifth Int. Congr. Photosynthesis. Ed. G.A. Akoyunoglou. International Science Services Balaban, Rehovot, Israel, Vol I: 129-142 (in press).
35. G.H. van Brakel, T.J. Schaafsma and J.J.S. van Rensen. Isr.J. of Chem. (in press, see also Ch 3 of this Thesis).

36. P. Heathcote and M.C.W. Evans (1981). Proc. Fifth Int. Congr. Photosynthesis. Ed. G.A. Akoyunoglou. International Science Services Balaban, Rehovot, Israel (in press).
37. A.W. Rutherford and J.E. Mullet (1981). Biochim.Biophys.Acta 635: 225-235.
38. H.A. Frank, M.B. McLean and K. Sauer (1979). Proc.Natl.Acad. Sci.USA 76: 5124-5128.
39. A.R. McIntosh, H. Manikowski and J.R. Bolton (1981). Proc. Fifth Int. Congr. Photosynthesis. Ed. G.A. Akoyunoglou. International Science Services Balaban, Rehovot, Israel (in press).
40. R. Tycko and C. Dismukes (1981). Proc. Fifth Int. Congr. Photosynthesis. Ed. G.A. Akoyunoglou. International Science Services Balaban, Rehovot, Israel (in press).
41. G.C. Dismukes, A. McGuire, R. Blankenship and K. Sauer (1978). Biophys.J. 21: 239-256.
42. R. Friesner, G.C. Dismukes and K. Sauer (1979). Biophys.J. 25: 277-294.
43. R.E. Blankenship. A. McGuire and K. Sauer (1975). Proc.Natl. Acad.Sci.USA 72: 4943-4947.
44. A.R. McIntosh, H. Manikowski, S.K. Wong, C.P.S. Taylor and J.R. Bolton (1979). Biochem.Biophys.Res.Comm. 87: 605-612.
45. S.J. van der Bent, T.J. Schaafsma and J.C. Goedheer (1976). Biochem.Biophys.Res.Comm. 71: 1147-1152.
46. G.H. van Brakel, J.J.S. van Rensen and T.J. Schaafsma (1981). Proc. Fifth Int. Congr. Photosynthesis. Ed. G.A. Akoyunoglou. International Science Services Balaban, Rehovot, Israel (in press).
47. A.R. McIntosh, H. Manikowski and J.R. Bolton (1979). J.Phys. Chem. 83: 3309-3313.
48. D. Holten, M.W. Windsor, W.W. Parson and M. Gouterman (1978). Photochem.Photobiol. 28: 951-961.
49. D. Holten, M.W. Windsor and W.W. Parson (1979). Springer Ser. Chem.Phys. 4: 126-133.
50. R.E. Blankenship (1981). Acc.Chem.Res. 14: 163-170.
51. A.J. Hoff (1981). In: ODMR Spectroscopy. Ed. R.H. Clarke. Wiley, New York.
52. G.R. Seely (1977). In: Primary Processes in Photosynthesis, Vol II of Topics in Photosynthesis. Ed. J. Barber. Elsevier, Amsterdam. Ch 1.

53. T.J. Schaafsma (1981). In: ODMR Spectroscopy. Ed. R.H. Clarke. Wiley, New York.
54. N.I. Krinsky (1979). Pure and Appl. Chem. 51: 649-660.
55. G. Öquist, G. Samuelson and N.I. Bishop (1980). Physiol.Plant 50: 63-70.
56. A.K. Chibisov (1969). Photochem.Photobiol. 10: 331-347.
57. A.K. Chibisov, A.V. Karayakin and M.Y. Zubrilina (1969). Biofizika 14: 925-927.
58. A.K. Chibisov (1972). Dokl.Akad.Nauk USSR 205: 142-145.
59. W. Potter and G. Levin (1979). Photochem.Photobiol. 30: 225-231.
60. M. Gouterman (1979). In: The Porphyrins Vol III. Ed. D. Dolphin. Academic Press, New York.
61. G.P. Gurinovich, A.N. Sevchenko and K.N. Solovyev (1968). Spectroscopy of chlorophyll and related compounds. Publishing House Science and Technology, Minsk. (English translation: National Technical Information Service, U.S. Dept. of Commerce, Springfield, VA 22151, USA). Ch 6.
62. The chemical and physical behavior of porphyrin compounds and related structures. Ed. A.D. Adler. Annals of the New York Academy of Sciences, Vol 206, New York. Ch 1.
63. S.J. Chantrell, C.A. McAuliffe, R.W. Munn and A.C. Pratt (1975). Coord.Chem.Rev. 16: 259-284.
64. T.J. Schaafsma (1981). Proc. Fourth Int. Sem. Energy Transfer in Condensed Matter. Prague (in press).
65. R.S. Mulliken (1939). J.Chem.Phys. 7: 339- .
66. E. Clementi, H. Clementi and D.R. Davis (1967). J.Chem.Phys. 46: 4725-4730.
67. J.D. Roberts and M.C. Caserio (1965). Basic principles of organic chemistry. Benjamin, New York. Ch 9.
68. W.J. van der Hart, J.J.C. Mulder and L.J. Oosterhoff (1972). J.Am.Chem.Soc. 94: 5724-5730.
69. M.J.S. Dewar (1969). The molecular orbital theory of organic chemistry. McGraw-Hill, New York. Ch 3.
70. D. Spangler, G.M. Maggiora, L.L. Shipman and R.E. Christoffersen (1977). J.Am.Chem.Soc. 99: 7478-7489.
71. W.T. Simpson (1949). J.Chem.Phys. 17: 1218-1221.
72. M. Gouterman (1961). J.Mol.Spectr. 6: 138-163.

73. M. Gouterman, G.H. Wagnière and L.C. Snyder (1963). *J.Mol. Spectr.* 11: 108-127.
74. J.D. Petke, G.M. Maggiora, L.L. Shipman and R.E. Christoffersen (1979). *Photochem.Photobiol.* 30: 203-223.
75. G.M. Maggiora, R.E. Christoffersen, J.A. Yoffe and J.D. Petke (1981). In: *Annals of the New York Academy of Sciences*, Vol 367, *Quantum Chemistry of Biomedical Sciences*, pp. 1-16. Eds. H. Weinstein and J.P. Green. New York Academy of Sciences, New York.
76. R.E. Christoffersen, D. Spangler, G.G. Hall and G.M. Maggiora (1973). *J.Am.Chem.Soc.* 95: 8526-8536.
77. P.-S. Song and W.E. Kurtin (1967). *J.Am.Chem.Soc.* 89: 4248-4249.
78. M. Sundbom (1968). *Acta Chem.Scand.* 22: 1317-1326.
79. R. Gáspár and R. Gáspár Jr. (1979). *Int.J.Quantum Chem.* 15: 567-578.
80. R.E. Christoffersen (1979). *Int.J.Quantum Chem.* 16: 573-604.
81. J.F. Kleibeuker (1977). Thesis, Wageningen. Ch 10 and Appendix.
82. J.F. Kleibeuker, R.J. Platenkamp and T.J. Schaafsma (1978). *Chem.Phys.* 27: 51-64.
83. S.S. Dvornikov, V.N. Knyukshto, K.N. Solov'ev and M.P. Tsvirko (1979). *J.Luminesc.* 18/19: 491-494.
84. S.S. Dvornikov, V.N. Knyukshto, K.N. Solov'ev and M.P. Tsvirko (1979). *Opt.Spectrosc.* 46: 385-388.
85. G.F.W. Searle, R.B.M. Koehorst, T.J. Schaafsma, B.L. Møller and D. von Wettstein (1981). *Carlsberg Res.Comm.* 46: 183-194.
86. B.R. Henry and W. Siebrand (1971). *J.Chem.Phys.* 54: 1072.
87. V. Lawetz, G. Orlandi and W. Siebrand (1972). *J.Chem.Phys.* 56: 4058-
88. G. Orlandi and W. Siebrand (1973). *J.Chem.Phys.* 58: 4513-4523.
89. F. Metz, S. Friedrich and G. Hohlneicher (1972). *Chem.Phys. Lett.* 16: 353-358.
90. D.A. Antheunis, J. Schmidt and J.H. van der Waals (1974). *Mol. Phys.* 27: 1521-1541.
91. D.A. Antheunis (1974). Thesis. Leiden. Ch V.
92. H.A. Frank (1977). Thesis. Boston.
93. E.W. Schlag, S. Schneider and S.F. Fischler (1971). *Ann.Rev. Phys.Chem.* 22: 465-526.

94. S.P. McGlynn, T. Azumi and M. Kinoshita (1969). Molecular spectroscopy of the triplet state. Prentice Hall, London. Ch V.
95. D.A. Antheunis (1974). Thesis. Leiden. Ch II.
96. P.-O. Löwdin (1950). J.Chem.Phys. 18: 365-375.
97. R.E. Christoffersen (1972). Adv.Quantum Chem. 6: 333-393.
98. R.A. Keller (1969). Chem.Phys.Lett. 3: 27-29.
99. R. Avarmaa (1979). Mol.Phys. 37: 441-454.
100. M.R. Wasielewski, J.R. Norris, L.L. Shipman, C.-P. Lin and W.A. Svec (1981). Proc.Natl.Acad.Sci.USA 78: 2957-2961.
101. R.H. Clarke, R.E. Connors, T.J. Schaafsma, J.F. Kleibeuker and R.J. Platenkamp (1976). J.Am.Chem.Soc. 98: 3674-3677.
102. W. Hägele, D. Schmid and H.C. Wolf (1978). Z.Naturforsch. 33a: 83-93.

2 MATERIALS AND METHODS

2.1 INTRODUCTION

In this chapter preparative and instrumental methods will be described. Optical techniques (fluorescence and absorption spectroscopy) and ESR were used to identify the determinant parameters of the primary photo-physical process(es) which occur in the systems studied, while ODMR were applied to characterize some of the more detailed features. The experiments were primarily designed to study the processes in algal cells. Extensive signal averaging was required for ODMR and ESR experiments because of the low signal to noise (S/N) ratio. We have also used chlorophyll-protein complexes offering the advantages of a better S/N ratio and of a more straightforward interpretation of the results. The composition of chlorophyll-protein complexes has turned out to be dependent on the isolation procedure followed. Similar phenomena have been extensively reported in the literature [1-4]. For example, complexes of different composition are obtained when thylakoid membranes from chloroplasts or algae are treated with various detergents. As shown in § 4.2 in more detail, the buffer used in the isolation procedure also influences the composition of the complex.

2.2 THE CULTIVATION OF THE ALGAE

Cells of the cyanobacterium *Synechococcus leopoliensis* (former name *Anacystis nidulans*, stock 1405/1 Cambridge) were grown at 25°C in Kratz and Myers medium C [5], pH = 7.8, in Erlenmeyer flasks of 1000 ml containing 250 ml medium, under continuous shaking and illumination (15 W/m²), while air enriched with 3% CO₂ was bubbled through the medium.

At least once a month part of the culture was transferred to fresh medium; normally the inoculum was 25 ml of the old culture. In the exponential growing phase the doubling time was approximately one day, somewhat depending on the moment of taking the inoculum.

For ODMR experiments or isolation of chlorophyll-protein complexes preferentially cells at the end of their logarithmic growing phase were taken.

The green alga *Scenedesmus obtusiusculus* was maintained on Beyerink agar slants of the following composition:

NH ₄ NO ₃	0.33 g/l
K ₂ HPO ₄	0.2 g/l
MgSO ₄ · 7H ₂ O	0.2 g/l
agar	1.5 %
FeSO ₄	6 mg/l
Na-citrate	4 mg/l
EDTA	2 mg/l
+ 2 ml/l trace elements solution A4+B7 according to Arnon [6].	

For their culturing an aliquot of algal cells from the slant was transferred into an Erlenmeyer flask which contained 250 ml of a medium of the following composition:

KNO ₃	2.5 g/l
KH ₂ PO ₄	0.136 g/l
MgSO ₄ · 7H ₂ O	0.5 g/l
FeSO ₄	6 mg/l
Na-citrate	4 mg/l
EDTA	2 mg/l
+ 2 ml/l trace elements solution A4+B7 according to Arnon [6].	

The cultivation was also carried out under continuous shaking and illumination, while air enriched with 3% CO₂ was bubbled through the medium. The growth rate was slightly less than for *Synechococcus leopoliensis*.

Usually cells were harvested after 1-2 weeks.

Copper-deficient cells of *Scenedesmus obtusiusculus* were grown by transferring about 25 ml of normal cells into the same medium, except for the presence of copper. The copper content of the algae could be gradually decreased by repeatedly inoculating this growing culture into fresh copper-free medium. In order to obtain a sufficiently copper-deficient culture, all glassware routinely was thoroughly rinsed with glass-distilled water. Growth rate was found to be little affected by copper deficiency.

To decrease the total paramagnetic ion content of the cells, they were grown in a medium containing no paramagnetic ions at all, except for 10^{-5} M Fe^{3+} . The procedure of rinsing glassware and repeated inoculation was also followed in this case. Under these conditions the growth rate was very slow, but after 4 weeks, cells could be harvested from a volume of 0.1 liter suspension. This amount was sufficient to carry out an adequate number of experiments. Without Fe^{3+} the cells did not multiply.

Mutants *Scenedesmus* #8 and C-6E from *Scenedesmus obliquus* were obtained as a gift from professor H. Senger, Marburg. The cells were maintained on agar slants containing the inorganic basal medium of Kessler et al. [8], enriched with 0.5% glucose and 0.5% yeast extract according to Senger and Bishop [9].

For growing the mutants, aliquots were taken from a slant under strictly sterile conditions and put into a dark incubator at 30°C in 1000 ml Erlenmeyer flasks containing 250 ml medium. In order to supply the cells with O_2 , the flasks were shaken each day by hand for a short period, during the experimental growth phase. After 2-3 weeks they were harvested.

We also tried to grow carotenoidless cells of *Synechococcus leopoliensis*, by adding DPA (diphenylamine) to the growth medium. DPA is known to inhibit carotenoid synthesis in photosynthetic bacteria (10 mg/liter) [10]. In cyanobacteria the carotenoids do not disappear completely at this DPA concentration, perhaps because of a lower permeability of the cell wall of cyanobacteria for DPA, as compared to bacteria [11]. Higher concentrations of DPA (30 mg/l) were found to kill the cells eventually, although they still were found to divide two or three times before dying.

A suitable method appeared to be growing the cells to halfway their exponential phase (3 days), then adding DPA (30 mg/l) and harvesting them after 3 days. Decay of the cell culture could be diminished by decreasing the intensity of the illumination. After this procedure the cells are expected to contain about 12% of the carotenoid content of normal cells. This approximated percentage was consistent with the extinction of the carotenoid absorption band at 492 nm of the final culture, compared with the extinction of the inoculum. This is what would be expected, if it is assumed that after DPA addition carotenoid synthesis is completely blocked during the next three cell divisions which were allowed before harvest.

2.3 ISOLATION OF CHLOROPHYLL-PROTEIN COMPLEXES

The mass of ~ 1000 ml algal culture in the late-logarithmic growing phase was centrifuged (12 min at 2400 g). The pellet of cells was resuspended and washed in medium A (0.3 M mannitol, 6.2 mM Tris, 5 mM MgCl_2 , 48 mM glycine, pH = 8.3). The resulting suspension was centrifuged again, resuspended in 40 ml medium A, and subsequently cooled in ice. The cell suspension was passed twice through a French Press at 1135 atm or thrice when the cells were older, because then the cell walls are apparently stronger. Intact cells were removed by centrifugation (15 min at 1500 g) and the supernatant was centrifuged again (30 min, 210,000 g) to remove phycocyanin pigments. The thylakoid membranes were now pelleted and resuspended by a Potter hand homogeniser in a small volume of medium A to obtain a suspension containing 2 mg ml^{-1} Chl-a. If not used immediately, the suspension was stored in liquid nitrogen. Chlorophyll concentration was measured according to McKinney [12].

SDS polyacrylamide gel electrophoresis (PAGE) was performed in a standard disc gel electrophoresis apparatus, fitted with a tap water cooling jacket (temperature ~ 15°C) and shielded from ambient light. For electrophoresis two kinds of buffer were used: TG buffer (6.2 mM Tris + 48 mM glycine, pH 8.3) and Pi buffer (100 mM sodium phosphate, pH 7.6). The gel composition was 5% acrylamide, 0.13% bisacrylamide, 0.1% TEMED (N,N,N',N'-tetramethylethylene-diamine), 0.05% SDS (sodium dodecylsulphate) and 1 mg/ml ammonium peroxodisulphate, dissolved in TG or Pi buffer containing 1 mM MgSO_4 . Preferentially, the gels were left standing overnight. The electrode buffers were 0.05% SDS + 1 mM MgSO_4 plus either TG or Pi buffer respectively. The sample (50 μg chlorophyll per gel) was applied to the surface of the gel after addition of mannitol (15% w/v) and in some cases bromophenolblue was added as a marker. After a short period at a low current, electrophoresis in TG buffer was carried out for 40 min at 3 mA for each gel, and in Pi buffer for 4 hrs at 10 mA.

After removing the gels from the enveloping glass tubes, the green bands were cut out to yield slices about 2-4 mm thick. These were stored in air-tight plastic bottles in liquid nitrogen until use.

The molecular weight of chlorophyll-protein bands after electrophoresis was estimated by comparing their mobilities with those of the following denatured protein markers [13]; *E. coli* β -galactosidase (130 kD), bovine serum albumin (68 kD), ovalbumin (54 kD) and chymotrypsin (26 kD). The proteins were denatured as described by Weber et al. [13]. Before carrying out electrophoresis, β -galactosidase and ovalbumin were applied to one gel and chymotrypsin and bovine serum albumin (5 μ g of each) to a second one, together with some bromophenolblue. The protein bands were stained with Coomassie Brilliant Blue. The R_f -values (distance travelled by protein from starting point divided by distance travelled by marker from starting point) were measured and plotted vs log(mol. weight).

A straight line should be found [13], as was usually observed. The R_f -values of the chlorophyll-protein complexes could be obtained using the aforementioned calibration, yielding an approximate value of their molecular weight. For chlorophyll proteins as well as for marker proteins the occurrence of polymerisation was observed, in particular, but not only, for concentrated samples.

The R_f -values of the standard proteins were found to be almost identical in a number of experiments; therefore it was not necessary to repeat a molecular weight determination for each electrophoresis experiment, as long as the bands were at the expected positions on the gel.

2.4 ELECTRON SPIN RESONANCE

ESR experiments were performed on a Varian E6 spectrometer (X-band), equipped with a cold-nitrogen gas variable temperature unit, permitting measurements down to 100 K. Cooling to ~ 5 K was achieved by using a helium flow cryostat (modified type ESR-9; Oxford Instruments). The sample within the cavity could be illuminated with high intensity light filtered through a saturated CuSO_4 solution (12 cm) and a UV cut-off Schott GG395 filter from a 1000 W Xe lamp yielding an intensity at the sample of $\sim 10,000$ W/m². When desired, intensity was diminished by placing neutral density filters (Balzers, type nr. 03 FNG) in the exciting beam.

Measurements on chlorophyll-protein complexes were performed on 1 mm slices cut from gels, which were impregnated at 0°C in the dark

with 65% w/w sucrose water solution in order to reduce light-scattering. The ESR tube was filled with gel slices and the space not occupied by gel was filled with sucrose solution. Freezing was always fast by inserting the tube into liquid nitrogen outside the cavity to avoid cracking of the sample. Finally the sample was placed in the precooled flow cyrostat.

0.5-20 mW of microwave power was applied at 100 K and 20-40 mW at 5 K. 100 kHz modulation amplitude was 1 Gauss, ESR time constant 0.3-1.0 sec.

ESR experiments with whole algal cells were performed in mainly the same way. The cells were suspended in the ESR tube in a mixture (2:1) of ethyleneglycol and water. A notified harmful effect of ethyleneglycol on the cells at room temperature could be diminished (although not completely prevented) by handling and freezing samples as quickly as possible, reducing the contact time of algae and ethyleneglycol at room temperature to a minimum. Glycerol is likely to have the same effects as ethyleneglycol. Probably it would have been better to suspend the algae in sucrose water mixture, as described for the Chl-protein complexes.

2.5 ABSORPTION DIFFERENCE SPECTROSCOPY

Absorption difference spectroscopy was applied to determine the P700 content of the CP-I complexes obtained by PAGE. In addition, from the kinetics of the P700 signals it could be deduced which fraction of the acceptors of P700 in the complexes were still functioning.

a. Absorption difference spectroscopy of chemically oxidised minus reduced P700 at room temperature

Slices cut from the electrophoresis gels were ground in a mortar with carborundum powder. This grinding was done either on ice or in a cold room. The sludge was centrifuged for 5 min. The supernatant, with $A_{675} \approx 0.1$, was split in two parts and the difference in the wavelength region 650 to 740 nm was run in a double beam spectrophotometer. The absorbance difference between the two samples may be maximally 3% of the A_{675} value. 0.5 mM ferricyanide (FeCy) was added to one of the samples and 2 mM ascorbate to the other. The

cuvette with FeCy was pre-illuminated for a short period to oxidise P700 and subsequently the difference spectrum of the two samples was recorded. The P700/Chl-a ratio could be evaluated from the peak height ratio at 700 nm and 675 nm in the difference spectrum.

b. Light minus dark absorption difference spectroscopy at room temperature

The gels were put in a 2 mm pathlength cuvette in an Aminco spectrophotometer (Aminco-Chance duochromator), equipped with a side illumination attachment. The sample was illuminated with an actinic beam from a tungsten lamp via Schott BG12 and BG18 filters. The photomultiplier was shielded from scattered light with a RG665 filter. The change of transmission of the gels, incubated with 0.5 mM MV and 5 mM ascorbate was measured at different wavelengths. The re-reduction of P700⁺ after switching off the light was rather slow and could be easily distinguished from rapid transients originating from Chl fluorescence.

c. Light minus dark absorption difference spectroscopy at 77K

Very thin gel slices, pre-incubated for at least 1 hr at 0°C in a saturated sucrose solution (66% w/w), were put in a 2 mm pathlength cuvette and dark adapted for 10 min. The contents of the cuvette were frozen by immersion in liquid nitrogen outside the spectrophotometer to diminish cracking of the sample which occurs to a much greater extent upon slow cooling. Subsequently the frozen sample was put into the pre-cooled sample holder of a spectrophotometer which is described in detail in [14] and [15].

In this apparatus the measuring beam passed alternately (2000 Hz) through an interference filter at the measuring wavelength (Balzers B40) and through an 800 nm interference filter (Balzers B40) and the difference of transmitted energy was registered. The actinic beam was from a tungsten source, filtered through a 675 nm interference filter (Balzers B40). The photomultiplier was shielded from the actinic beam by using a chopper rotation at the same frequency as of the alternating measuring beam, in such a way, that the photomultiplier was only open when the sample was illuminated with measuring light. Also in this case the sample was impregnated in sucrose solution, forming a low temperature glass.

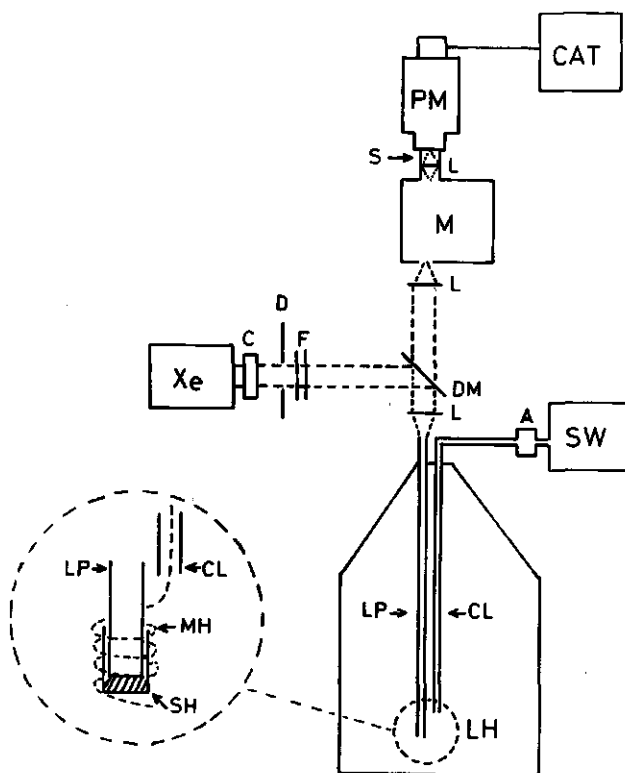


Figure 2.1 Schematic diagram of ODMR spectrometer (for details see text). LH: liquid helium container; LP: light pipe; CL: coaxial line; MH: microwave helix; SH: sample holder; Xe: Xenon lamp; C: CuSO_4 filter; D: diaphragm; F: optical glass filters; DM: dichroic mirror; L: lenses; M: monochromator; S: light shield and lens holder; PM: photomultiplier; CAT: computer for averaging of transients; A: microwave amplifier; SW: swept microwave source.

2.6 OPTICALLY DETECTED MAGNETIC RESONANCE

For ODMR experiments a modified version of the spectrometer described by van der Bent et al. [16] was used (see Fig. 2.1). For optical excitation a 900 Watt Xenon lamp (Osram) was employed with a saturated CuSO_4 solution filter in series with Schott BG12 and

GG395 filters. This gave a light beam with a half maximum bandwidth between 370 and 465 nm (see Fig. 2.2). The light was reflected by a dichroic mirror (Schott type 312) and focussed into a quartz light guide (1 m, 5 mm \varnothing , Suprasil, Schott). A sample was put into a PTFE cuvette with a height of 15 mm, inner diameter 5 mm, and wall-thickness 0.25 mm, snugly fitting around the lower end of the quartz light guide.

This construction resulted in a light flux of about 4000 W/m^2 at the surface of the sample. When a lower intensity was desired, neutral density filters were placed in the exciting beam.

Alternatively an Ar laser (Coherent Radiation CR 3) was used as an excitation-source. For broad-band excitation a monochromator (0.25 m Spex minimate) was put into the exciting beam if desired.

For kinetic measurements a mechanical chopper was put into the exciting beam (maximum chopping frequency 3200 Hz).

The quartz rod together with the sample was inserted into a cryostat, containing liquid helium, liquid nitrogen or another cooling fluid. Fluorescence emitted by the sample passed through the quartz rod and the dichroic mirror and was focussed into an EMI-9659 QB with extended S20 spectral sensitivity or a RCA C31034A (GaAs cathode) photomultiplier via a monochromator or an interference filter. The RCA C31034A tube is about 10 times more sensitive in the region of the measurements, but the opening is much smaller, so care was

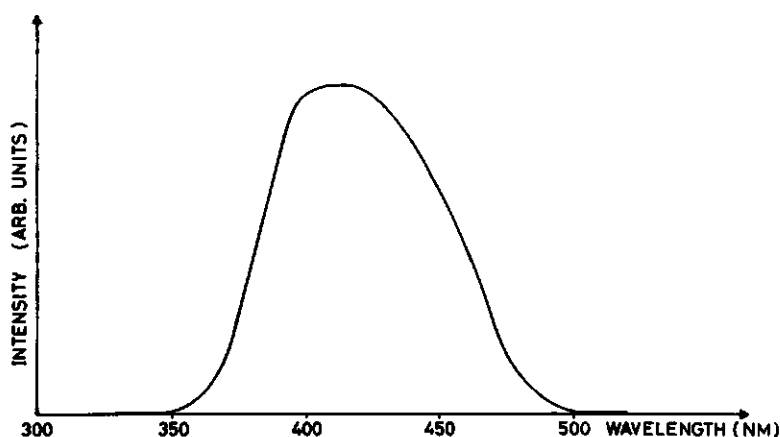


Figure 2.2 Intensity profile of the excitation light beam used in ODMR experiments and low temperature fluorescence measurements, measured at the place of the sample in the set-up of Fig. 2.1. Filters used Schott GG395 and BG12 (3 mm thick).

taken for proper focussing of fluorescence light.

With this spectrometer also fluorescence and excitation spectra at low temperature were recorded.

Microwave power from a Hewlett-Packard 8620 C/86220 A sweep generator, equipped with an Avantek UA-405 microwave amplifier (max. output 100 mW), was applied to the sample via a RG-213/U Amphenol cable and a coaxial line of stainless steel tubes with the following dimensions: inner tube with an outer diameter of 3 mm and wall thickness of 0.5 mm, outer tube with an outer diameter of 8 mm and a wall thickness of 0.25 mm, ending in a four-turn wave helix of copper wire (1 mm \varnothing) wound in a helix of 5.7 mm inner \varnothing , surrounding the sample. Microwave power at the sample was measured to be 40 mW, using a single loop of 1 mm \varnothing copper wire connected to a 423 A(neg) HP detector crystal. Sweep range was typically 10-1300 MHz, swept in 1 sec. Care had to be taken, that the resonance lines were traversed in a time which should be longer than the longest of lifetimes of the triplet sublevels in order to avoid asymmetric distortion and displacement of the resonance lineshape. In our ODMR experiments, the resonances (fwhm 40 MHz) were traversed in $\frac{40}{1300}$ sec \approx 30 msec, which is longer than the longest lifetime of Chl-a in vivo of about 5 msec (see § 4.3.2). Under our conditions a symmetrical lineshape was always observed. Moreover, it was checked by sweeping at a lower rate that no displacement of the resonance position occurred as a result of a too high a sweep rate.

Signals were fed into a PAR C4203 signal averager. A simple RC-filter was used for signal to noise improvement. The experimental RC-time was adapted to the required time-resolution.

For precise frequency determination of the top of the resonance profile a Systron Donner 1017 frequency counter was used. To determine the resonance-frequency we used the following procedure: a relatively narrow frequency sweep was made across the ODMR transition with precisely known start and stop frequencies on either side of the resonance profile. The sweep was made both in forward and reverse direction through the ODMR transition, because the position of the resonance maximum may be shifted in the direction of the sweep (see Fig. 2.3 A and B). Subsequently, the same range was swept with microwave power output only at a marker frequency ν_M adjusted to the estimated center of the ODMR transition (trace C in

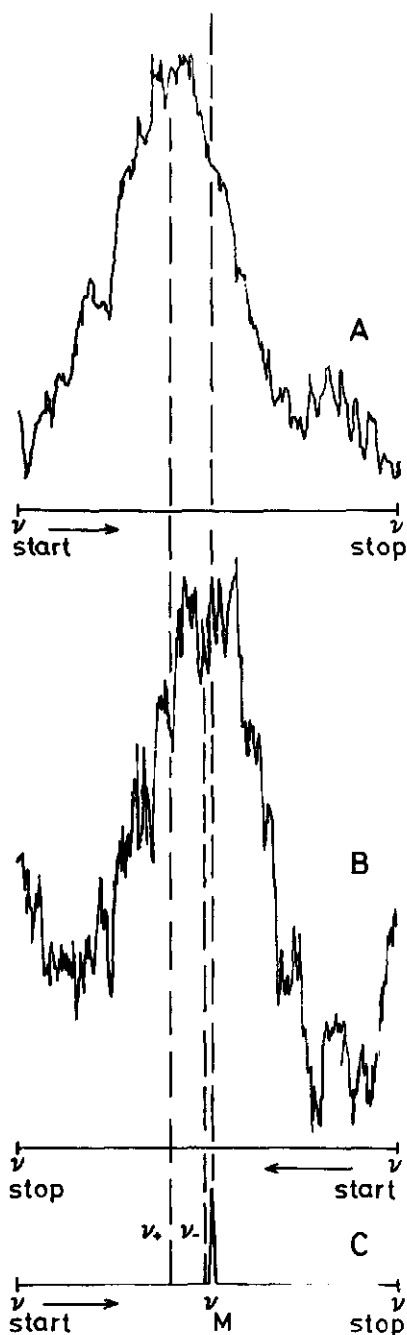


Figure 2.3 Illustration of the method applied for accurate frequency calibration of ODMR resonance spectra.

- A. ODMR resonance profile scanned in forward direction.
- B. ODMR resonance profile scanned in reversed direction. Scanning direction is indicated by arrows.
- C. marker; frequency determined by frequency counter.

Fig. 2.3). This frequency was first estimated on the screen of the CAT from the position of the maximum of the ODMR transition and precisely determined by using the frequency counter. The position of the top of the ODMR transition was subsequently determined with reference to this fixed frequency and using the scale calibration as shown in figs 2.3 A and B. The average frequency of both the forward and reverse swept spectra (ν_+ and ν_-) was taken to be the frequency of the ODMR transition. The accuracy obtained in this way was ± 5 MHz, limited by the S/N ratio of the signals.

Microwave power was amplitude-modulated with 15 V square wave pulses from a function generator (Farnell). Frequency modulation was achieved by a Wavetek 185 sweep generator; FM width was 350 kHz at 100 kHz carrier frequency.

For ODMR experiments whole cells of algae were taken from the culture, centrifuged (5 min, 3000 g) and the pellet was resuspended in as little as possible of growth medium (final Chl-a conc. $\sim 0.5 - 1$ mg/ml⁻¹). Any additives were added at this moment and left in contact with the algae to incubate for the time required for the specific chemical.

Resuspension of pelleted algae in glycerol or ethyleneglycol-water mixture was found to affect the fluorescence spectra of the algae, so most experiments were performed in the growth medium. Gel slices were used as such.

2.7 REFERENCES

1. J.P. Markwell, J.P. Thornber and M.P. Skrdla (1980). *Biochim. Biophys. Acta* 591: 391-399.
2. B. Lagoutte, P. Setif and J. Duranton (1980). *Photosynthesis Res.* 1: 3-16.
3. J.P. Thornber (1975). *Ann. Rev. Plant Physiol.* 26: 127-158.
4. J.P. Thornber, J.P. Markwell and S. Reinman (1979). *Photochem. Photobiol.* 29: 1205-1216.
5. W.A. Kratz and J. Myers (1955). *Am. J. Bot.* 42: 282-287.
6. D.I. Arnon (1938). *Am. J. Bot.* 25: 322-325.
7. J.J.S. van Rensen (1971). *Meded. Landbouwhogeschool Wageningen* 71-9: 1-80.
8. E. Kessler, W. Arthur and J.E. Brugger (1957). *Arch. Biochem.* 71: 326-335.

9. H. Senger and N.I. Bishop (1972). *Plant Cell Physiol.* 13: 633-649.
10. E.C. Wassink and G.H.M. Kronenberg (1962). *Nature* 194: 553-554.
11. T. Ogawa, L.P. Vernon and H.Y. Yamamoto (1970). *Biochim.Biophys.Acta* 547: 188-197.
12. G. McKinney (1941). *J.Biol.Chem.* 140: 315-322.
13. K. Weber, J.R. Pringle and M. Osborn (1972). in: *Methods in Enzymology*, Vol. XXVI: 3-27. Eds. C.H.W. Hirs and S.N. Timasheff, (1972), Academic Press, New York.
14. R.E. Kendrick and C.J.P. Spruit (1973). *Photochem.Photobiol.* 18: 139-144.
15. C.J.P. Spruit (1971). *Meded.Landbouwhogeschool Wageningen* 71-21: 1-6.
16. S.J. van der Bent, P.A. de Jager and T.J. Schaafsma (1976). *Rev.Sci.Instr.* 47: 117-121.

3 THEORY OF ODMR

3.1 INTRODUCTION

This chapter is meant to present a non-exhaustive overview of theoretical aspects, relevant to our ODMR experiments. We limit ourselves to two subjects: amplitude and shape of signals (§3.2) and the sign of ODMR signals (§3.3).

For the amplitude of ODMR signals a simple expression is derived, containing constants readily accessible for experiments. The mechanism of sign reversal of ODMR signals, observed for the triplet state of Chl-a in whole algal cells, and in chlorophyll-protein complexes, has so far received little attention and turns out to be useful to explain the results of our experiments.

3.2 AMPLITUDE AND SHAPE OF ODMR SIGNALS

3.2.1 Amplitude

The purpose of this paragraph is to express the amplitude of ODMR signals in relation to triplet sublevel populations and rate constants of the processes involved. In continuation of previous work [1-4], we derive a simple expression containing constants readily accessible for experiment; its validity can be checked by comparing experimental results with their predicted values.

The first question we would like to answer is: how many molecules are excited into their triplet state per unit of time, under our experimental conditions? In Fig. 3.1 a simple diagram is presented of the three lowest electronic states (Fig. 3.1A) and triplet sublevels (Fig. 3.1B) involved in an ODMR experiment. S_0 , S_1 and T_0 stand for ground state, first excited singlet and lowest excited triplet state, respectively; k_{ex} is the rate constant for optical excitation from S_0 and contains the excitation light intensity, k_f and k_d are the radiative and radiationless decay rate constants of S_1 to S_0 decay, k_{isc} represents the rate constant of intersystem

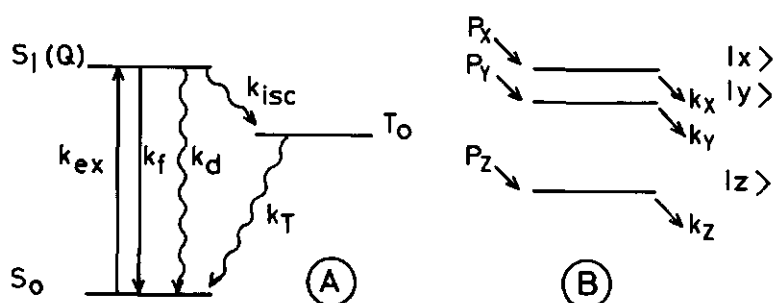


Figure 3.1 Level diagram of lowest electronic states (A) and spin sublevels of T_0 (B) involved in ODMR experiment. Symbols are defined in the text.

In Fig. 3.1A wavy arrows indicate radiationless processes, fully drawn arrows radiative processes.

crossing (ISC) $S_1 \rightarrow T_0$ and k_T is the mean rate constant of $T_0 \rightarrow S_0$ decay. All k 's are expressed in s^{-1} . For dilute solutions k_{ex} can be determined in the following way, provided Beer's law is valid: Following the treatment in [5], for a given excitation light intensity I_0 (in number of photons $\cdot cm^{-2} \cdot s^{-1}$), the number of absorbed photons (in $cm^{-3} \cdot s^{-1}$) I_A is given by

$$I_A = 2300 \cdot \epsilon \cdot c \cdot I_0 \quad (3.1)$$

where the concentration of solute molecules absorbing in the wavelength region of interest is expressed in $mol \cdot l^{-1}$, and the extinction coefficient ϵ is expressed in $l \cdot mol^{-1} \cdot cm^{-1}$.

The rate constant k_{ex} is related to I_A by

$$I_A = k_{ex} [S_0] \quad (3.2)$$

in order to arrive at kinetic equations (3.4a-c) containing first order rate constants only. When $[S_0]$ is expressed in number of molecules $\cdot l^{-1}$, combination of (3.1) and (3.2) yields

$$k_{\text{ex}} = \frac{2300}{N_{\text{AV}}} \varepsilon \cdot I_0 \quad (3.3)$$

N_{AV} is Avogadro's number.

For Chl-a in vitro, $\varepsilon \approx 1.2 \cdot 10^5 \text{ l} \cdot \text{mol}^{-1} \cdot \text{cm}^{-1}$ (solvent: ether) [6]. For our experiments, I_0 was experimentally determined to be $(4 \pm 1) \times 10^{17} \text{ photons} \cdot \text{cm}^{-2} \cdot \text{s}^{-1}$. I_0 should represent the integrated intensity over the excitation profile. Actually we have used the effective average wavelength of the excitation profile (see Fig. 2.2), yielding

$$k_{\text{ex}} \approx 250 \text{ s}^{-1}$$

This figure represents an upper limit, however, for our experiments, since the samples which have been studied do not obey Beer's law, as they contain particles with high local pigment concentration. In addition, there is considerable scattering of excitation-light for samples, consisting of frozen gels or aqueous suspensions of algae. The rate of excitation is $\sim 250 \text{ s}^{-1}$ only for chlorophyll molecules at the surface of the interface of the sample and the lightpipe.

Now we have determined the rate constant for optical excitation, the next question to be answered is: How is the fluorescence intensity related to the triplet population and kinetic constants under our experimental conditions?

Again referring to Fig. 3.1A, the intersystem crossing process $S_1 \rightarrow T_0$ is completely radiationless. Generally k_T contains a radiative and a radiationless part. For chlorophylls and other photosynthetic pigments, however, k_T is almost exclusively radiationless, because the phosphorescence yield is known to be low (quantum yield $\approx 5 \times 10^{-5}$) [7,8,9] and can be neglected for our purposes.

In Fig. 3.1B the population rate for a molecule to enter triplet sublevel $|i\rangle$ ($i = x, y, z$) after excitation to S_1 and subsequent ISC to T_0 , is called P_i , expressed in $\text{mol} \cdot \text{l}^{-1} \cdot \text{s}^{-1}$ as follows from (3.5). The decay rate constants of the individual sublevels are denoted by k_i (in s^{-1}).

In the experiments described in this thesis the optical pumping cycle includes the group of excited singlet states associated with the Soret absorption band. This group of states, subsequently de-

noted by B-states, consists of no less than ten different electronic states (see § 1.4). The Q-states, associated with the long wavelength absorption band, consist of two excited singlet states [10]. For reasons of simplicity this detour is omitted in the kinetic model, in accordance with the treatment in [2]. After excitation into B-states, decay occurs to Q-states by internal conversion and vibrational relaxation with a rate constant k_{ic} , which is in the order of 10^{11} s^{-1} [11]. It is assumed that this process dominates ISC from B-states to higher excited triplet levels. For a more detailed description of the electronic states of chlorophyll we refer to § 1.4. As a result of rapid radiationless deactivation the B-states have a low steady state population. Because the time resolution of our experiments is $\approx 0.1 \text{ ms}$, it is permissible to assume that any change in excitation rate to B-states instantaneously results in an identical change in population rate to S_1 , the lowest Q-state, and therefore excitation to B-states can be regarded as equivalent to excitation to S_1 .

The time dependence of the population of the states S_0 , S_1 and T_0 are governed by a set of differential equations, as outlined by [1, 2, 12, 13]:

$$\frac{d[S_0]}{dt} = -k_{ex}[S_0] + (k_f + k_d)[S_1] + k_T[T_0] \quad (3.4a)$$

$$\frac{d[S_1]}{dt} = k_{ex}[S_0] - (k_f + k_d)[S_1] - k_{isc}[S_1] \quad (3.4b)$$

$$\frac{d[T_0]}{dt} = k_{isc}[S_1] - k_T[T_0] \quad (3.4c)$$

where the concentration of molecules in the denoted electronic states is expressed in $\text{mol} \cdot \text{l}^{-1}$.

With reference to Fig. 3.1 a total population rate P of the triplet state T_0 can be defined as

$$P = k_{isc}[S_1] \quad (3.5)$$

and accordingly for an individual sublevel $|i\rangle$

$$P_i = k_{isc}^{(i)} [S_1] \quad (3.5a)$$

Evidently,

$$P = \sum_i P_i \quad (3.6)$$

For later use we also define relative populating rates p_i as

$$p_i = \frac{P_i}{P} \quad (3.7)$$

where $\sum_i p_i = 1$ and $0 \leq p_i \leq 1$.

From (3.4b) it can be seen that in a steady state situation, when $d[S_1]/dt = 0$

$$P = \frac{k_{isc} k_{ex} [S_0]}{k_f + k_d + k_{isc}} \quad (3.8)$$

and using (3.2)

$$P = \frac{k_{isc}}{k_f + k_d + k_{isc}} \cdot I_A \quad (3.9)$$

For an individual sublevel

$$P_i = \frac{k_{isc}^{(i)}}{k_f + k_d + k_{isc}^{(i)}} \cdot I_A \quad (3.10)$$

which shows that the population rate of a triplet sublevel is proportional to the absorption rate of the optical pumping cycle.

In addition, the following relation holds

$$[S_0] + [S_1] + [T_0] = [N] \quad (3.11)$$

where $[N]$ is the chlorophyll concentration in $\text{mol} \cdot \text{l}^{-1}$. N is the maximum amount of molecules that can be subjected to the ODMR experiment.

From (3.4) and (3.11) it can be derived, that under steady state conditions the fluorescence intensity I_f is given by

$$I_f = \frac{k_{ex}k_f}{k_{ex} + k_{isc} + k_f + k_d} ([N] - [T_0]) \quad (3.12)$$

(cf. [14]). The excitation light intensity is weak enough that stimulated emission $S_n \rightarrow S_0$ can be neglected.

Under our experimental conditions I_f is found to be approximately 10^{-1} Einstein $\cdot l^{-1} \cdot s^{-1}$, using $k_{ex} \approx 250 s^{-1}$, as previously derived, $k_{isc} \approx 1.3 \cdot 10^8 s^{-1}$ (for spinach chloroplasts [15]), $k_f \approx k_d \approx 10^9 s^{-1}$ [16], and the relative triplet population is known to be less than 5% (§ 3.4). The concentration of molecules $[N]$ is $\approx 10^{-3}$ M (§ 2.6).

Eqn (3.12) represents the sought relation between the fluorescence intensity, the triplet population, and the relevant kinetic constants. In order to make use of this equation, it is necessary to define the limits of its applicability and to establish its relation with fluorescence fading experiments, as reported in § 4.3.

It can be shown that the steady state population of S_1 will always be low under our experimental conditions. From (3.4b) it follows that

$$\frac{[S_1]}{[S_0]} = \frac{k_{ex}}{k_{isc} + k_f + k_d} \quad (3.13)$$

and using the same values as in (3.12) for the rate constants, $[S_1]/[S_0]$ is approximately $\approx 10^{-7}$, i.e. the concentration of molecules in S_1 can be neglected with respect to the population of S_0 , or with respect to the population of T_0 . This is clear from

$$\frac{[T_0]}{[S_0]} = \frac{k_{isc}k_{ex}}{(k_{isc} + k_f + k_d)k_T} \quad (3.14)$$

which equals $\sim 10^{-2}$, again using the same values as in (3.12). It is assumed that $k_T \approx 10^3 s^{-1}$, based on the experimental results described in § 3.4.

Several conclusions can be drawn from (3.14). The limits of applicability are imposed by k_{ex} , which can be varied for each experiment, resulting in a change of the $[T_0]/[S_0]$ ratio. The triplet population is only linearly dependent on k_{ex} , when $[T_0] \ll [S_0]$. This follows from the relationship $[S_0] = [N] - [T_0] - [S_1]$, to be sub-

stituted as denominator in the left-hand side of (3.14), where $[N]$ is constant and $[S_1]$ always remains a small quantity. Under the circumstances of our experiments $[T_0]$ can be neglected with respect to $[S_0]$. Thus $[T_0]/[S_0] \approx [T_0]/[N]$, and $[T_0]$ becomes linearly dependent on k_{ex} . The value of 10^{-2} for $[T_0]/[S_0]$ must be regarded as representative for the conditions of our experiments. This estimate is a reasonable one, as can be seen by comparison with the results of the experiments of fluorescence fading (§4.3), where the relative amount of triplets is determined.

The relationship (3.14) can also be written as

$$\frac{[T_0]}{[S_0]} = \frac{k_{ex}k_{isc}}{(k_{isc} + k_f + k_d)k_T} = \frac{k_{ex}}{k_T} \phi_T \quad (3.15)$$

where ϕ_T is the triplet yield defined as

$$\phi_T = \frac{\text{number of absorbed photons leading to triplets}}{\text{number of absorbed photons}}$$

as usual (see e.g. [5]). From fluorescence fading experiments (§4.3), it is found that $[T_0]/[S_0] \approx 2 \times 10^{-2}$. Using $k_{ex} \sim 250 \text{ s}^{-1}$, $k_T \sim 10^3 \text{ s}^{-1}$ results in

$$\phi_T \gtrsim 0.1$$

This value is substantially lower than those reported in the literature [17]. Our ϕ_T represents a lower limit, since the value of $k_{ex} = 250 \text{ s}^{-1}$ only applies to those molecules which are at the interface between the light-pipe and the sample, due to scattering of excitation light by the sample. Molecules located deeper in the sample have a lower value of k_{ex} . In addition ϕ_f (the fluorescence yield), and thus ϕ_T , strongly depend on temperature: ϕ_f has been found to increase at decreasing temperature, *in vitro* [17-19] as well as *in vivo* [20-22]. This phenomenon has been rationalized by invoking an excited triplet state very close to S_1 , serving as an efficient pathway for ISC at relatively high temperature [18,19,23]. At 4.2 K this pathway may well become much less efficient, resulting in a lower value of ϕ_T (see also § 1.4). Our measurements only allow a reliable value of ϕ_T , under our conditions, i.e. at low temperature, etc.

We are now in a position to discuss expressions relating the amplitude of the ODMR signals with changes in the triplet population, and/or kinetic constants.

In an ODMR experiment the fluorescence intensity is changed by applying microwaves resonant with the frequency difference between one or more pairs of triplet sublevels $|i\rangle$ (Fig. 3.1B). The change of fluorescence ΔI_f is easily derived from (3.12) and is given by

$$\Delta I_f = \frac{-k_{ex}k_f}{k_{ex} + k_{isc} + k_f + k_d} \Delta[T_0] \quad (3.16)$$

Several expressions for ΔI_f have appeared already in the literature. It is helpful to compare some of these expressions with (3.16).

Avarmaa et al. [4] have derived an expression relating the relative change of fluorescence, δI_f , with the relative change in the triplet population

$$\delta I_f = \frac{\Delta I_f}{I_f} = \gamma \frac{[\Delta T_0]}{[T_0]} \quad (3.17)$$

where γ is a dimensionless parameter.

It is shown that

$$\gamma = - \frac{[T_0]}{[S_0]} \quad (3.18)$$

where γ can also be expressed in kinetic constants by eqn (3.14). For $\gamma \ll 1$ - 'weak excitation' limit - γ is a measure of the relative amount of triplets $[T_0]/[N]$.

On the other hand Van der Bent et al. [24] used the following approach: For every triplet sublevel $|i\rangle$ a rate equation can be formulated:

$$\frac{d[N_i]}{dt} = -k_i[N_i] + P_i \quad (3.19)$$

where $[N_i]$ represents the concentration of molecules in sublevel $|i\rangle$, and

$$\sum_i [N_i] = [T_0] \quad (3.20)$$

Solving (3.19) under steady state conditions, $d[N_i]/dt = 0$ for all i , yields steady state populations $[N_i^0]$ of triplet sublevels

$$[N_i^0] = \frac{P_i}{k_i} \quad (3.21)$$

Now it can be derived that under continuous illumination and irradiation with resonant microwaves connecting a pair of sublevels $|i\rangle$ and $|j\rangle$ the change of fluorescence will be

$$\Delta I_f = -A(k_i - k_j)(k_i + k_j)^{-1}([N_i^0] - [N_j^0]) \quad (3.22)$$

where A is an experimental constant. Using (3.17) A can be identified as

$$A = \gamma \frac{I_f}{[T_0]} \quad (3.23)$$

Eqn (3.17) makes it possible to estimate $\Delta[T_0]/[T_0]$, since δI_f follows from the experiments of §4.2 to be about 1% for $|x\rangle \rightarrow |z\rangle$ and $|y\rangle \rightarrow |z\rangle$ ODMR transitions, and γ can be determined from fluorescence fading experiments (§4.3) to be $(2-3) \times 10^{-2}$. This shows that $\Delta[T_0]/[T_0]$ will be about 0.03 - 0.05, a not unreasonable value in view of the relative populations of the different sublevels observed for Chl-a *in vivo* in algae (see §5.2) and *in vitro* [25], as well as for bacteriochlorophyll in photosynthetic bacteria [26]. γ will always be small in the 'weak excitation limit', and consequently a small relative change of the fluorescence intensity will correspond with a large relative change in triplet population.

From (3.22) it can be seen that there are two possible reasons for not observing an ODMR transition between two triplet sublevels. Firstly the populations of both sublevels may be equal, and secondly the decay rate constants may be equal. These cases can be interrelated in view of (3.21), because the steady state populations contain populating rates as well as decay rate constants. These two may be related, as discussed in § 1.4, because they contain similar

matrix elements.

From (3.22) it follows that the intensity of ODMR signals cannot be simply related to the total triplet population, i.e.

$$\Delta I_f = -A(k_i - k_j)(k_i + k_j)^{-1} \left\{ \frac{P_i}{k_i} - \frac{P_j}{k_j} \right\} \quad (3.24)$$

which cannot be written as a simple function of $[T_0]$, unless further assumptions, e.g. about the behaviour of P_i and k_i relative to each other, are made.

3.2.2 The shape of ODMR resonance transitions

The shape of ODMR resonance lines for algae and chlorophyll-protein complexes from algae is found to be Gaussian. This is demonstrated in Fig. 3.2 for the ODMR lineshape of the D+E transition of a CP-I complex isolated from *Anacystis nidulans*. This is in agreement with the observation of a Gaussian ODMR lineshape for reaction centers of photosynthetic bacteria [27].

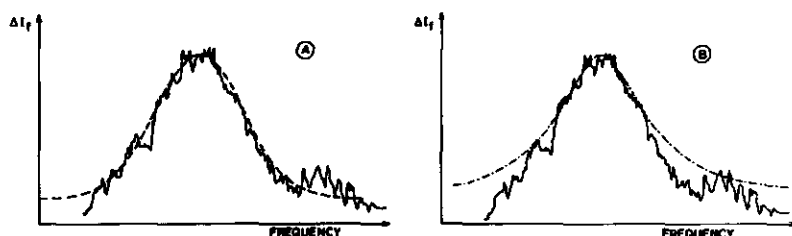


Figure 3.2 Comparison of a D+E resonance line of a chlorophyll-protein complex CP-I from *Anacystis nidulans* with a Gauss curve (A) and a Lorentz curve (B) (scanning rate 150 MHz/s, time constant 10 ms, microwave power 40 mW).

The good fit in A is typical also for the other resonances in this chlorophyll-protein complex, as well as for resonances found in whole cells.

The area under a Gaussian spectrum is given by [28]

$$A = 1.0643 y_m \Delta \nu_{1/2} \quad (3.25)$$

with y_m the amplitude of the resonance line and $\Delta\nu_{1/2}$ the fwhm value of the ODMR transition. Thus the intensity of ODMR transitions can only be compared by their amplitudes when the linewidths are identical.

Finally it is noted that the ODMR transitions are inhomogeneously broadened. From the fact that $\Delta\nu_{1/2} \approx 10^7 \text{ s}^{-1}$ and noting that the lifetime of the triplet state is $\sim 10^{-3} \text{ s}$, which would give rise to a lifetime broadening of 10^3 Hz , we can conclude that homogeneous broadening is not the dominant broadening mechanism. This is consistent with the observation of a Gaussian ODMR lineshape. The Gaussian lineshape also excludes the occurrence of fast exchange between different sites.

3.3 THE SIGN OF ODMR SIGNALS

3.3.1 Introduction

In whole algal cells the triplet state of Chl-a can be detected by monitoring the fluorescence band at $\sim 715 \text{ nm}$. This triplet state has almost exactly the same ZFS-values as the triplet state of Chl-a *in vitro*. The striking difference between both is that in algal cells the triplet is detected by an increase of fluorescence intensity upon microwave saturation (§3.2), while in Chl-a *in vitro* the triplet is detected as a decrease.

This result is underlined by the measurements on chlorophyll-proteins, where most of the chlorophyll is still in its native environment, yielding positive ODMR signals, reflecting an increase of fluorescence, whereas also some chlorophyll - as judged from the low temperature fluorescence spectrum - is present, which has lost its original surrounding, yielding negative triplet signals, just as Chl-a *in vitro* (see Fig. 1, §3.4).

This paragraph discusses the mechanisms that can give rise to this sign reversal of ODMR signals.

In general the sign of ODMR signals is related to the change of the total triplet population, due to microwave irradiation, by

$$\Delta I_f \sim - \Delta[T_0] \quad (3.26)$$

where ΔI_f is the change of fluorescence intensity and $\Delta[T_0]$ the change in total triplet population.

Note the minus sign: an increase of triplet population implies a decrease of the population of the ground state, yielding an immediate decrease of fluorescence at the time scale of our experiments.

Four mechanisms can be conceived to be responsible for the sign reversal of the ODMR signals *in vivo* with respect to those *in vitro*:

- 1) radical pair mechanism
- 2) site effects
- 3) energy transfer
- 4) spin-lattice relaxation.

§3.3.2 discusses the radical pair mechanism (RPM). The effect of energy transfer is discussed in §3.3.4, and in addition the possible influence of site effects, through a change of sublevel kinetics. The theoretical framework on ISC, developed in §1.5, is used in §3.3.3 to predict the effects of hydrogen-bonding to ring V oxygen atoms of Chl-a, on sublevel kinetics and the sign of the ODMR signal.

The effect of spin-lattice relaxation is discussed in §3.3.4.

3.3.2 The radical pair mechanism

As mentioned in §1.3.1, the triplet state of reaction centres of photosynthetic bacteria (P870) [26,29-31] and of plants [31-33], as measured by ESR, exhibits an unusual spin polarization pattern, that cannot arise from spin-orbit coupling in a single molecule [8], but can be nicely explained by invoking a radical pair mechanism (RPM).

The principles of this mechanism have been explained by several authors [26,31].

The first step in this RPM, immediately following optical excitation, is the formation of a radical pair, as occurs in photosynthetic systems by the charge separation in reaction centres.

When the two radicals of the pair are far enough apart, the individual spins of the separated electron-hole pair precess independently with respect to the hyperfine tensor axis system of each radical, when no external field is applied, with a frequency, determined by the nuclear hyperfine tensorial elements. Because this frequency is different for both radicals, mixing of singlet with

triplet states in the radical pair occurs. In this way the spin state of the recombination product is determined by the difference in precession frequency of the spin of electron and hole in the radical pair and the time elapsed between separation and recombination.

When the external magnetic field is applied, the triplet state of the radical pair has three sublevels $|1\rangle$, $|0\rangle$, $|-1\rangle$, which can be expressed as linear combinations of the zero-field sublevels $|x\rangle$, $|y\rangle$ and $|z\rangle$.

Theoretically it can be shown - as is confirmed by experiments on the recombination product - that the $|0\rangle$ sublevel is preferentially populated with respect to the $|\pm 1\rangle$ sublevels in high external field [31].

In zero-field, however, it is not so easily seen, how the radical pair triplet sublevels are populated. We will not attempt to treat this case exhaustively, since our present purpose is only to show that sign reversal of ODMR triplet signals can occur by the RPM.

Therefore, we consider a situation, where charge separation proceeds from a donor D to an acceptor A, so that the pair $^1(D^+A^-)$ is created in a singlet state. We assume that there is no exchange interaction between the two radicals of the pair, but the $^1(D^+A^-)$ pair state is mixed with the triplet $^3(D^+A^-)$ state by an interaction of the electron spin on A^- with a foreign spin $S' = \frac{1}{2}$.

For such a situation the interaction of the unpaired electron spins $S^{(A)}$ on A^- with the foreign spin S' can be represented by the spin hamiltonian H' as

$$H' = S^{(A)} \cdot \underline{A} \cdot S' \quad (3.27)$$

where \underline{A} is a tensor, describing hyperfine and/or exchange interaction. The hyperfine interaction is assumed to be limited to one nuclear spin S' with $I = \frac{1}{2}$ on A^- ; the exchange interaction may occur between the unpaired electron on A^- and a third electronic spin $S^{(c)}$, e.g. on a second acceptor. *In vivo*, this could represent an unpaired spin on ubiquinone associated with iron.

After diagonalizing the H' matrix, starting with the basis set

$$\begin{aligned}\phi_1 &= \alpha\alpha\alpha_N; \phi_2 = \alpha\alpha\beta_N; \phi_3 = \alpha\beta\alpha_N; \phi_4 = \alpha\beta\beta_N \\ \phi_5 &= \beta\alpha\alpha_N; \phi_6 = \beta\alpha\beta_N; \phi_7 = \beta\beta\alpha_N; \phi_8 = \beta\beta\beta_N\end{aligned}\quad (3.28)$$

where the first two symbols α and β are those of the unpaired spins on D^+ and A^- , and α_N and β_N are the spin functions of S' , eigenfunctions are obtained which contain spinfunctions of all three triplet sublevels with equal weight [34], clearly giving rise to identical rates of triplet formation for all three triplet sublevels of the radical pair on a long time scale. When charge recombination: ${}^3(D^+A^-) \rightarrow ({}^3D)A$ occurs, we assume that the triplet spin orientation does not change, i.e. a radical pair in the $|x\rangle$ spin state is transformed into an $|x\rangle$ state of the recombined product. Since the $|x\rangle$, $|y\rangle$ and $|z\rangle$ spin states equally occur in the radical pair, the populating rates of the $|x\rangle$, $|y\rangle$ and $|z\rangle$ triplet sublevels of the recombination product $({}^3D)A$ are predicted to be identical, provided the elapsed time is long enough. Note that this result is obtained for A in (3.27) in a tensorial form, i.e. the hyperfine or exchange interaction may include anisotropic terms.

The decay of $({}^3D)A$ to the ground state still proceeds by spin-orbit coupling. This means that the $|z\rangle$ sublevel, which for chlorophylls has the smallest decay rate constant of the three, ends up with the largest steady state population, since $p_x = p_y = p_z$ and $n_i = p_i/k_i$ ($i = x, y, z$).

This situation gives rise to positive signals in the ODMR experiment. Upon irradiation with microwaves, population is transferred from the slowly decaying sublevel $|z\rangle$ to the faster decaying sublevels $|x\rangle$ and $|y\rangle$, resulting in a decrease of total triplet population and an increase of fluorescence intensity, according to (3.26).

In order to discuss our experimental results in algal cells, we must first note that under the circumstances of our experiments on PSI containing chlorophyll-protein complexes, isolated from algae, the reaction centres are predominantly irreversibly oxidized, resulting in D^+A , in terms of our previous example. This system cannot produce triplets. For the small reversibly oxidized component in these complexes charge recombination is too slow to allow detection of triplets at the reaction centre.

This fact does not completely exclude the RPM as a possible

cause for ODMR sign reversal. The observed triplets may be located in shallow traps in the antenna pigment surrounding the reaction centre. The occurrence of such traps becomes evident by cooling the sample to cryogenic temperature. In such traps radical pair formation and charge recombination may occur, yielding polarized triplets and positive ODMR.

In our view this possibility is not very likely, because the existence of donor-acceptor couples in antenna pigment has never been firmly established by experiments.

3.3.3 Site effects

Ligands are known to have several effects on the spectroscopic properties of chlorophylls [35-39].

For the following discussion, it is first necessary to make a distinction between nucleophilic ligation to the central metal ion, by pyridine, MTHF, ethanol, water, etc., and electrophilic ligation to side chains, in Chl-a primarily the oxygen atoms attached to ring V (O_1 , O_2 in Fig. 1.4), by hydrogen-bonding with ethanol, water, etc. In this paragraph we will only be concerned with the effect of hydrogen-bonding to the oxygen atoms O_1 and O_2 . As a result of the discussion of §1.5 it can now be said that hydrogen-bonding to these oxygen atoms has an appreciable effect on the triplet state kinetics, since these atoms play an important role in spin-orbit coupling.

Ligation to the central metal ion has effects on the optical spectra or on zero-field splitting parameters, but these effects arise from interaction with the π -electrons in low electronic states that do not contribute to the SOC, see Table 1.2. Any effects observed on the triplet state kinetics, upon ligation of Mg in chlorophylls, therefore, is ascribed to a change in the T_0 - S_0 energy separation, via the energy-gap law [40]. It is expected that a change in triplet state kinetics due to ligation of Mg is equal for all three triplet sublevels, since the energy-gap law can be related to spin-state independent Franck-Condon factors [41]. Therefore, ligation to Mg is not expected to result in ODMR sign reversal, since the steady-state populations of all three triplet sublevels change with the same relative amount, and their relative

ordering is not changed. Even the σ -electrons, shared between the metal ion and the four pyrrole nitrogen atoms, contribute only little to the SOC, because they are too high in energy [10] to be important.

Our present purpose is to show, that sign reversal of ODMR signals can occur as a result of ligation to side chains of Chl-a.

The amplitude and signs of ODMR signals are determined by the population differences between triplet sublevels, as explained in §3.2. Let us consider two arbitrarily chosen sublevels. If the faster decaying sublevel has the higher population, the sign of the ODMR transition is predicted to be negative, corresponding to a decrease of fluorescence intensity (see Fig. 3.3a), according to (3.26). Hydrogen-bonding to an oxygen atom attached to ring V, likely to occur *in vivo* [42-44], lowers the energies of the MO's in which the n -electrons of this oxygen atom participate. Thus, these orbitals contribute less to the first order HT terms in (1.9). The effect on the populating rates is predicted to be larger than on the decay rate constants, because of the difference in the energy denominator: for the populating process $E(S_1) - E(S_n)$, ($n \neq 1$), and for the decay $E(S_0) - E(S_n)$, ($n \neq 0$), the latter clearly being the largest of the two. A change in the energy of one or a few of the S_n will have the largest effect on $E(S_1) - E(S_n)$.

Since this difference is a first order effect for the $|x\rangle$ and $|y\rangle$ sublevels in Chl-a, and a second order effect for the $|z\rangle$ sublevel, the $|x\rangle$ and $|y\rangle$ sublevels are affected more, i.e. their populating rate will be lowered more than the populating rate of the $|z\rangle$ sublevel.

This results in a decrease of the population of $|x\rangle$ and $|y\rangle$ with respect to the population of $|z\rangle$, and may eventually result in a sign reversal of one or both of the ODMR transitions.

In Fig. 3.3 this effect is schematically shown in an order of decreasing $|x\rangle$ and $|y\rangle$ populating rates. It is believed to occur for Pheo-a [12,45] and for Chl-b [36] *in vitro*, and may also occur for Chl-a *in vivo*.

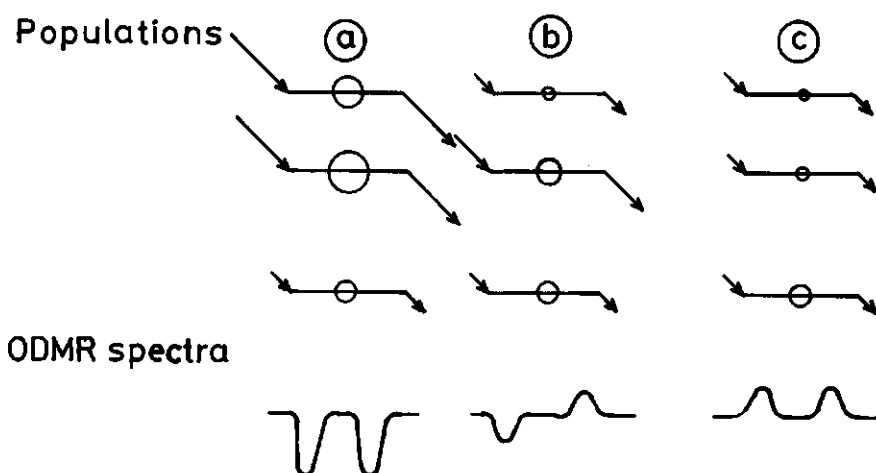


Figure 3.3 Effect of ligation of oxygen-containing side-groups of Chl-a on the sign of its ODMR transitions.

A schematic diagram for the effect of ligation at the side chains of Chl-a on the relative populations of triplet sublevels and the resulting ODMR spectra.

In the upper part of the figure the size of the circles represents the population of the triplet sublevels. The lower part represents the ODMR spectra that would result. The length of the arrows indicates the magnitude of populating rates and decay rate constants.

3.3.4 Fluorescence detected magnetic resonance (FDMR) of whole algae and the *Anacystis nidulans* CP-I complex

This paragraph consists of a paper, accepted for publication in the Israel Journal of Chemistry.

Its main purpose is to demonstrate, that both singlet energy transfer between antenna pigment chlorophyll and traps within this system, as well as ligation at oxygen containing side chains of Chl-a may give rise to sign reversal of ODMR signals. This paragraph does not provide a firm conclusion which of both mechanisms applies to the sign reversal observed in whole algae and chlorophyll-protein complexes, isolated from these algae.

Additional experimental results relevant to this problem are presented in §4.3.

FLUORESCENCE DETECTED MAGNETIC
RESONANCE (FDMR) OF WHOLE ALGAE
AND THE *ANACYSTIS NIDULANS* CP-I
COMPLEX

by

G.H. van Brakel, T.J. Schaafsma and
J.J.S. van Rensen

SUMMARY

Fluorescence-detected magnetic resonance (FDMR) spectra have been obtained at 4.2 K and at zero magnetic field of the photoexcited chlorophyll-a triplet state in blue-green and green algae, as well as in a Photosystem 1 chlorophyll-protein (CP-I) complex, isolated from the blue-green alga *Anacystis nidulans*. FDMR spectra of the CP-I complex recorded by monitoring the ~720 nm fluorescence emission, exhibit sign reversal with respect to FDMR resonances obtained at ~680 nm. This phenomenon can be attributed to the effects of singlet-singlet energy transfer to a chlorophyll trap in the P.S.-I antenna, or to different triplet state kinetics in both species. Remarkably narrow 2E resonances of <10 MHz width are reported for several types of algae.

ACKNOWLEDGEMENT

The authors are deeply indebted to Drs. W.J. Vredenberg and J.C. Wesseliuss for stimulating discussions and kind assistance for culturing algae. Mr. W.J. Vermaas has been of great help in carrying out the reported experiments. *Scenedesmus* C-6E algae were generously made available by Dr. H. Senger.

INTRODUCTION

Fluorescence-detected magnetic resonance (FDMR) [1] is an offspring of the recently developed optically detected magnetic resonance (ODMR) in zero magnetic field [2-4]. It is a convenient technique to study non-phosphorescent triplet states of photosynthetic pigments [1,5-11] and has been successfully applied to bacterial reaction centres [12-15], chloroplasts [16,17] and algae [18-20]. Recently, chlorophyll-a (Chl-a) FDMR signals have been observed in several Chl-a and Chl-a/b protein complexes isolated from barley [21,22] and in whole chloroplasts [23]. In these systems, photo-excited short-lived triplet states of chlorophylls may serve as natural spin-probes, which do not cause distortions of their native protein environment. Provided the triplet state properties of the chlorophyll probe are measured with sufficient accuracy and its location within the photosynthetic unit is unambiguously determined, FDMR of the pigment-probe can yield valuable information about the structure of its environment, proximity of other, interacting chlorophylls and those photosynthetic processes, in which chlorophyll is directly involved [17,29].

This paper focusses on the application of FDMR to the study of the photosynthetic apparatus of algae by making use of FDMR transitions in chlorophyll triplets, generated within this apparatus by illumination with visible light. These transitions are observed in whole cells of the blue-green alga *Anacystis nidulans*, as well as in a well-known chlorophyll-protein complex, denoted CP-I [24], isolated from these algae.

It is the purpose of this report to discuss and evaluate the various mechanisms which may cause sign-reversal of *in vivo* chlorophyll triplet FDMR-spectra with respect to those of chlorophyll *in vitro*. S-S ET has been invoked to explain sign-reversal of FDMR transitions in bacterial reaction centres with respect to those of *in vitro* bacterio chlorophyll [14].

The CP-I complex contains 40 chlorophyll-a (Chl-a) molecules, one P700 reaction centre, 1-2 β -carotenes, traces of xanthophylls,

quinones, galacto- and phospholipids, but no pheophytin-a or cytochromes [24]. All compounds are embedded in a 110 kD molecular weight protein.

By treatment with SDS, the ratio of Chl-a : P700 in these complexes is much lower than in intact algae, where it is ~500:1. In both cases Chl-a is part of a pigment antenna system, funneling excitation energy into the P700 reaction centre at a picosecond time-scale, and thus the energy-transfer properties of CP-I are of great importance to understand the primary steps of photosynthesis immediately after the system has absorbed a visible photon. The Chl-a triplets observed in this complex are very likely identical to those found in the parent alga, i.e. they are probably located in that part of the algae photosynthetic unit which is constituted by the CP-I complex.

The principles of fluorescence-detected magnetic resonance in zero magnetic field have been reviewed by several authors [2-4].

An electronic triplet state has three magnetic substates, denoted as spin states; in the absence of an external magnetic field, these three spin states denoted by $|x\rangle$, $|y\rangle$ and $|z\rangle$ have energies corresponding to the eigenvalues of the zero field spin Hamiltonian.

$$H = -(X\hat{S}_x^2 + Y\hat{S}_y^2 + Z\hat{S}_z^2) \quad (1)$$

\hat{S}_x , \hat{S}_y and \hat{S}_z are the spin operators such that the eigenvalue of $\hat{S}^2 = \hat{S}_x^2 + \hat{S}_y^2 + \hat{S}_z^2$ equals $S(S+1) = 2$ when expressed in units of \hbar^2 and $\hat{S}_i|i\rangle = 0$; x, y, z refer to a molecule-fixed axis system. Microwave induced transitions between spin states occur when microwaves with frequency ν satisfy the resonance condition

$$\Delta E = \frac{h\nu}{c} \quad (2)$$

where c is the velocity of light in $\text{cm} \cdot \text{sec}^{-1}$, ΔE is expressed in cm^{-1} and

$$\Delta E = |X-Y|, |Y-Z|, |X-Z| \quad (3)$$

Since changes induced by microwaves in the populations of spin states lead to small changes in the S_0 ground state population, due

to the different decay rate constants of the individual spin states, these changes in the populations of states can be monitored via the fluorescence intensity. The changes in the fluorescence intensity are in general small (typically $\sim 1-0.1\%$) but detectable due to the high sensitivity of light detectors. For the detailed influence of the microwave irradiation on the fluorescence intensity we refer to previous papers [6,25].

Since the sum of the energies $X+Y+Z$ equals zero, it is convenient to use the zero-field splitting parameters D and E defined by

$$D \equiv \frac{1}{2}(X+Y) - Z = -3/2 Z \quad (4a)$$

$$E \equiv \frac{1}{2}(X-Y) \quad (4b)$$

Then microwave transitions occur at energies $2E$, $D-E$ and $D+E$, corresponding to the transitions between states $|x\rangle \leftrightarrow |y\rangle$, $|y\rangle \leftrightarrow |z\rangle$, and $|x\rangle \leftrightarrow |z\rangle$, respectively.

At sufficient amplitude, resonant microwave radiation, connecting spin states $|i\rangle$ and $|j\rangle$, equalizes their populations. The resulting change in fluorescence intensity ΔI_f is given by [27]

$$\Delta I_f = -A(k_i - k_j)(n_i^0 - n_j^0)(k_i + k_j)^{-1} \quad (5)$$

where A is an instrumental constant, k_i and k_j are decay constants of spin levels i and j and n_i^0 and n_j^0 are steady-state populations of these levels. Eqn. (5) has been derived in the absence of spin-lattice relaxation between triplet spin levels.

EXPERIMENTAL

Anacystis nidulans were grown in Kratz and Myers medium C [26] at pH 7.8, in 3% CO₂-enriched air at 20°C under continuous illumination (15 W/m²). They were harvested after 3-7 days for disc electrophoresis on acrylamide gel after SDS treatment in phosphate buffer (pH 7.6) [28]. The green bands were cut out and stored in liquid nitrogen until use. The P700/chlorophyll-a ratio was estimated to be 1/40 by measuring the reduced (2 mM neutralized ascorbate) minus the oxidized (1 mM ferricyanide) difference spectrum [29] on a Cary 14R spectrophotometer equipped with a scattered light attachment.

Mutant C-6E of *Scenedesmus obliquus* was taken from stock in agar slant and grown for 10-20 days in a dark incubator at 30°C in a 1000 ml Erlenmeyer flask containing 250 ml of inorganic medium according to [30], modified after [31] with glucose (0.5%) and yeast extract (0.5%).

The FDMR measurements were carried out at 4.2 K on a laboratory-constructed apparatus described previously [27] to which minor modifications have been made in order to improve the signal to noise ratio. A frequency sweep of 10-1300 MHz was made in 1 sec at constant microwavepower and under continuous high intensity (4000 W/m²) illumination with blue (400-450 nm) light from a 900 Watt high-pressure Xe lamp (Osram XBO). Up to 2¹⁷ sweeps were recorded and stored in a CAT. Fluorescence spectra at 4.2 K were measured with the same apparatus.

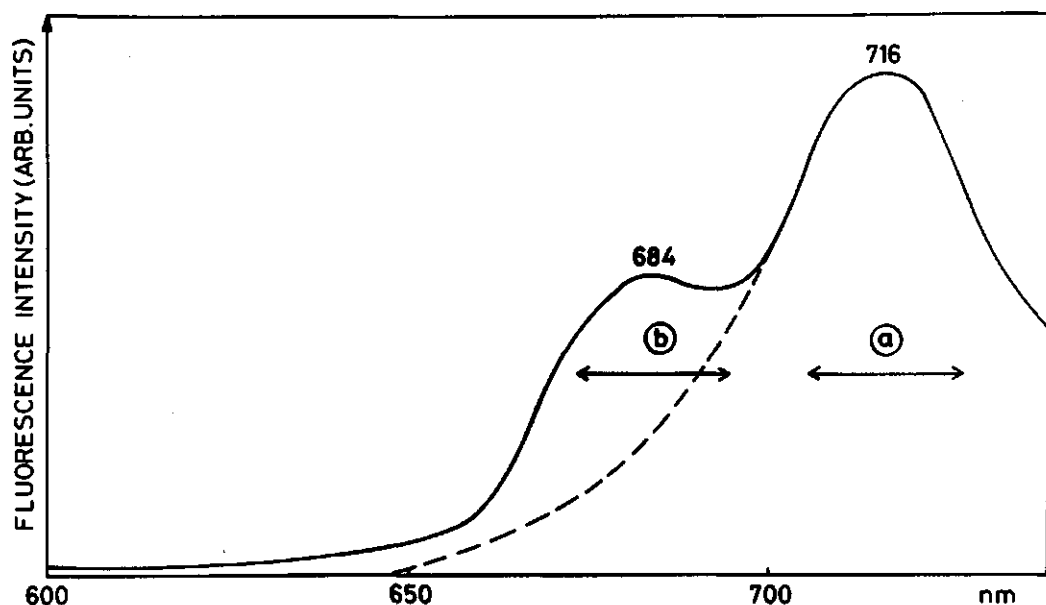


Figure 1 4.2 K surface-excited fluorescence spectrum of CP-I complex in polyacrylamide gel from *Anacystis nidulans*. Detection bandwidth 20 nm (\longleftrightarrow). Fluorescence spectrum of sample immediately after preparation. The 684 nm band appears upon standing at room temperature under ambient light. Regions a and b, indicated by arrows, have been monitored to obtain FDMR spectra, shown in Figs 2a and b. The width of the arrows corresponds with the detection bandwidth used in the FDMR experiments.

RESULTS

The 4.2 K fluorescence spectrum of the CP-I complex, isolated from *Anacystis nidulans* (wild type) blue-green algae is presented in Fig. 1. The relative intensities of the bands with maxima at 684 nm and 716 nm strongly depends on temperature as well as sample-treatment. Lowering the temperature from room temperature to liquid-helium temperature causes the 716 nm band to appear. Prolonged exposure (>2 hrs) of the sample to ambient light at room temperature increases the 684 nm band intensity at the expense of the band at longer wavelength. Monitoring the fluorescence emission in regions a and b indicated in Fig. 1, triplet FDMR spectra of the CP-I complex are obtained as shown in Figs 2a and b. The widths of the optical detection bands have been indicated in Fig. 1. Note the opposite signs of the D+E and D-E transitions at ~735 and ~965 MHz, in the spectra of Figs 2a and b, and their slightly different resonance frequencies.

Fig. 3 represents a typical FDMR spectrum, obtained at 4.2 K of the green alga *Scenedesmus obliquus* C-6E mutant, monitoring the fluorescence emission in a 20 nm region around the 693 nm maximum. Note the small linewidth of ~8 MHz of the 2E transition at 228 MHz, as compared to the corresponding linewidths of 40 MHz of the D+E and D-E transitions at 763 and 994 MHz.

The zero-field splitting parameters of the observed triplets for the CP-I complex and several types of algae have been collected in Table I.

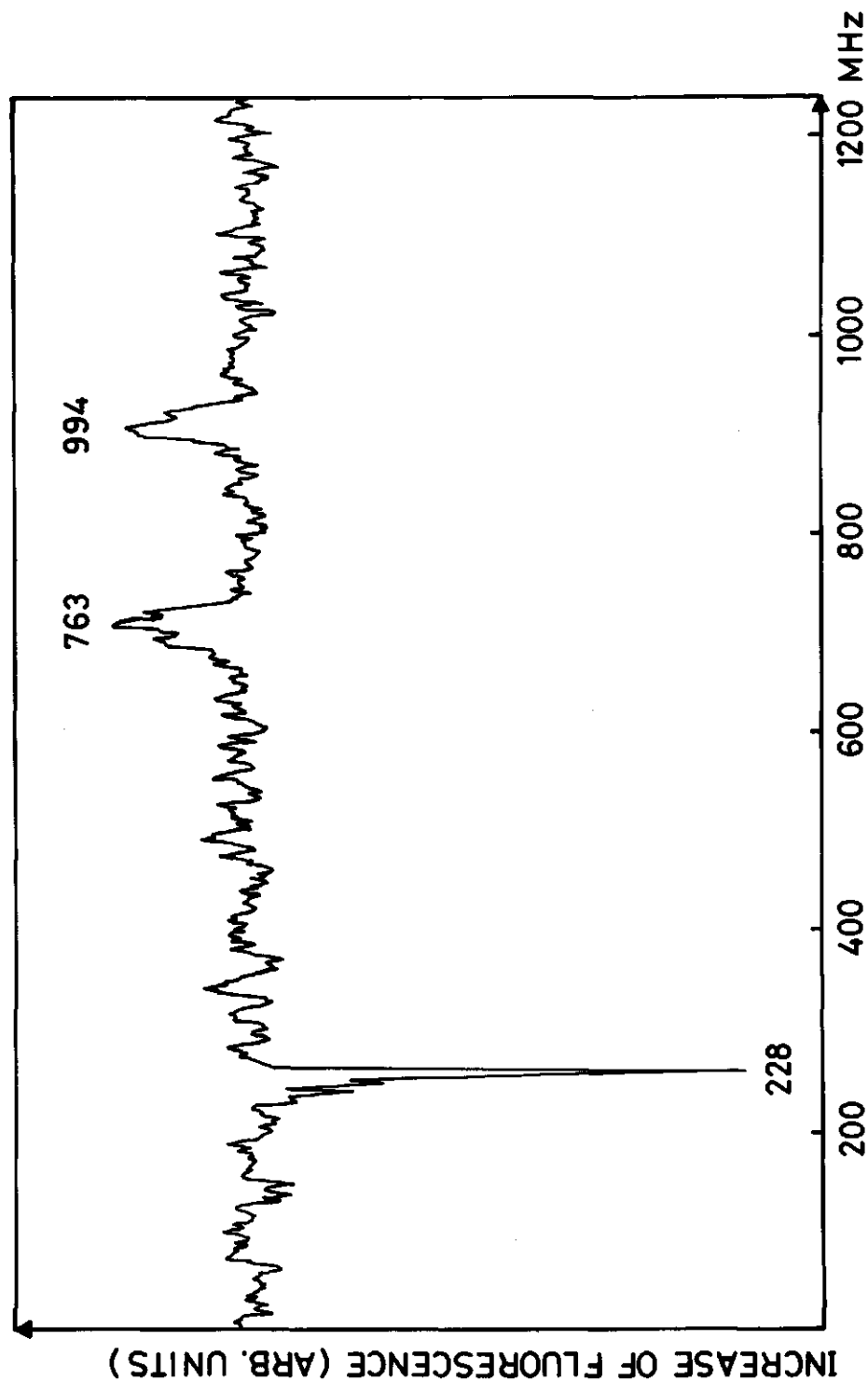


Figure 3 4.2 K FDMR spectrum of *Scenedesmus obliquus* C-6E mutant. Detection wavelength 693 nm; bandwidth 20 nm. Sweep rate 1300 MHz/s; microwave power 40 mW; number of accumulated spectra: 210; medium: water.

Table I Zero-field splitting parameters D and E of chlorophyll-a.
T = 4.2 K.

Environment	λ_f^a (nm)	D ($\times 10^4 \text{ cm}^{-1}$)	E ($\times 10^4 \text{ cm}^{-1}$)	$\Delta I_f/I_f^b$ (%)	Ref.
Chl-a.L/n-C ₈	669	309 \pm 4	42 \pm 4	-	7,10
Chl-a.L ₂ /n-C ₈	687	291 \pm 5	38 \pm 4	+	7,10
(Chl-a.L ₂) ₂ /n-C ₈	725	286 \pm 5	31 \pm 5	+	7,10
CP-I complex	684	283 \pm 4	38 \pm 4	- 5×10^{-3}	20,30,*
" "	716	284 \pm 4	38 \pm 4	+ 6×10^{-3}	20,30,*
<i>Anacystis nidulans</i>	717	289 \pm 4	38 \pm 4	+ 5×10^{-3}	18-20
<i>Scenedesmus</i> C-6E	693	287 \pm 5	38 \pm 5	+ 10×10^{-3}	20,*

* this work

a. Monitoring wavelength region. b. Sign of $\Delta I_f/I_f$ refers to increase of fluorescence resulting from microwave absorption by the triplet state of Chl-a. The figure represents the average for the D+E and D-E transitions. If no quantitative data are available, only the sign of $\Delta I_f/I_f$ is given.

DISCUSSION

Referring to Fig. 4, and solving the steady-state kinetic equations for an isolated molecule, i.e. $k_1 = k_2 = 0$, it is easy to derive a relation between the fluorescence intensity I_f and the steady-state number of triplets $N(T_0)$

$$I_f = \frac{k_f k_{ex}}{k_f + k_{isc} + k_{ex}} [N - N(T_0)] \quad (6)$$

where N is the total (and maximum) number of guest molecules in the sample, which can be subjected to the ODMR experiment. For $N(T_0) \ll N$, the relative change of the fluorescence intensity $\frac{\Delta I_f}{I_f}$ resulting from a change $\Delta N(T_0)$ follows from (6):

$$\frac{\Delta I_f}{I_f} = - \frac{\Delta N(T_0)}{N} \quad (7)$$

Note, that the relative changes of the fluorescence intensity and the triplet state population have opposite sign. This applies to the situation where the change of $N(T_0)$ is brought about by absorption of resonant microwaves by a pair of spinlevels of T_0 , so that the populations of these levels are equalized. The intensity of the exciting light remains constant. For a guest molecule acting as a trap for singlet-excitation from a dilute bath of surrounding guest molecules, we may again solve the steady-state kinetic equations, using the singlet-singlet energy-transfer equation:



where the superscript "tr" denotes trap-molecules, followed by



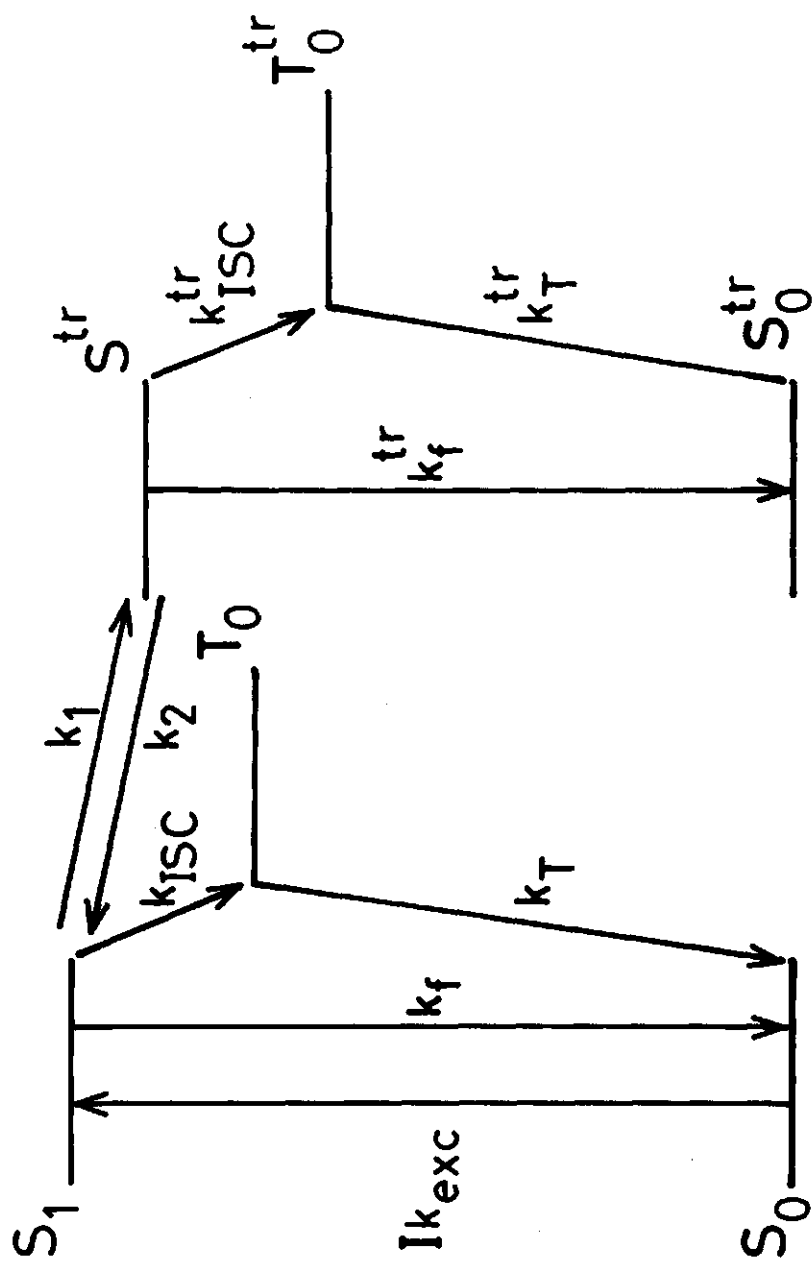


Figure 4 Kinetic scheme for singlet-singlet energy transfer from energy levels of antenna pigment (left) to those of traps (right, labelled "tr").

and noting that

$$N(S_0) \approx N_b$$

$$N(S_0^{tr}) + N(T_0^{tr}) \approx N_{tr} \quad (9)$$

where $N(S_0)$, $N(S_0^{tr})$, $N(T_0^{tr})$ define the number of groundstate molecules in the bath, the number of groundstate traps, and the number of triplet state traps. In (9) the steady-state populations of S_1 and S_1^{tr} have been neglected, assuming a low optical excitation level. N_b and N_{tr} represent the total number of molecules in the bath and the total number of traps. The result for I_f is given by

$$I_f = \frac{k_f k_{ex} N_b}{k_f + k_{isc} + k_1 [N_{tr} - N(T_0^{tr})]} \quad (10)$$

if the rate of $S_1^{tr} \rightarrow S_1$ backtransfer, $k_2 N_b \ll k_{isc}^{tr} + k_f^{tr}$. As expected for $k_1 = 0$, eqn. (10) reduces to (6) under the condition $k_{ex} I \ll k_{isc} + k_f$, i.e. low excitation level. For $T_0^{tr}/N^{tr} \ll 1$, the relative fluorescence change is easily derived from (10):

$$\begin{aligned} \frac{\Delta I_f}{I_f} &= \frac{k_1 N_{tr}}{k_f + k_{isc} + k_1 N_{tr}} \cdot \frac{\Delta N(T_0^{tr})}{N_{tr}} \\ &= \frac{\Delta T_0^{tr}}{N_{tr}} \quad \text{if } k_1 N_{tr} \gg k_f + k_{isc} \end{aligned} \quad (11)$$

Note, that now $\frac{\Delta I_f}{I_f}$ and ΔT_0^{tr} have equal sign. Thus, the signs of all three FDMR transitions of a chlorophyll-triplet at D+E, D-E, and 2E are inverted with respect to those of the isolated molecules, if this triplet is detected by monitoring the fluorescence of the surrounding pigment-bed, and the triplet molecule is the end-product of singlet-singlet energy transfer from the pigment-bed.

The fluorescence quantum yield $\phi_f \approx I_f / k_{ex} N_b$ can be brought into the form

$$\phi_f^{-1} = (\phi_f^0)^{-1} + \frac{k_1}{k_f} \cdot [N_{tr} - N(T_0^{tr})] \quad (12)$$

where ϕ_f^0 represents the fluorescence quantum yield of the isolated molecule, i.e. if $k_1 = 0$. Eqn. (12) closely resembles the Duysens-Vredenberg relation [32]

$$\phi_f^{-1} = A + BN(\text{open}) \quad (13)$$

between the fluorescence yield of antenna chlorophyll in bacterial reaction centres and the fraction of centres which are open for energy-transfer.

A and B are positive constants and can be determined from experiment [32]. A similar expression relating the change in fluorescence intensity and the effect of saturating microwaves on the triplet population of bacterial reaction centres has been derived by Hoff and Gorter de Vries [14].

Comparing (12) and (13) shows that $N(T_0^{tr})$ can be identified as the number of closed traps. If the number of traps which are excited into their triplet state approaches N_{tr} , singlet-excitation cannot be transferred to the trap and the fluorescence yield is close to that of the isolated molecule.

There are two other models involving energy transfer between surrounding chlorophyll molecules and the triplet trap observed by FDMR.

Firstly, we may assume that the triplet state of a Chl-a species emitting at ~684 nm can be observed *directly* by monitoring its 'own' fluorescence emission at 684 nm, as well as *indirectly* by detecting at 716 nm. Singlet excitation of the 684 nm species is transferred to a collection of molecules emitting at 716 nm, and competes with $S_1 \rightarrow T_0$ intersystem crossing in the 684 nm species. Then, a change $\Delta N(T_0)$ of the 684 nm species, induced by microwave absorption, should be observable also by detecting at 716 nm, i.e. by its effect on the fluorescence emission of an energy-sink red-shifted with respect to the 684 nm species. By a similar analysis as presented for the model of Fig. 4, it is predicted that the relative changes of the 716 nm fluorescence intensity and the triplet population of the 684 nm species again have the same sign. Monitoring the fluores-

cence at 684 nm, however, produces opposite signs of $\frac{\Delta I_f}{I_f}$ and $\frac{\Delta T_0}{T_0}$. This model can be eliminated since it predicts the observed ODMR frequencies to be identical, when monitoring at 684 and 716 nm, in contrast with experiment (Figs. 2a and b). Furthermore, the amplitude of ODMR signals observed at 716 nm should increase with increasing ratio of the 680 nm vs the 716 nm species. Experimentally, no dependence is observed.

In densely-packed pigment-protein complexes, triplet-triplet energy transfer may occur by triplet-excitons [30], created by optical excitation, followed by intersystem-crossing in a bed of pigment molecules with (almost) degenerate states.

Exciton-trapping occurs at pigments at chemical or physical defects, allowing observation by ODMR. If T-T energy transfer is dominant, and if we neglect direct optical excitation of the traps, a kinetic model similar to that in Fig. 4 predicts the relation:

$$\frac{\Delta I_f}{I_f} \approx - \frac{k_T}{k_1 N_b} \frac{\Delta N(T_0^{tr})}{N_{tr}} \quad (14)$$

between the relative changes in fluorescence of the pigment-bed and the triplet population of the traps.

In (14) N_b is the total number of molecules in the pigment-bed from which T-T energy transfer takes place to the trap. Clearly, T-T energy transfer does not produce the experimental sign reversal of ODMR transitions in the CP-I complex.

Summarizing, out of the three energy-transfer mechanisms discussed before, only S-S energy transfer from pigment-bed to trap remains as a possible candidate for sign reversal of 684 nm vs 716 nm FDMR signals, monitored by pigment-bed fluorescence.

This model can explain the sign reversal of Chl-a FDMR signals observed at 684 nm and 716 nm in CP-I particles isolated from *Anacystis nidulans* and presented in Figs 2a and b. FDMR transitions, observed at 735 (D-E) and 965 MHz (D+E) by monitoring the 684 nm fluorescence emission band (Fig. 2b) are then assigned to the triplet state of Chl-a isolated from the remaining part of the antenna pigment-protein complex. This Chl-a species migrates together with

the CP-I complex in electrophoresis, and not as free Chl-a. Consequently, the 684 nm FDMR transitions should be ascribed to Chl-a still attached to the protein, but out of reach for singlet-singlet energy transfer from the other pigment molecules by partial unfolding of the complex. Frequencies and signs of these transitions correspond to those of Chl-a *in vitro* [7,10,11].

Positively signed ODMR transitions at 740 MHz and 977 MHz (Fig. 2a) observed by monitoring the antenna pigment fluorescence at 716 nm (Fig. 1), would originate from triplet state Chl-a trapped in the native CP-I complex. Under these conditions singlet-singlet energy transfer from surrounding pigment molecules to the trap would result in sign-reversal of the ODMR transitions, as discussed before.

Several objections can be made against this mechanism, however. Inspection of Figs. 2a and b reveals that the amplitude-ratio of transitions at 977 and 740 MHz in Fig. 2a is different from that for the 965 and 735 MHz transitions in Fig. 2b. The ET model predicts the 684 and 716 nm signals to be of opposite sign but with constant amplitude-ratio, between high- and low-frequency transitions. Also, pigment-bed fluorescence is unlikely to be emitted from fluorescent chlorophyll traps which are very different from those giving rise to triplet formation. Consequently, it is difficult to conceive how triplets are formed in a limited number of traps, whereas no triplets are assumed to be formed in the surrounding pigment-bed.

As an alternative for the ET mechanism, we may look for the effects of Chl-a triplet state kinetics, assuming that the triplet state of the 716 nm Chl-a species may have modified kinetics with respect to that of the isolated molecule, fluorescing at 684 nm. Indeed, it has been observed for a very similar compound, pheophytin-a, dissolved in n-octane, doped with ethanol, that one of the ODMR transitions (D+E) changes sign, when the monitoring fluorescence wavelength window is shifted over the fluorescence emission band [19]. This effect is expected to occur upon ligation or complexing of the molecule by polar solvents, due to changes in the contributions of excited singlet states to the spin-orbit coupling matrix elements for the three triplet spin levels [11,34].

Table II presents some results on the effect of different ligands

Table II Environmental effect on triplet state kinetics and signs of ODMR transitions

Compound	Solvent	Level	$\frac{a_{k_i}}{k_t} (\%)$	$P_i (\%)$	$a_{\Delta n_i}$	$2E^b$	$D-E^b$	$D+E^b$
Chl-a	MTHF	$ x\rangle$	33	31	-0.06			
		$ y\rangle$	60	60	-0.04	-	+	+
		$ z\rangle$	7.5	11	+0.10			
Chl-a	EtOH	$ x\rangle$	19	25	+0.07			
		$ y\rangle$	72	65	-0.06	+	+	-
		$ z\rangle$	10	10	-0.02			
Chl-b	MTHF	$ x\rangle$	31	35	+0.06			
		$ y\rangle$	64	60	-0.02	+	-	-
		$ z\rangle$	4.5	4	-0.03			
Chl-b	EtOH	$ x\rangle$	25	27	-0.01			
		$ y\rangle$	69	66	-0.04	+	+	+
		$ z\rangle$	5	7	+0.06			

- (a) $\Delta n_i^0 \equiv \left[\frac{P_i}{k_i} / \sum_i \frac{P_i}{k_i} \right] - 1/3$ represents the fractional deviation from uniform steady state distribution of molecules over the three spin-levels. For such a uniform distribution $n_x^0 = n_y^0 = n_z^0 = 0.33$; k_i = total decay rate of spin-level $|i\rangle$, $k_T \equiv 1/3 \sum_i k_i$.
- (b) Entries in these columns represent signs of FDMR transitions, as predicted from the values of Δn_i^0 and k_i and eqn. (5).

on the triplet state kinetics of Chl-a and b and the signs of the FDMR transitions of these pigments. Note that Chl-a in solid MTHF at ~ 100 K, where the kinetic data of Table II have been obtained [35], is in a biligated state with two MTHF solvent molecules attached to the Mg^{2+} ion. Removal of one ligand generally shifts the fluorescence wavelength from ~ 685 to 670 nm and changes the FDMR signs of the D-E and D+E transitions from positive (as in Table II) to negative [10]. The data for Chl-a in EtOH demonstrate that sign reversals may result from a change of ligand interaction, since EtOH also interacts with the ring-V keto group through hydrogen bonding [35].

Similar sign reversals are predicted for Chl-b in MTHF vs EtOH on the basis of measured triplet state kinetics in both solvents. Thus, the positive signs of the 716 nm Chl-a transitions in Fig. 2a may also be the result of ligation of Chl-a to at least two nearby ligands, presumably protein sidegroups.

The observed zero-field splitting parameters, the position of the fluorescence band, and even the signs of the D-E and D+E transitions of the chlorophyll triplet observed by monitoring the 716 nm fluorescence, are in close agreement with the data for the $(\text{Chl-a} \cdot 2\text{H}_2\text{O})_2$ *in vitro* dimer [7,10] (see Table I). This dimer has been proposed as a model for the P.S.-I reaction centre [36]. Yet, the observed resonances at 716 nm are unlikely to originate from chlorophyll triplets localized on the P.S.-I reaction centre. Under our experimental conditions it is irreversibly photo-oxidized [37], and then is unable to act as a trap for chlorophyll triplets. Rather, the observed triplets should be located in shallow traps in the antenna system.

The present results suggest, that the architecture of the antenna system contains chlorophylls with parallel orientation, similar to that in the water-linked dimer and the P700 reaction centre. The so-called *in vitro* dry dimer $(\text{Chl-a})_2$, suggested as a possible building block for the antenna [38], does not fluoresce and therefore is not observed by FDMR. The main difference between the traps observed at 716 nm by FDMR and the reaction-centre trap is the coupling of the latter to electron-acceptors at close distance.

Unfolding of the complex, which slowly occurs at room temperature in the gel, removes pigment-pigment as well as environmental

interactions, and shifts the pigment fluorescence from 716 to 684 nm. Since the 684 nm emission belongs to Chl-a still bound to the protein in some way, the main contribution to the blue-shift is believed to come from removing pigment-pigment interactions.

From the ZFS values and the fluorescence spectrum of Chl-a in the unfolded complex, it is not possible to draw firm conclusions about its immediate surroundings: as shown by Table II and according to data from ref. 10, the FDMR signals observed at 684 nm should have positive signs, if Chl-a were biligated at Mg^{2+} . Furthermore, the *in vitro* biligated species fluoresces at 687 nm, red shifted with respect to the Chl-a fluorescence in unfolded CP-I. A 680 nm fluorescent Chl-a species has been observed [10] monoligated at Mg^{2+} and hydrogen bonded to the ligand at the ring V keto group. Unfortunately, no FDMR could be obtained of this species.

In conclusion, the 716 nm species is likely to be Chl-a, interacting with other parallel oriented, nearby chlorophylls, each chlorophyll being held in position by at least two protein ligands interacting with the Mg^{2+} ion, and possibly a third, hydrogen bonded to the ring V keto group. Upon unfolding, the interaction between chlorophylls is removed. Probably, the number of ligands is reduced at the same time.

At 4.2 K spin-lattice relaxation may be fast enough to compete with spin-level decay. The resulting Boltzmann equilibrium would give rise to positively signed FDMR transitions. Further cooling to 2 K does not have a significant effect on the FDMR spectrum, however, eliminating spin-lattice relaxation as a possible cause for the observed sign reversal of the 716 nm transitions.

The fluorescence spectrum of the CP-I complex closely resembles that of the long-wavelength region of the intact blue-green alga *Anacystis nidulans* from which it is isolated. Upon cooling from room temperature to 4.2 K the 720 nm band intensifies considerably in both cases. Furthermore, the zero field splitting values D and E derived from FDMR transition-frequencies of the complex are close to those in blue-green algae, as is evident from Table I. These observations are in agreement with the generally accepted view, that the fluorescence spectrum of CP-I largely originates from Chl-a in

the antenna-pigment [39].

The FDMR spectrum of the C-6E mutant of the green alga *Scenedesmus obliquus*, which lacks Photosystem II and contains no carotenoids in Photosystem I, exhibits positive D+E and D-E transitions at 763 MHz and 994 MHz, as shown in Fig. 3, and an unusually narrow 2E transition (8 MHz fwhm). Such narrow 2E transitions have not been found for wild type *Scenedesmus*. The absence of Photosystem II and/or carotenoids is not a necessary requirement of observing narrow 2E transitions, because similar narrow resonances have been found for *Anacystis nidulans* and *Chlorella vulgaris* [11,19]. Presently, the conditions for observing these narrow resonances is not understood.

The large variation in linewidth of the FDMR transitions in *Scenedesmus* C6-E and several other algae is remarkable. Close inspection of D+E and D-E resonances suggests the presence of an inhomogeneous structure within the transition-profile. The 2E transition consists of one dominant, narrow peak and several weak satellites. Its inhomogeneous structure is much less pronounced than for the D+E and D-E resonances. The most simple explanation for the strong variations of linewidth involves a wider distribution of D- than of E-values.

Thus, the $|z\rangle$ spin-level is selectively broadened, as well as those FDMR transitions involving this level. By contrast, the $|x\rangle$ and $|y\rangle$ spin-levels are approximately equidistant, almost independent from the variation in D-values. For a planar molecule, the D-value is proportional to $\langle r^{-3} \rangle$, where r is the distance between triplet spins. Interaction of the central Mg^{2+} ion of Chl-a with ligands primarily affects D [10] and does not discriminate between the in-plane molecular x and y axes, i.e. it shifts the energies of the $|x\rangle$ and $|y\rangle$ spin-levels with approximately the same amount, leaving the E-value almost unaffected by ligation to Mg^{2+} . Tentatively, we suggest that the selective broadening of the Chl-a $|z\rangle$ spin-level reflects the presence of various Mg^{2+} ligand interactions with the surrounding protein. This also could explain why the sharp 2E transition is not always observed in different samples of algae. A subtle change in the protein-structure induced by preparation conditions, is all what is needed to destroy the uniform in-plane perturbation by the protein-environment of the pigment-mole-

cule, and results in broadening of the 2E transition beyond detection, due to its low integrated intensity. This may also be the reason for the absence of 2E transitions in FDMR spectra of the CP-I complex and Chl-a *in vitro* [10,20].

We point out that highly uniform pigment environments have also been invoked to explain the extreme and unexpected narrowness of all three FDMR transitions of bacterial reaction centres [12]. If this explanation is correct, the local environment of the pigment, provided by the *in vivo* protein-structure, must be highly uniform with respect to each of the three molecular axes of the pigment. We suggest that the antenna complex in algae represents an example of a photosynthetic pigment in a protein environment which is more uniform with respect to lateral pigment-protein interactions than in a direction perpendicular to the plane of the pigment molecule.

REFERENCES

1. W.G. van Dorp, T.J. Schaafsma, M. Soma and J.H. van der Waals (1973). *Chem.Phys.Lett.* 21: 221-225.
2. M.A. El-Sayed (1972). In: *Spectroscopy*, MTP Int.Rev. of Sci: Phys.Chem.Ser.One (A.D. Buckingham, cons.ed., D.A. Ramsy, vol. ed.), Vol 3. Butterworths, London and University Park Press, Baltimore, Maryland. p. 119.
3. A.L. Kwiram (1972). In: *Magnetic Resonance*, MTP Int.Rev. of Sci: Phys.Chem.Ser.One (A.D. Buckingham, cons.ed., C.A. McDowell, vol.ed.), Vol 4. Butterworths, London and University Park Press, Baltimore, Maryland. p. 271.
4. H. Maki and J.A. Zuclich (1975). In: *Topics in Current Chemistry*, Vol 54. Springer Verlag, New York. p. 116-163.
5. R.H. Clarke and R.H. Hofeldt (1974). In: *Excited States of Biological Molecules*, Proc.Int.Conf. of Excited States of Biol. Molecules, Lisbon, Portugal, April 18-24. Eds: J.B. Birks and S.P. McGlynn. Wiley, New York. pp. 309-313.
6. R.H. Clarke and R.H. Hofeldt (1974). *J.Chem.Phys.* 61: 4582-4587.
7. R.P.H. Kooyman, T.J. Schaafsma and J.F. Kleibeuker (1977). *Photochem.Photobiol.* 26: 235-240.
8. R.H. Clarke, R.E. Connors, T.J. Schaafsma, J.G. Kleibeuker and R.J. Platenkamp (1976). *J.Am.Chem.Soc.* 98: 3674-3677.
9. R.P.H. Kooyman, T.J. Schaafsma, G. Jansen, R.H. Clarke, D.R. Hobart and W.R. Leenstra (1979). *Chem.Phys.Lett.* 68: 65-70.
10. R.P.H. Kooyman (1980). Thesis. Agricultural University, Wageningen.
11. T.J. Schaafsma (1981). In: *Triplet state ODMR spectroscopy, Techniques and applications to biophysical systems*. Ed.: R.H. Clarke. Wiley, New York (in press).
12. R.H. Clarke, R.E. Connors, J.R. Norris and M.C. Thurnauer (1975). *J.Am.Chem.Soc.* 97: 7178-7179.
13. A.J. Hoff (1976). *Biochim.Biophys.Acta* 440: 765-771.
14. A.J. Hoff and H. Gorter de Vries (1978). *Biochim.Biophys.Acta* 503: 94-106.

15. A.J. Hoff in ref. 11.
16. A.J. Hoff and J.H. van der Waals (1976). *Biochim.Biophys.Acta* 423: 615-620.
17. A.J. Hoff, Govindjee and J.C. Romijn (1977). *FEBS Lett.* 73: 191-196.
18. S.J. van der Bent, T.J. Schaafsma and J.C. Goedheer (1976). *Biochem.Biophys.Res.Comm.* 71: 1147-1152.
19. S.J. van der Bent (1977). Thesis. Agricultural University, Wageningen.
20. G.F.W. Searle, G.H. van Brakel, W.F.J. Vermaas, A. van Hoek and T.J. Schaafsma (1980). *Proc. 5th Int. Congr. Photosynthesis, Kallitea, Greece (in press).*
21. G.F.W. Searle and T.J. Schaafsma (1981). *Proc. 4th Int. Sem. on Energy, Transfer in Condensed Matter, Prague (in press).*
22. G.F.W. Searle, R.B.M. Koehorst, T.J. Schaafsma, B.L. Møller and D. von Wettstein (1981). *Carlsberg Comm.* 46: 183-194.
23. R.H. Clarke, S.P. Jagannathan and W.R. Leenstra (1980). *Photochem.Photobiol.* 32: 805-808. See also: *Lasers in Photomedicine and Photobiology*. Eds: R. Pratesi and C.A. Sacchi (1980). Springer Verlag, Berlin. pp. 171-174.
24. J.P. Thornber, R.S. Alberte, F.A. Hunter, J.A. Shiozawa and K.-S. Kan (1976). *Brookhaven Symp.Biol.* 28: 132-148.
25. W.G. van Dorp, W.H. Schoemaker, M. Soma and J.H. van der Waals (1975). *Mol.Phys.* 30: 1701-1721.
26. W.A. Kratz and J. Myers (1955). *Am.J.Bot.* 42: 282-287.
27. S.J. van der Bent, P.A. de Jager and T.J. Schaafsma (1976). *Rev.Sci.Instr.* 47: 117-121.
28. J.W. Kleinen Hammans, L.P.L.M. Rabou and H.Q. Pietersen (1977). *Photochem.Photobiol.* 26: 235-240.
29. T.V. Marsho and B. Kok (1971). In: *Methods in Enzymology*. Vol XXIII. Ed.: A. San Pietro. Acad. Press, New York. pp. 515-522.
30. E. Kessler, W. Arthur and J.E. Bruggen (1957). *Arch.Biochem.* 71: 326-335.
31. N.I. Bishop in ref. 29, pp. 130-143.
32. W.J. Vredenberg and L.N.M. Duysens (1963). *Nature* 197: 355-357.
33. J. Jortner, S.A. Rice, J.L. Katz and S.I. Choi (1965). *J.Chem. Phys.* 42: 309-323.

34. J.P. Lemaistre and A.H. Zewail (1979). Chem.Phys.Lett. 68: 302-308.
35. J.F. Kleibeuker (1977). Thesis. Agricultural University, Wageningen.
36. L.L. Shipman, T.M. Cotton, J.R. Norris and J.J. Katz (1976). Proc.Natl.Acad.Sci.USA 73: 1971.
37. G.H. van Brakel, T.J. Schaafsma, J.J.S. van Rensen, J.W. Kleinen Hammans. Biochim.Biophys.Acta (to be published).
38. J.J. Katz, J.R. Norris and L.L. Shipman (1976). Brookhaven Symposia in Biology 28: 17.
39. Symposion on Chlorophyll organization and energy transfer in photosynthesis, Ciba Foundation 1978 (1979). Ciba Found.Symp. 61, new series. Excerpta Medica, Amsterdam.

3.3.5 Conclusions

Four mechanisms have been discussed that can give rise to sign reversal of the ODMR transitions of Chl-a *in vivo* compared to Chl-a *in vitro*.

Of these the spin-lattice relaxation effect has been excluded as a possibility, because of the absence of a temperature effect. The radical pair mechanism has been considered less probable, because the ODMR triplet of Chl-a appears to be located in the antenna pigment and not in the reaction centres. So the mechanisms of energy transfer and the effects of ligation (site-effects) are left over as possible candidates.

It can be argued (see §3.3.4) that the relative size of the two triplet signals D+E and D-E belonging to one species of Chl-a should be identical for the Chl-a fluorescing at 715 nm, and the Chl-a fluorescing at 685 nm in chlorophyll-proteins, when the energy transfer mechanism is operative. This is not observed, and based on this fact preference is given to the site-effects as the cause of sign reversal.

This argument cannot be considered to have absolute validity, however, since also between *in vivo* experiments, some variation in the relative sizes of the two triple signals is observed.* Determinations of the triplet sublevel kinetics as reported in §4.3 should provide the decisive answer, whether the sign reversal of ODMR species is due to a change in triplet state sublevel kinetics or to energy transfer.

* This is due to changes in microwave field amplitude at the resonance frequencies for different experiments. Recent experiments [46] have confirmed, that this is indeed the cause for the variation in relative size of the D+E and D-E resonances. In fact, for one experimental run, both resonances detected at 684 and 716 nm have almost equal, but opposite amplitudes [46]. Thus there is no preference left for the site-effects based on this argument.

3.4 REFERENCES

1. R.H. Clarke and R.H. Hofeldt (1974). *J.Chem.Phys.* 61: 4582-4587.
2. W.G. van Dorp, W.H. Schoemaker, M. Soma and J.H. van der Waals (1975). *Mol.Phys.* 30: 1701-1721.
3. R. Avarmaa (1979). *Mol.Phys.* 37: 441-454.
4. R. Avarmaa and T.J. Schaafsma (1980). *Chem.Phys.Lett.* 71: 339-344.
5. N.J. Turro (1967). *Molecular Photochemistry*. Benjamin, New York. p. 73.
6. D. Mauzerall (1977). In: *Photosynthesis I, Encyclopedia of Plant Physiology, New Series Volume 5*, Eds. A. Trebst and M. Avron. Springer, Berlin. pp. 117-124.
7. A.A. Krasnovskii Jr., N.N. Lebedev and F.F. Litvin (1974). *Dokl.Akad.Nauk SSSR* 216: 1406-1409.
8. J.F. Kleibeuker (1977). Thesis, Landbouwhogeschool Wageningen.
9. A.W.H. Mau and M. Puza (1977). *Photochem.Photobiol.* 25: 601-603.
10. J.D. Petke, G.M. Maggiora, L.L. Shipman and R.E. Christoffersen (1979). *Photochem.Photobiol.* 30: 203-223.
11. M. Asano and J.A. Koningstein (1981). *Chem.Phys.* 57: 1-10.
12. S.J. van der Bent (1977). Thesis, Landbouwhogeschool Wageningen.
13. R.G. Lawler (1973). In: *Progress in Nuclear Magnetic Resonance Spectroscopy*, Vol. 9. Eds. J.W. Emsley, J. Feeney and L.H. Sutcliffe. Pergamon Press, Oxford. pp. 147-210.
14. G.H. van Brakel, T.J. Schaafsma and J.J.S. van Rensen (1981). *Isr.J.Chem.* (In press).
15. N.E. Geacintov, G.E. Swenberg, A.J. Campillo, R.C. Hyer, S.L. Shapiro and K.R. Winn (1978). *Biophys.J.* 24: 347-359.
16. J. Lavorel and A.-L. Etienne (1977). In: *Primary Processes of Photosynthesis, Topics in Photosynthesis, Vol. 2*. Ed. J. Barber. Elsevier/North Holland Biomedical Press, Amsterdam. pp. 203-268 and references therein.
17. G.P. Gurinovich, A.N. Sevchenko and K.N. Solovyo (1968). *Spectroscopy of Chlorophyll and Related Compounds*. Publishing House Science and Technology, Minsk. (English translation: National Technical Information Service, U.S. Dept. of Commerce, Springfield, VA 22151, USA).

18. S.S. Dvornikov, V.N. Knyukshto, K.N. Solov'ev and M.P. Tsvirko (1979). *Opt.Spectroscopy (USSR)* 46: 385-388.
19. S.S. Dvornikov, V.N. Knyukshto, K.N. Solov'ev and M.P. Tsvirko (1979). *J.Luminescence* 18/19: 491-494.
20. R.A. Avarmaa, S.M. Kochebey and R.P. Tamkivi (1979). *FEBS Lett.* 102: 139-142.
21. C.P. Rygersberg and J. Ames (1978). *Biochim.Biophys.Acta* 502: 152-160.
22. C.P. Rygersberg and J. Ames (1980). *Biochim.Biophys.Acta* 593: 261-271.
23. T.J. Schaafsma (1981). In: *ODMR Spectroscopy*. Ed. R.H. Clarke. Wiley, New York. (In press).
24. S.J. van der Bent, P.A. de Jager and T.J. Schaafsma (1976). *Rev.Sci.Instr.* 47: 117-121.
25. J.F. Kleibeuker (1977). Thesis, Landbouwhogeschool Wageningen. Ch. 10.
26. A.J. Hoff (1981). In: *ODMR Spectroscopy*. Ed. R.H. Clarke. Wiley, New York. (In press).
27. A.J. Hoff (1976). *Biochim.Biophys.Acta* 440: 765-771.
28. C.P. Poole Jr. (1967). In: *Electron Spin Resonance*. Interscience Publishers, Wiley, New York.
29. P.L. Dutton, J.S. Leigh and M. Seibert (1972). *Biochem.Biophys. Res.Comm.* 46: 406-413.
30. R.A. Mushlin, P. Gast and A.J. Hoff (1980). *Chem.Phys.Lett.* 76: 542-547.
31. R.E. Blankenship (1981). *Acc.Chem.Res.* 14: 163-170.
32. A.W. Rutherford, D.R. Paterson and J.E. Mullet (1981). *Biochim. Biophys.Acta* 635: 205-214.
33. H.A. Frank, M.B.McLean and K. Sauer (1979). *Proc.Natl.Acad.Sci. USA* 76: 5124-5128.
34. J.G.M. van Rens, G. Jansen and T.J. Schaafsma. Private communication.
35. R.P.H. Kooyman, T.J. Schaafsma and J.F. Kleibeuker (1977). *Photochem.Photobiol.* 26: 235-240.
36. R.P.H. Kooyman (1980). Thesis. Wageningen. Ch. 5.
37. J.S. Brown (1977). *Photochem.Photobiol.* 26: 319-326.
38. T.M. Cotton, P.A. Loach, J.J. Katz and K. Ballschmitter (1978). *Photochem.Photobiol.* 27: 735-749.

39. B. Voigt, D. Leopold, B. Hieke and P. Hoffmann (1979). *Stud. Biophys.* 75: 93-94.
40. J.F. Kleibeuker, R.J. Platenkamp and T.J. Schaafsma (1978). *Chem.Phys.* 27: 51-64.
41. D.A. Antheunis (1974). Thesis. Leiden.
42. M. Lutz (1977). *Biochim.Biophys.Acta* 460: 408-430.
43. M. Lutz, J.S. Brown and R. Rémy (1979). CIBA Foundation Symposium 61, *Excerpta Medica*, Amsterdam. 105-125.
44. G.F.W. Searle, R.B.M. Koehorst, T.J. Schaafsma, B.L. Møller and D. von Wettstein (1981). *Carlsberg Res.Comm.* 46: 183-184.
45. T.J. Schaafsma, S.J. van der Bent and R.P.H. Kooyman (1978). XXth Congress Ampère, Tallinn.
46. G.F.W. Searle, private communication.

4.1 INTRODUCTION

This chapter reports the detection and characterization of ODMR spectra of the triplet state of Chl-a, as well as triplet state kinetics in several algae and in a chlorophyll protein complex CP-I, isolated from wild type *Anacystis nidulans*.

The discussion of the results, presented in the following paragraphs, aims at answering the following questions:

1. In which part of the photosynthetic apparatus is the Chl-a triplet detected in algae, located? As shown in §§4.2 and 4.3, the triplet is likely to be located in the antenna pigment of PSI, in view of a comparison of the Chl-a triplet state properties in the CP-I complex and in whole algae, and considering the oxidation state of the PSI reaction centre under the conditions of our experiments, as discussed in §4.5.
2. Why are Chl-a triplets not always detected in CP-I complexes and algae? What is the possible role of carotenoids? The results of §4.2 and the discussion in §4.5 represent attempts to find an answer to these questions.
3. Are the Chl-a triplets detected in algae and CP-I complexes identical? For this purpose we have made a comparison of low temperature fluorescence spectra, ODMR frequencies and triplet state kinetics, as discussed in §4.5.
4. Is the sign reversal of ODMR spectra detected at ~ 715 nm vs ~ 685 nm in CP-I complexes, and the positive sign of the ODMR signal detected at ~ 720 nm in algae, due to a fundamental change of Chl-a triplet state kinetics, or to energy transfer? Both mechanisms have been proposed and discussed in §3.3.4, without providing a decisive answer.

4.2 CHLOROPHYLL TRIPLETS AND ENERGY TRANSFER IN ISOLATED PSI CHLOROPHYLL PROTEINS FROM BLUE-GREEN ALGAE

This paragraph contains a paper in press, to be published in the Proceedings of the Fifth International Congress on Photosynthesis, Volume I, pp. 129-142, Ed. G.A. Akoyunoglou, International Science Services Balaban, Rehovot, Israel (1981). This Congress was held at Chalkidiki, Greece, Sept. 1980.

CHLOROPHYLL TRIPLETS AND ENERGY TRANSFER IN ISOLATED PSI CHLOROPHYLL PROTEINS FROM BLUE-GREEN ALGAE

G.F.W. Searle, G.H. van Brakel, W.F.J. Vermaas, A. van Hoek and T.J. Schaafsma

Department of Molecular Physics, Agricultural University,
de Dreijen 6, 6703 BC WAGENINGEN, the Netherlands

Abstract

1. CPI particles have been prepared from the blue-green algae *Synechococcus cedrorum* and *Synechococcus leopoliensis* using sodium dodecyl sulphate, followed by purification with gel electrophoresis. Using tris-glycine buffer pH 8.3 the amount of free chlorophyll found is minimal. The CPI particles show a pronounced long wavelength emission band (for *S. cedrorum* near 720 nm and for *S. leopoliensis* near 712 nm), and very little 680 nm emission.
2. An ODMR (optically detected magnetic resonance) signal in the F720 emission is only detected for CPI particles prepared from *S. leopoliensis* when phosphate buffer replaces tris-glycine in the electrophoresis step. An initial study of the chlorophyll triplet sublevel population/depopulation kinetics gave an estimate for the triplet lifetime in CPI of between 5 and 10 ms at 4.2 K. The triplet yield in CPI is very low compared to chlorophyll *in vitro*.
3. In CPI prepared by tris-glycine electrophoresis (m.wt. 165 kD) the electron acceptors A₁, A₂ and A (maybe also B) appear to be functional. Under the conditions of the ODMR experiment P700 should be present in the oxidized radical cation form: P700⁺. However, CPI prepared in phosphate buffer (m.wt. 85 kD) contains no functional electron acceptors, even the primary acceptor A₁ appears not to function normally, and the oxidation state of P700 under ODMR experimental conditions is still uncertain.
4. The source of the chlorophyll triplets seen by ODMR in phosphate prepared CPI would appear to be intersystem crossing (S₁ → T₀) in the photosystem I antenna chlorophyll a, as the

slow oxidation and reduction kinetics of P700 observed in these preparations would rule out a radical pair mechanism. However, the location of the triplets (on reaction centre or antenna chlorophyll) remains to be determined.

5. It is also possible that a carotenoid (probably not β -carotene) can act as a quencher of chlorophyll triplets. This carotenoid (a carotenoid-protein?) can be removed from the CPI by electrophoresis in phosphate buffer; and also to a greater extent for CPI from *S. leopoliensis* than from *S. cedrorum*. Carotenoids contribute to the long-wavelength emission but not the minor 680 nm emission band.
6. A theoretical treatment is still required to describe population/depopulation kinetics of the three sublevels of chlorophyll triplets in a chlorophyll-protein such as CPI, and to account for the different sign of the ODMR signal measured in the fluorescence bands at 680 nm and 720 nm. A possible model is presented.
7. Measurements of chlorophyll fluorescence lifetimes and fluorescence anisotropy (wavelength-resolved and time-resolved) are planned to test further the model of energy transfer and chlorophyll triplet quenching in CPI.
8. The relationship between the chlorophyll triplet states seen in whole algae and in isolated CPI remains to be established.

Introduction

Chlorophyll in the triplet state has been observed in photosynthetic systems *in vivo* using the ODMR (optically detected magnetic resonance) technique [1,2], although compared to triplet yields for *in vitro* chlorophyll the levels detected are low. The origin of these chlorophyll triplets is still uncertain, but two possible mechanisms have been proposed: a spin-inversion of a radical ion pair at the reaction centre, in which electron donation away from the reaction centre is blocked (as seen in photosynthetic bacteria, ref. 3); and intersystem crossing from the excited singlet state chlorophyll in the antenna pigment systems.

It is also not clear whether the ODMR signal seen in whole cells in the long wavelength emission band arises from triplet chlorophyll in photosystem I (PSI) or photosystem II (PSII) - see ref. 4. The

disruption of photosynthetic membranes with detergents allow the physical separation of the two photosystems so that the localization of the triplets is open to experiment. The observation of high yields of triplets [5] in the green alga mutant *Scenedesmus obliquus* C-6E, which lacks PSII [6], and the absence of detectable triplets in *Scenedesmus* mutant No. 8, which lacks PSI, indicated that PSI could be the source of the ODMR signal. Therefore the present investigation was initiated on PSI chlorophyll-proteins, purified with SDS (sodium dodecyl sulphate) from blue-green algae (a good source of PSI as a much higher proportion of the chlorophyll is associated with PSI compared to green algae or higher plants). These chlorophyll-proteins also have the advantage over intact cells of being simpler systems to carry out experiments at the molecular physical level, and are moreover well-characterized biochemically.

An important consideration in these ODMR experiments is the oxidation state of the PSI reaction centre (P700) at 4 K under continuous illumination.

A major difference between ODMR measurements on chlorophyll solutions in organic solvents and on chlorophyll-proteins, is the presence of energy transfer between chlorophyll molecules in the latter, both in the singlet and triplet states. This could probably lead to differences in population and depopulation rates of the three triplet sublevels *in vivo* compared to *in vitro*, and also to triplet quenching processes. Therefore excitation energy transfer studies are an essential complement to the ODMR measurements.

Materials and methods

The algal strains used were *Synechococcus cedrorum* and *Synechococcus leopoliensis* (*Anacystis nidulans*). These were grown in Kratz and Myers C medium [7] at pH 7.8, in 3% CO₂-enriched air at 20°C, and under moderate intensity illumination from fluorescent tubes (TL 33). 250 ml of algal suspension was placed in a 1 litre erlenmeyer flask and this was shaken continuously until the cells were harvested after 3-7 days.

2-3 flasks were harvested by centrifugation at 2400 xg for 10 min. The cell pellet was washed once with the mannitol/tris-gly-

cine/Mg²⁺ (MGTM) medium (0.3 M mannitol + 6.2 mM N-trishydroxymethyl-amino-methane + 48 mM glycine + 5 mM MgCl₂, pH 8.3), and resuspended in about 30 ml of the same medium. The cells were then broken in a French press at 1200 atmospheres pressure (20,000 p.s.i.), two passages giving 90% cell breakage (as measured by chlorophyll released from the cells). The remaining whole cells were removed by centrifugation at 2400 xg for 20 min, and the supernatant was then further centrifuged at 200,000 xg for 30 min to give a thylakoid pellet, substantially free of phycocyanin.

This thylakoid pellet was resuspended using a Potter hand homogenizer with teflon plunger in 1.0 - 1.5 ml MTGM medium to give a chlorophyll concentration of 1.5 - 2.0 mg Chl/ml (chlorophyll measured according to MacKinney [8] in 80% acetone using $A_{1\text{ mg/ml}}^{663} = 82.04$). A solution of 2% (w/v) SDS (British Drug Houses, Analytical Reagent grade) in MTGM medium was added to give a final SDS: chlorophyll ratio of 20:1 (w/v) and a final SDS concentration of 1.20 - 1.33% (w/v). The thylakoid suspension was immediately centrifuged at 40,000 xg for 10 min at 10°C, and the supernatant used for electrophoresis.

SDS polyacrylamide gel electrophoresis was performed in a standard disc gel electrophoresis apparatus, fitted with a tap water cooling jacket (temperature ~15°C) and shielded from room lighting. The gel composition was: 5% acrylamide, 0.13% bisacrylamide, 0.1% TEMED (N,N,N',N'-tetra methylethylenediamine), 0.05% SDS and 1 mg/ml ammonium persulphate, dissolved in TG medium (6.2 mM N-trishydroxymethylaminomethane + 48 mM glycine, pH 8.3) containing 1 mM MgSO₄. When the gels were run in phosphate buffer, the tris-glycine was replaced by 100 mM sodium phosphate, pH 7.6. The sample (50 µg chlorophyll per gel) was applied to the gel surface after addition of mannitol (15% w/v) and bromophenol blue as marker. After a short period (5-10 min) at low current, electrophoresis was carried out for 40 min at 3 mA/gel for gels in TG buffer, and for 4 hours at 10 mA/gel for gels in phosphate buffer. The electrode buffers consisted of 0.05% SDS + 1 mM MgSO₄, plus either TG or 100 mM sodium phosphate respectively. After removing the gels from the glass tubes, the green bands were cut out with a razor blade giving slices about 2-4 mm thick. These were stored in air-tight plastic bottles in liquid nitrogen until use.

The molecular weight of chlorophyll-protein bands on electrophoresis were estimated by comparison of their mobilities with those of denatured protein markers [9] - *E coli* β -galactosidase (130 kD), bovine serum albumin (68 kD), ovalbumin (43 kD) and chymotrypsinogen (26 kD) were used. Protein bands were stained with Coomassie Brilliant Blue.

The isolated chlorophyll-proteins in the gel were characterized by absorption spectra at room temperature using a Shimadzu UV-200 spectrophotometer with correction for scattering, and by fluorescence emission and excitation spectra at 77 K using a Perkin-Elmer MPF-2A spectrofluorimeter, equipped with a Hamamatsu R-928 photomultiplier, or at 4.2 K using the ODMR apparatus.

The ODMR measurements were carried out at 4.2 K on a laboratory-constructed apparatus described previously [10], to which minor modifications have been made to improve the signal/noise ratio 4-5 fold. A frequency sweep (round trip time 1 s) 10-1300 MHz was made at constant microwave power and under continuous high intensity (4000 W/m²) blue illumination from a high-pressure Xe lamp filtered through CuSO₄ solution. During the period of each measurement (2-12 hours) up to 10¹⁹ sweeps were recorded, stored in a CAT and the averaged signal read out digitally.

Electron paramagnetic resonance (EPR) measurements were performed on a Varian E3 or E6 EPR spectrometer (X-band) equipped with a device to allow sample cooling with cold N₂ gas. The range of microwave power used was 0.5 - 20 mW, with a modulation of 1 gauss, and a time constant of 0.3 - 1.0 s. The cavity could be illuminated with high intensity blue light (Xe lamp with CuSO₄ filter). For measurements at 20 K the E6 was equipped with a He cryostat and higher microwave powers (20-40 mW) were used.

P700 absorbance difference measurements were carried out at room temperature and at 77 K, for CPI in gel slices and for CPI extracted from the gel by grinding at 0°C in a mortar with buffer and carborundum powder. At room temperature, for the extract a ferricyanide minus ascorbate chemical difference spectrum could be made, whilst P700 in gel slices could be best measured from light-induced bleaching, using a modified Aminco spectrophotometer equipped with side illumination (blue-green actinic light, Schott BG12, 4 mm + BG18, 4 mm), after preincubation of the gel slices with 0.5 mM methylvio-

logen and 5 mM ascorbate. The molar extinction coefficient of $64\ 000\ \text{cm}^{-1}$ reported by Hiyaama and Ke [11] was used. For absorbance kinetic measurements at 77 K dark-adapted gel slices were preincubated at 4°C in a saturated sucrose solution, so that on freezing they remained non-scattering. The change in the absorbance difference between a given wavelength and the reference wavelength (800 nm) was measured on side illumination with red actinic light (675 nm). In order to overcome interference from prompt fluorescence, measuring and actinic light beams were allowed to fall on the sample alternately through a chopper (frequency 2 kHz).

Results

In Fig. 1 the pattern of pigmented bands (unstained) seen on gel electrophoresis in phosphate buffer (A) and tris-glycine (B) is shown. The two closely-spaced bands in (A) often merge into one broad band. The fast-running yellow-brown band (often seen together with a blue phycocyanin band, and also containing free chlorophyll) is characteristically intense in phosphate gels and may indicate a preferential removal of carotenoids from the chlorophyll proteins by phosphate. It is possible that bands 2-4 represent different oligomers of CPI (e.g. monomer, dimer and tetramer).

The procedure for SDS incubation and tris-glycine gel electrophoresis described here allows us to prepare chlorophyll-proteins from *Synechococcus* with the appearance of relatively little free chlorophyll (i.e. not bound to protein).

The chlorophyll-protein bands were characterized by their fluorescence emission spectra (Fig. 1). In phosphate both bands a and b showed a pronounced long wavelength emission band (we shall denote this fluorescence as F720 although the wavelength of maximum emission was found to differ for *S. cedrorum* and *S. leopoliensis* and also to shift slightly from preparation to preparation). In tris-glycine band 1 showed an emission maximum at 680 nm with very little F720, whilst 2-4 gave pronounced F720 emission, 5 showed a maximum at 685 nm with very little F720. In general, electrophoresis in phosphate buffer led to higher F720/F680 ratios in the chlorophyll-proteins compared to tris-glycine electrophoresis.

It should be stressed that the CPI fractions were found to be

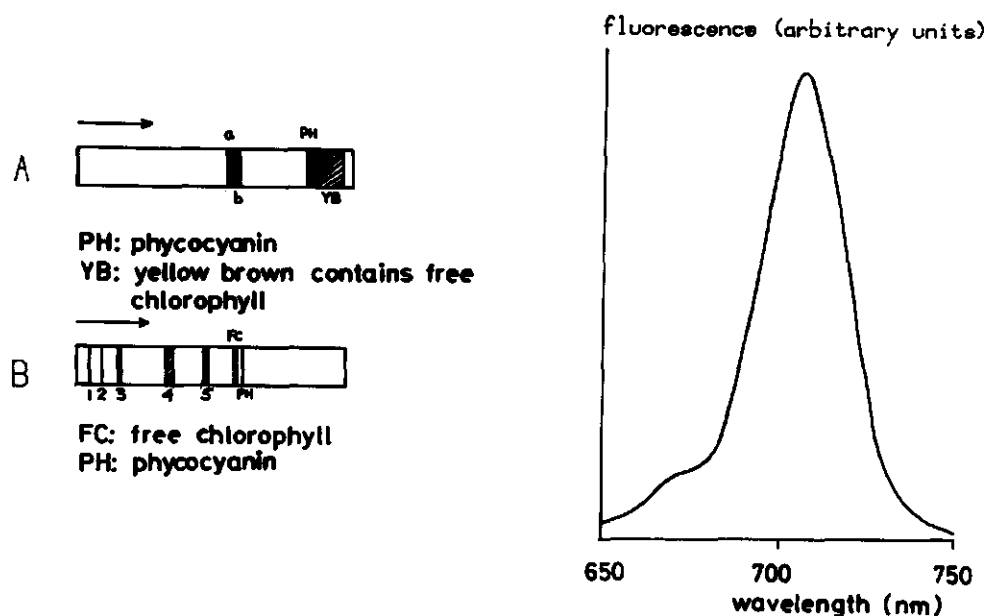


Figure 1 Unstained gel electrophoresis pattern in (A) phosphate buffer and (B) tris-glycine. Also the fluorescence emission spectrum of bands a+b (CPI) from *S. leopoliensis* at 77 K is shown.

rather stable whilst remaining in the gel, as judged by the fluorescence emission spectrum at 77 K: little change occurred in the ratio F720/F680 over a period of 1-2 days at 0°C in the dark. On the basis of these emission data we attribute bands a and b, and 2-4 to photosystem I chlorophyll (see for example ref. 12), and we shall denote them all as CPI. The isolation from *Synechococcus* of low molecular weight CPI fractions, which have pronounced F720 emission and minimal fluorescence at 680-685 nm is an indication of the close association of F720 with the antenna chlorophyll in the immediate environment of the PSI reaction centre.

The CPI fractions present in gel slices were investigated for an ODMR signal in the 720 nm fluorescence band. After measurements on the various CPI fractions (shown in Fig. 1) prepared from *S. cedrorum* and *S. leopoliensis* we conclude that the ODMR signal can only be detected in CPI from *S. leopoliensis* prepared by electrophoresis

in phosphate buffer. We have not detected an ODMR signal at 720 nm in CPI from *S. cedrorum*, nor from CPI prepared by electrophoresis in tris-glycine buffer.

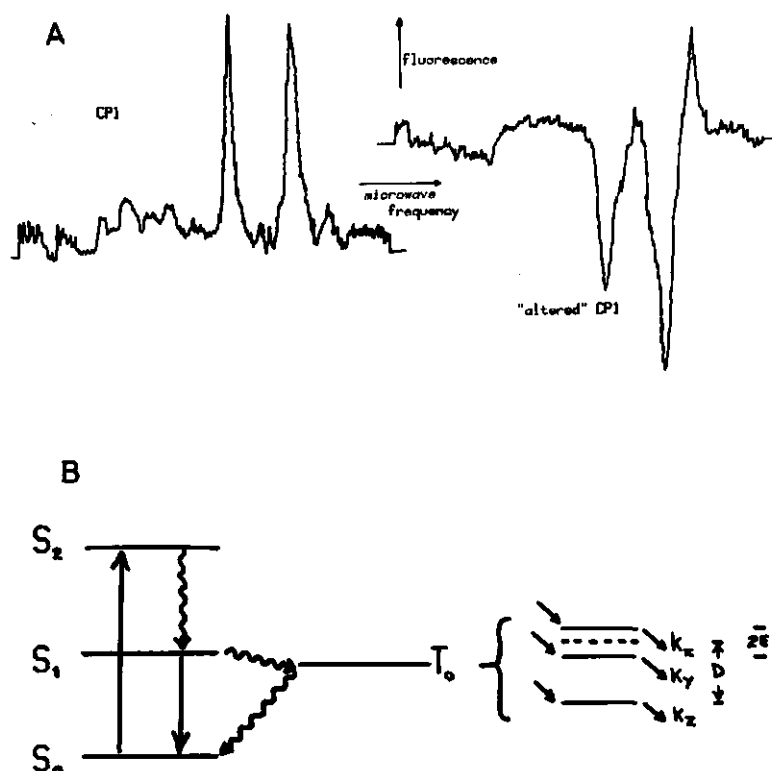


Figure 2a ODMR spectra at 4 K of CPI from *S. leopoliensis* prepared in phosphate buffer. Microwave frequency scan 0-1300 MHz.

Figure 2b Levelscheme for ODMR experiments.

Fig. 2a shows an ODMR spectrum of CPI from *S. leopoliensis* in F720, appearing as an increase ('up' signal) in the chlorophyll fluorescence yield at the resonant microwave frequencies 735 ± 5 (D-E) and 985 ± 5 (D+E) MHz. For definitions of D, E and kinetic constants, see Fig. 2b. The ODMR spectrum measured in the 685 nm emission band of a non-CPI chlorophyll protein is distinct from the CPI F720 ODMR spectrum in two respects: the chlorophyll fluorescence yield decreases ('down' signal) at the microwave resonant

frequencies, and also the frequencies are usually shifted slightly. This shift is, however, small and may be positive or negative compared to the 'up' signal, which suggests that the chlorophyll forms present in the triplet state in the two cases are very similar, i.e. monomeric (although a completely plane parallel dimer of chlorophyll would also show similar frequencies). When the 'up' and 'down' signals are measured simultaneously in the same sample (an 'altered' CPI showing F680 in addition to F720), there is a small but significant difference between the frequencies of the 'up' and the 'down' signals. This suggests that the 'up' ODMR signal does not arise from the same chlorophyll triplet population that gives rise to the 'down' signal.

The average lifetime of the three triplet sublevels in CPI has been estimated using a modulated light source as described by van Dorp et al. [13]. Both $|x\rangle \rightarrow |z\rangle$ and $|y\rangle \rightarrow |z\rangle$ transitions are stimulated simultaneously by microwave irradiation to equalize the population of all three sublevels, and the small decrease in the fluorescence intensity during the light-on period is ascribed to a build-up of the total triplet population. Although we have difficulty in saturating with microwave power, initial measurements in the 720 nm fluorescence emission band indicate a triplet lifetime for chlorophyll in CPI at 4.2 K of 5-10 ms. The population/depopulation kinetics of the three triplet sublevels can also be estimated by maintaining the excitation light at a constant level in the ODMR apparatus, and applying a fixed frequency (one of the two resonant frequencies) microwave irradiation at a modulated amplitude. The recovery of the fluorescence to the original level on reducing the microwave power gives a measure of the depopulation rate constant of the lowest level (k_z), this being considerably smaller than those for the other levels (k_x and k_y). Initial measurements have been made on the 'altered' CPI (showing F680 as well as F720), at both resonant microwave frequencies for both 680 nm and 720 nm emission bands, and in all four cases the value for k_z was between 10 and 50 ms⁻¹. It is hoped to obtain more precise measurements to allow any difference between k_z for F680 and F720 to be observed - as this would be additional evidence that the ODMR signal in F720 does not arise from the same triplet population that gives rise to the ODMR signal in F680.

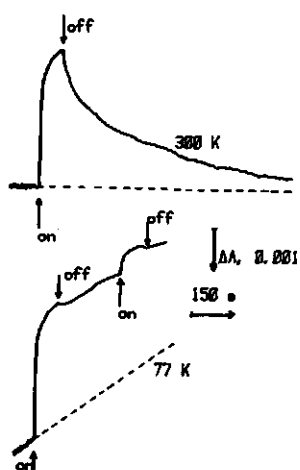


Figure 3a Light-induced absorbance changes at 705 nm in dark-adapted *S. leopoliensis* CPI (electrophoresis in tris-glycine). Actinic light on and off where shown.

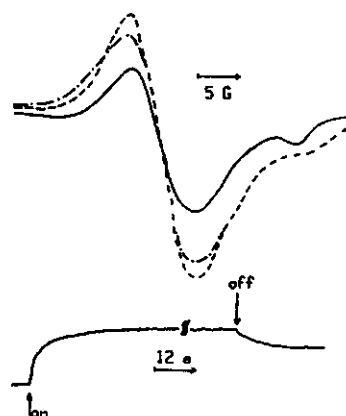


Figure 3b Light-induced spectra changes in the same gels at 110 K. Dark-adapted signal (—); signal after illumination (---); signal after a further dark period (-.-.). Intensity changes measured at the maximum.

Fig. 3 shows the P700 absorbance and EPR oxidation-reduction kinetics measured in CPI in gel slices prepared in tris-glycine buffer. At room temperature photo-oxidation of P700 on illumination of a dark-adapted sample is rapid (within the instrumental response) and the re-reduction in the dark is complete. At 77 K photo-oxidation is still rapid but re-reduction is incomplete (about 15%); warming to room temperature allows complete re-reduction. The EPR spectrum of CPI shows the typical signal of the $P700^+$ cation radical with a linewidth of 8.5 gauss. The light-induced EPR signal at 110 K has a rapid risetime, and is only partially reversible in the dark (about 15%), as seen also for the absorbance changes.

Fig. 4 shows similar data for the phosphate prepared CPI, and it is seen that the P700 oxidation-reduction kinetics in this case are rather slow. At room temperature the light-induced absorbance decrease is fully reversible in the dark; however, at 77 K it is irre-

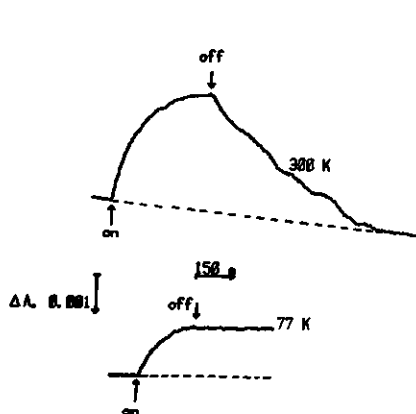


Figure 4a Light-induced absorbance changes at 697 nm in dark-adapted *S. leopoliensis* CPI (electrophoresis in phosphate buffer). Actinic light on and off where shown.

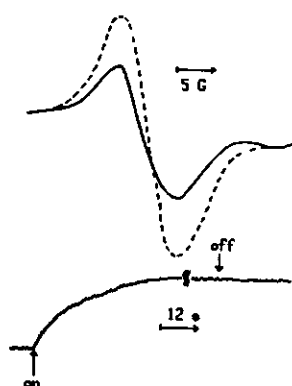


Figure 4b Light-induced EPR spectra changes in the same gels at 110 K. Dark-adapted signal (—) and signal after illumination (---). Intensity changes were measured at the maximum.

versible (although warming to room temperature allows complete re-reduction), and moreover the extent of P700 oxidation in the light is less than at room temperature. In the EPR experiment at 110 K dark-adapted CPI shows a slow growing-in of the light-induced signal, which is irreversible in the dark - in good agreement with the absorbance measurements.

We have also investigated the possible role of carotenoids in the quenching of chlorophyll triplet states in CPI, and Fig. 5 shows the absorption spectra of CPI fractions which have been extracted out of the gel to allow a comparison of their spectra in the region 450-500 nm without any distortion from scattering and self-shielding. The same sample of SDS-treated thylakoid extract was electrophoresed in tris-glycine or phosphate buffer containing gels. It is apparent that electrophoresis in phosphate causes an appreciable loss of carotenoids from the CPI compared to tris-glycine.

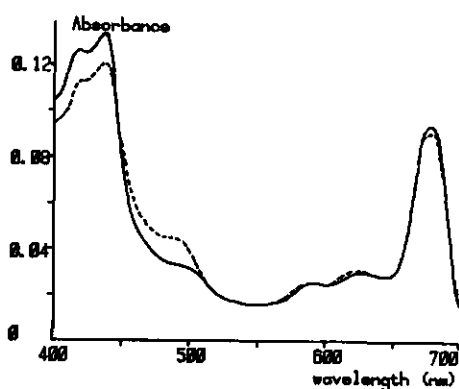


Figure 5 Absorption spectra of CPI from *S. leopoliensis* extracted out of the gel after electrophoresis in phosphate buffer (—) or tris-glycine (---).

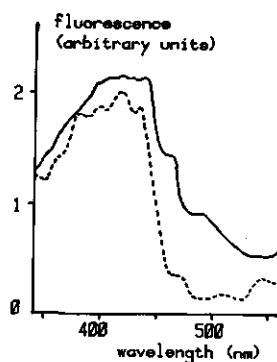


Figure 6 Chlorophyll fluorescence excitation spectra for emission at 715 nm (—) and 675 nm (---) from *S. leopoliensis* CPI (phosphate buffer).

The carotenoid composition of the CPI preparations has not been measured; however, we have investigated the β -carotene content specifically through chlorophyll fluorescence excitation spectra. β -carotene is reported to be the only carotenoid which transfers excitation energy to chlorophyll [12]. The excitation spectra for emission at 715 and 675 nm for CPI prepared in phosphate buffer is shown in Fig. 6. It is apparent from the pronounced peaks at 470 and 500 nm that β -carotene is present in this preparation of CPI which shows ODMR-detectable triplets. CPI prepared in tris-glycine also shows similar spectra. A striking feature is the ability of β -carotene to transfer energy to the chlorophyll form emitting at 715 nm, but the absence of any contribution to 675 nm emission.

The molecular weights of the CPI preparations have been estimated from their mobilities on the electrophoresis gel and the appearance of ODMR-detectable chlorophyll triplets appears to be related to the loss of some protein (carotenoid-protein?). CPI prepared from *S. leopoliensis* in tris-glycine has a molecular weight of 165,000 kD, and this decreases to 85,000 kD in phosphate buffer. The CPI prepared in phosphate buffer from *S. cedrorum*, which shows no ODMR signal, has a molecular weight of 110,000 kD.

Discussion

In tris-glycine gels the rapid photo-oxidation of P700 in CPI at 77 K (Fig. 3) indicates the presence of the electron acceptor A (and maybe also B). If we extrapolate the findings at 77-110 K to 4 K for tris-glycine prepared CPI - and this is probably valid as the rapid kinetics indicate a more or less intact electron acceptor chain so that the oxidation-reduction kinetics should be temperature-independent below about 100 K (see for example ref. 14) - then P700 will be completely oxidized under the conditions of the ODMR experiment. As $P700^+$ is a radical it can stimulate intersystem crossing so that the presence of the PSI reaction centre in the oxidized form is probably the cause of the absence of chlorophyll triplet states in tris-glycine-prepared CPI, whether the triplets are located near the reaction centre or in the antenna chlorophyll.

On the other hand, in phosphate-prepared CPI the P700 oxidation-reduction kinetics are very slow at 77-110 K, indicating the loss of or disruption of the components of the electron acceptor chain, and, moreover, the irreversibility of the photo-oxidation of P700 at 77 K (Fig. 4) indicates that even the primary acceptor A_1 is not functioning normally. Under these circumstances it is not justifiable to extrapolate our findings at 77 K to 4 K, and the oxidation state of P700 in the phosphate-prepared CPI under the conditions of the ODMR experiment is therefore still uncertain. However, it can be concluded that the chlorophyll triplets observed in ODMR cannot arise by a radical pair mechanism.

Mathis has demonstrated the ability of carotenoids to quench chlorophyll triplets [15] and we have presented evidence that quenching by a carotenoid (not β -carotene) could be occurring in CPI. The identity of the carotenoid responsible has not been established, but *Synechococcus* is known to contain hydroxylated carotenoids (xanthophylls) in large amounts [16]. The carotenoid content of the algae could be a source of variability in the triplet level in the isolated CPI, as it is strongly dependent on physiological growth conditions [17], and carotenoid in tris-glycine prepared CPI could be a contributory cause of the absence of ODMR signals.

The contribution of β -carotene to fluorescence emission at 720 nm

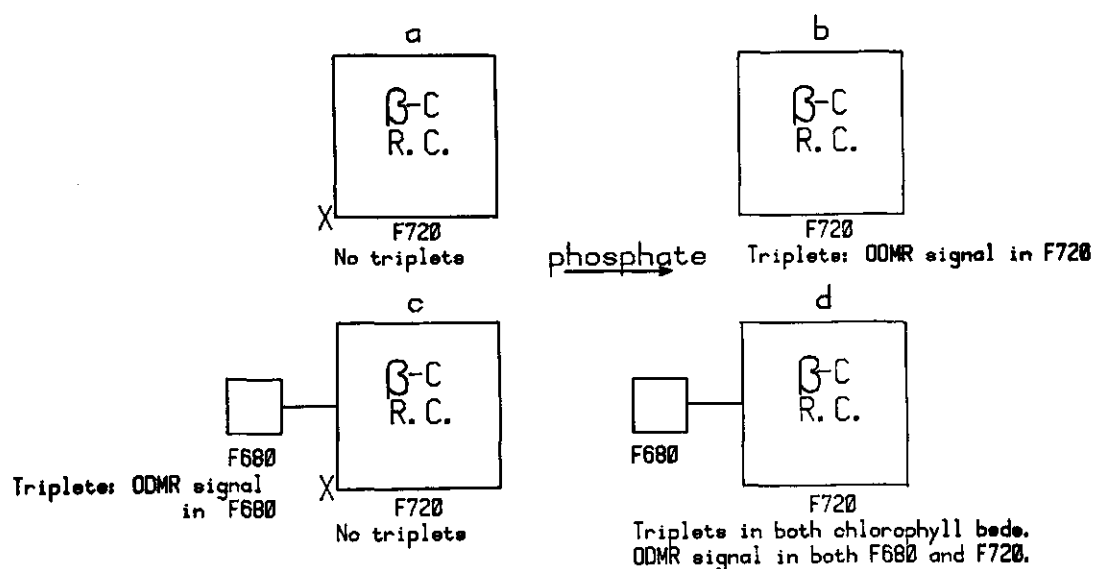


Figure 7 Proposed model for energy transfer in CPI.

R.C.: reaction centre (P700).

β -C : β -carotene

X : xanthophyll, or other unknown quenching species (c) and (d) represent 'altered' CPI in which short wavelength emission (F680) is present in addition to F720

but not to that at 680 nm is also a valuable piece of information in constructing a model for energy transfer in CPI (Fig. 7).

In Fig. 7, (a) and (b) differ from (c) and (d) in that one or more of the chlorophyll molecules in CPI has become 'unfolded' or isolated from the bulk of the chlorophylls. Situations (b) and (d) differ from (a) and (c) in that the chlorophyll triplet quencher X is no longer bound to the periphery of the CPI particle. As energy transfer between isolated and bulk chlorophylls does not occur in (c), the F680 triplet is not quenched by X. From this model we can also understand why energy absorbed by β -carotene is not transferred by singlet energy transfer to F680 (i.e. no contribution of carotenoid to the F680 fluorescence excitation spectrum, see Fig. 6). The β -carotene at the reaction centre can transfer energy to the F720 emitting dimers in the bulk, but energy transfer to the isolated chlorophyll is prevented.

The isolated chlorophyll is not detached from the CPI, but is connected to the rest of the particle through a polypeptide chain, which has become unfolded, thus giving rise to the 'altered' CPI. Because of its isolation this chlorophyll should have properties similar to that of chlorophyll *in vitro*, including a high triplet yield, a long fluorescence lifetime (~ 4 ns) and fluorescence emission at ~ 680 nm. However, because it is still protein-bound, its absorption spectrum should not differ significantly from that of the bulk chlorophyll. Interestingly the group of Gross has found that the ionic composition of the medium can indeed affect energy transfer in CPI (as seen by chlorophyll fluorescence yield changes), and also affect protein tertiary structure [18].

An alternative model to that shown in Fig. 7 is one in which the triplet state of the 'unfolded' chlorophyll is responsible for both ODMR signals (at F680 and F720). In this model, the 'unfolded' chlorophyll cannot be completely isolated with regard to energy transfer and the resonant microwave frequencies and triplet kinetics in F680 should be identical.

The size and sign of the ODMR signal is not only dependent on the total triplet population but also on the relative populations of the three triplet sublevels [19]. It is possible that interaction between chlorophyll molecules and the amino acid side groups of the protein, or between chlorophyll molecules themselves, could

give rise to a different relative population of these levels to that measured for chlorophyll *in vitro*.

References

1. S.J. van der Bent, T.J. Schaafsma and J.C. Goedheer (1976). Biochem.Biophys.Res.Comm. 71: 1147-1152.
2. A.J. Hoff and J.H. van der Waals (1976). Biochim.Biophys.Acta 423: 615-620.
3. W.W. Parson, R.K. Clayton and R.J. Cogdell (1975). Biochim.Biophys.Acta 387: 265-278.
4. A.J. Hoff, Govindjee and J.C. Romijn (1977). FEBS Lett. 73: 191-196.
5. G.H. van Brakel, unpublished results.
6. T. Ogawa and L.P. Vernon (1970). Biochim.Biophys.Acta 197: 292-301.
7. W.A. Kratz and J. Myers (1955). Am.J.Bot. 42: 282-287.
8. G. MacKinney (1941). J.Biol.Chem. 140: 315-322.
9. K. Weber, J.R. Pringle and M. Osborn (1972). In: Methods in Enzymology, Vol XXVI. Eds: C.H.W. Hirs and S.N. Timasheff. Academic Press, New York. pp. 3-27.
10. S.J. van der Bent, A. de Jager and T.J. Schaafsma (1976). Rev. Sci.Instrum. 47: 117-121.
11. T. Hiyama and B. Ke (1972). Biochim.Biophys.Acta 267: 160-171.
12. J.C. Goedheer (1969). Biochim.Biophys.Acta 172: 252-265.
13. W.G. van Dorp, W.H. Schoemaker, M. Soma and J.H. van der Waals (1975). Mol.Phys. 30: 1701-1721.
14. P. Mathis, K. Sauer and R. Remy (1978). FEBS Lett. 88: 275-278.
15. P. Mathis (1969). Photochem.Photobiol. 9: 55-63.
16. H. Stransky and A. Hager (1970). Arch.Mikrobiol. 72: 84-96.
17. J.C. Goedheer (1976). Photosynthetica 10: 411-422.
18. E.L. Gross and J. Grenier (1978). Arch.Biochem.Biophys. 187: 387-398.
19. S.J. van der Bent (1977). Thesis. Wageningen.

4.3 ODMR OF ALGAE

The triplet state of Chl-a was first detected by van der Bent et al. [1] in whole algal cells by use of the ODMR technique.

An ODMR spectrum of the cyanobacterium *Anacystis nidulans* is shown in Fig. 4.1. A similar spectrum of the green alga *Scenedesmus obtusiusculus* detected in the region 716-736 nm (see Fig. 4.4) is presented in Fig. 4.3. The D and E values and detection wavelengths of various algae are listed in Table 4.1a, together with some results for one mutant alga, for CPI isolated from *A. nidulans*, and for Chl-a *in vitro*. From this table it is evident that the triplets can be assigned to Chl-a. The 4.2 K fluorescence spectra of *A. nidulans* and *S. obtusiusculus* are presented in Figs 4.2 and 4.4. For experimental details, see §§2.2 and 2.6. In *A. nidulans* the triplet is detected only in the 719 nm fluorescence band. Detecting in the region of the other fluorescence peak (672 nm) does not produce ODMR signals of Chl-a triplets. Similarly, in *S. obtusiusculus* ODMR signals are only detected in the 726 nm band and not in the 696 nm band. The fluorescence bands at 719 nm (Fig. 4.2) and 726 nm (Fig. 4.4) arise from Chl-a, and are generally ascribed to Chl-a belonging to PSI [4]. The 672 nm fluorescence in *A. nidulans* mainly originates from phycocyanin, whereas also some light-harvesting pigments contribute to this band [4].

During the first stages of the project, it appeared that triplets in *A. nidulans* are only detected when DCMU is added, in a concentration $>10^{-5}$ M. Till now, it has remained obscure, however, why adding DCMU helps in detecting the Chl-a triplet. Its function is clearly not to block electron flow between PSI and PSII, for such electron transport has so far not been demonstrated at 4.2 K. Furthermore, other agents, which are also known to block electron transport between both photosystems, do not give rise to detectable amounts of triplets. Table 4.2 compiles the results of adding several agents, as well as the effect of preillumination prior to freezing, upon the detectability of triplets.

It appeared, that it is sometimes possible to detect triplets in *S. obtusiusculus* and always in *S. C-6E* without adding DCMU. To confuse the situation even more, in wild type algae occasionally no triplets are detected at all, DCMU added or not. This may be caused

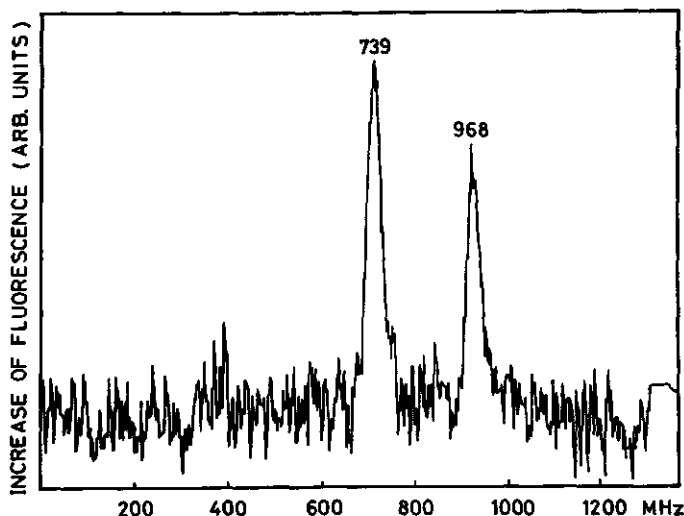


Figure 4.1 ODMR spectrum of a frozen aqueous suspension of *Anacystis nidulans* whole cells. $T = 4.2$ K. Detection wavelength 719 nm; bandwidth 20 nm. Microwave power ~ 40 mW. Sweep rate 1300 MHz/S. $[DCMU] = 10^{-5}$ M. Number of accumulated spectra 2^{15} .

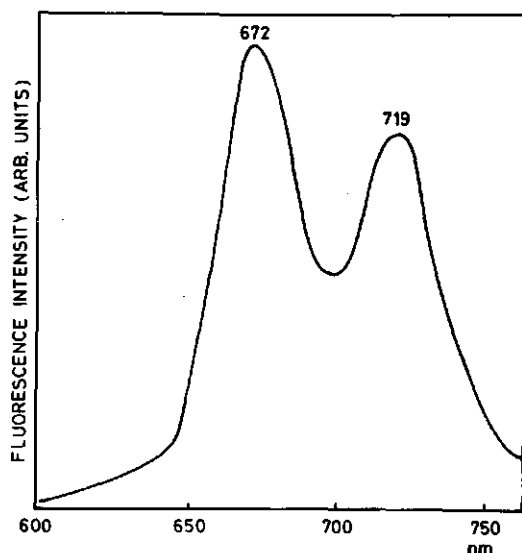


Figure 4.2 Fluorescence spectrum of a frozen aqueous suspension of *Anacystis nidulans* whole cells. $T = 4.2$ K. Detection bandwidth 20 nm. The excitation profile is given in §2.6.

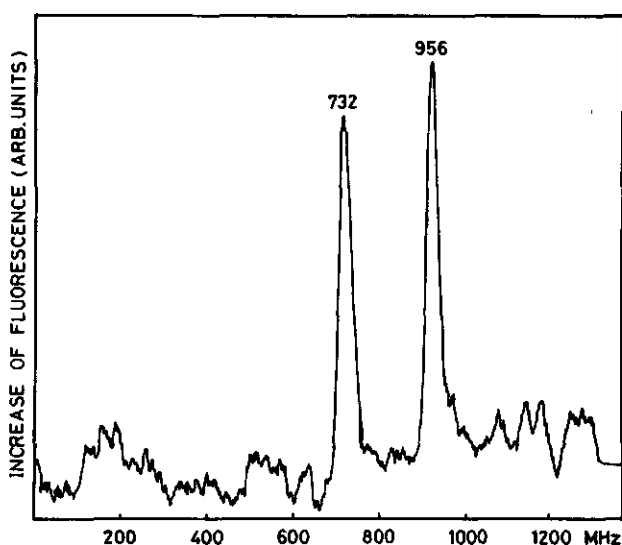


Figure 4.3 ODMR spectrum of *Scenedesmus obtusiusculus* wild type whole cells. Detection wavelength 726 nm. Other experimental conditions as in Fig. 4.1.

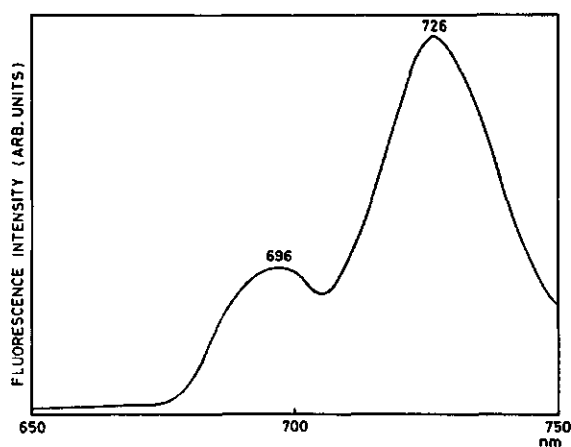


Figure 4.4 Fluorescence spectrum of *Scenedesmus obtusiusculus* wild type whole cells. Experimental conditions as in Fig. 4.2.

Table 4.1a Zero-field splitting parameters of Chl-a at 4.2 K

Species	$\lambda_f^a)$ (nm)	$D^b)$ ($\times 10^{-4} \text{ cm}^{-1}$)	$E^b)$ ($\times 10^{-4} \text{ cm}^{-1}$)	Ref.
<i>Anacystis nidulans</i>	719	280	40	
<i>Scenedesmus obtusiusculus</i>	726	281	38	
<i>Scenedesmus</i> mutant C-6E	713 ^{c)}	286	39	
	693	287	38	[2]
	688	282	38	
<i>Porphyridium cruentum</i>	~ 720	283	37	[1]
<i>Euglena gracilis</i>	~ 720	297	37	[1]
<i>Chlorella</i>	~ 720	288	38	[1]
CP-I (from <i>A. nidulans</i>)	716	280	38	
	684	286	38	
(Chl-a.H ₂ O) ₂ in n-octane	725	286	31	[3]
Chl-a.Pyr ₂ in n-octane	686	283	40	[3]

a) detection fluorescence wavelength region

b) the accuracy of D and E is $5 \times 10^{-4} \text{ cm}^{-1}$

c) in the absence of DCMU.

Table 4.1b Zero-field splitting parameters of the species observed by ODMR at 713 nm in *Scenedesmus* C-6E in the presence of DCMU

Species	$\lambda_f^a)$ (nm)	$D^b)$ ($\times 10^{-4} \text{ cm}^{-1}$)	$E^b)$ ($\times 10^{-4} \text{ cm}^{-1}$)	Ref.
S. C-6E	713	338	44	
Pheophytin-a in MTHF	(ESR)	341	33	[5]

a) fluorescence detection wavelength

b) accuracy $\pm 5 \times 10^{-4} \text{ cm}^{-1}$

Table 4.2 Effect of various inhibitors and preillumination on Chl-a triplet detection in *Anacystis nidulans*

Inhibitor	Physiological effect	Effect on triplet detection ^{a)}
DCMU	blocks electron transport between PSI and PSII	+
DBMIB	"	-
KCN	"	-
dithionite	universal reductant	+
ferricyanide	artificial acceptor for PSI, oxidizes P700 (in the dark)	-
DCPIP/asc/DCMU	maintains P700 in the reduced state	+

preillumination	oxidizes P700	-

a) + = triplet observed by ODMR

- = no triplet observed by ODMR

by growth conditions or seasonal effects, although care has been taken to standardize procedures.

The divergence in the effects of agents both reducing or oxidizing P700 (see Table 4.2) is another indication, that we are not observing triplets arising from P700, as argued in §4.2.

Finally, we note that the fluorescence intensity of frozen algae suspensions, used in ODMR experiments, is not related to the total number of algal cells in the sample, because we have employed front-surface excitation, avoiding self-absorption effects. The fluorescence spectra have not been corrected for photomultiplier spectral response.

For the ODMR spectrum of *S. C-6E* whole cells we refer to §3.3.4. The ZFS values of Chl-a in this alga detected at various fluorescence wavelengths have been included in Table 4.1a. The corresponding 4.2 K fluorescence spectrum of this alga is presented in Fig. 4.5.

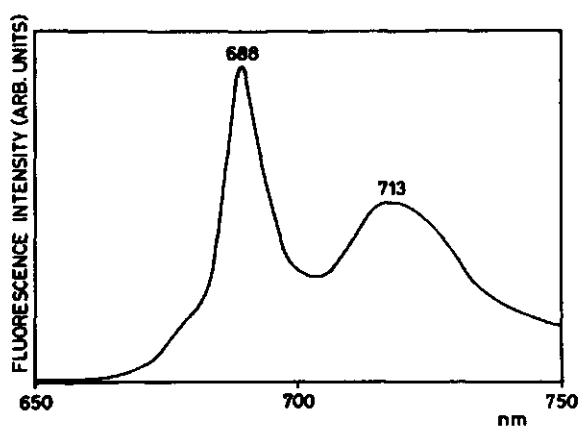


Figure 4.5 Fluorescence spectrum of *Scenedesmus* C-6E mutant whole cells. Experimental conditions as in Fig. 4.2.

The fluorescence spectra, shown in Figs 4.2, 4.4 and 4.5, have been obtained at low resolution (20 nm), corresponding to the detection bandwidth of ODMR spectra. This rather large bandwidth was necessary to obtain an acceptable S/N ratio in ~4 hrs accumulation time, using a signal averager, as described in §2.6, for ODMR Spectra.

The low temperature fluorescence spectra contain more structure than is revealed by Figs 4.2, 4.4 and 4.5, as is demonstrated by a 2 nm resolved fluorescence spectrum of *A. nidulans* and *S. obtusiusculus* (Figs 4.6 and 4.7).

In the presence of DCMU, *S. C-6E* exhibits a new ODMR spectrum detected at the 714 nm band, replacing that of Chl-a, detected at the same wavelength, in the absence of DCMU (see Table 4.1a). ZFS values derived from this new ODMR spectrum are presented in Table 4.1b, together with ZFS values of pheophytin-a *in vitro*.

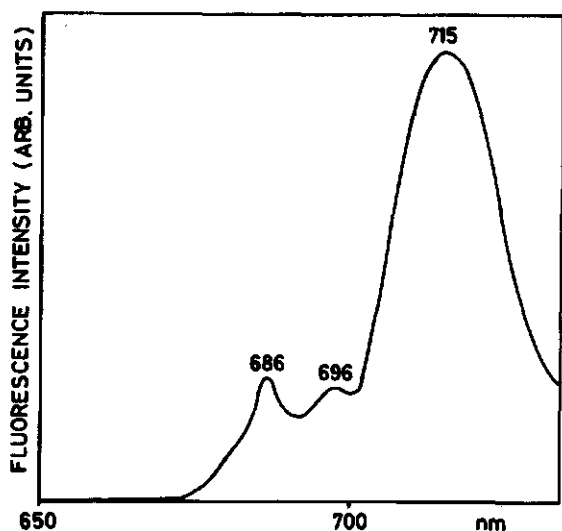


Figure 4.6 Fluorescence spectrum of a frozen aqueous suspension of *Anacystis nidulans* whole cells. $T = 4.2$ K. Detection bandwidth 2 nm.

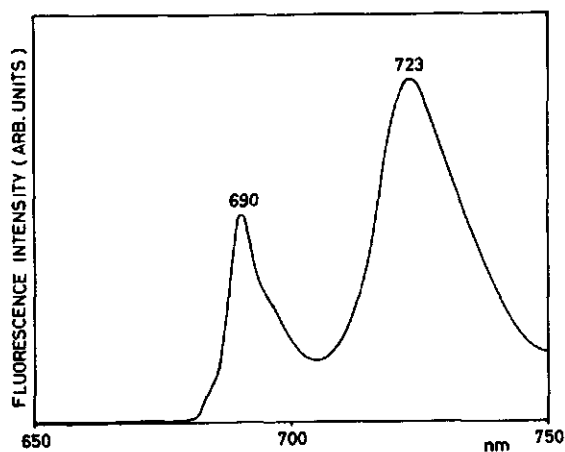


Figure 4.7 Fluorescence spectrum of a frozen aqueous suspension of *Scenedesmus obtusiusculus* whole cells. $T = 4.2$ K. Detection bandwidth 2 nm.

$$I_f(0) = N k_{ex} \phi_f \quad (4.7)$$

and

$$I_f(\infty) = I_f(0) \frac{k_T}{k_T + k_{ex}\phi_T} \quad (4.8)$$

The last equation permits the calculation of the decay constant k_T , corrected for the effect of excitation $k_{ex}\phi_T$:

$$k_T = (k_T)_{\text{measured}} \cdot \frac{I_f(\infty)}{I_f(0)} \quad (4.9)$$

Thus, by adjusting the exciting light intensity, we are able to approach the value of k_T as close as is practical by the S/N ratio for a given duration of the experiment. In practice, we have used neutral density filters, such that $k_{ex} \leq 250 \text{ s}^{-1}$. Assuming that $\phi_T \leq 0.5$ for Chl-a, eqn (4.9) predicts, that the measured decay constant deviates $\sim 10\%$ from the real value k_T of $\sim 1000 \text{ s}^{-1}$ for Chl-a.

A similar treatment as given above applies to the case, where we take into account the presence of three sublevels in T_0 . Now the $I_f(t)$ curve contains $k_i + \phi_T^i \cdot k_{ex}$ ($i = x, y, z$), analogous to (4.4c). It is evident, that the largest deviation from the real value of k_i occurs for the level with the largest ϕ_T^i if $k_{ex} \neq 0$.

The amplitudes c_3^i ($i = x, y, z$) in $I_f(t)$ in fact are a direct measure for the steady-state populations $n_i(\infty)$, as can be seen from (4.6). However, the decay constant of a particular triplet sublevel cannot be determined from the FF curve, if it does not carry any population, e.g. because ϕ_T for that level is close to zero. In this respect the FF method is more limited than the microwave induced fluorescence response method.

In the FF experiments, described in this chapter, we have employed a chopped laser beam, such that the leading edge of the excitation pulse has a risetime of $\sim 0.5 \text{ ms}$. Analysis of the effect of this limited time resolution on measured decay constants and amplitudes (steady-state populations) has revealed, that decay constants can be measured, which are significantly larger than the reciprocal

risetime of the excitation pulse. Naturally, the accuracy of measured decay constants continuously decreases in that region. This automatically shows up by the use of a non-linear exponential fit-program, containing standard deviations. The amplitudes, however, are affected in a systematic way, and increasingly come out too low, if the measured decay constant more and more exceeds the reciprocal risetime of the excitation pulse.

For the microwave induced change of fluorescence intensity $\Delta I_f(t)$, of a system of chlorophyll-proteins under continuous illumination with exciting light, under ODMR conditions, the following relations have been derived [10].

Microwaves on:

$$\Delta I_f(t) = \alpha \{ e^{-\frac{1}{2}(k_x + k_y)t} - 1 \} \quad (4.10)$$

Microwaves off:

$$\Delta I_f(t) = \beta \left\{ \frac{1}{k_x} e^{-k_x t} - \frac{1}{k_y} e^{-k_y t} \right\} \quad (4.11)$$

for application of microwaves resonant with the transition between triplet sublevels $|x\rangle$ and $|y\rangle$. Similar expressions are valid for $|x\rangle \leftrightarrow |z\rangle$ and $|y\rangle \leftrightarrow |z\rangle$ transitions. In (4.10) and (4.11) k_i have been defined before, α and β are proportionality constants, containing instrumental parameters, kinetic constants of the $S_0 \rightarrow S_1$ process and the $T_0 \rightarrow S_0$ process and the steady-state populations of the individual triplet sublevels. It is assumed, that the intensity of the exciting light is sufficiently low to linearize the kinetic equations and that the microwave power is sufficiently high for immediate saturation of the transition.

Again the fluorescence curves $\Delta I_f(t)$ can be fitted to a multi-exponential by a non-linear computer program.

4.4.2 Results

The kinetic constants, obtained for the CP-I complex and *Scenedesmus* C-6E, by the two methods, described in §4.4.1, of fluorescence fading (FF) and microwave induced response of fluorescence (MIRF), are given in Table 4.3.

Unfortunately, the S/N ratio was too low to allow an accurate determination of steady-state populations.

In Table 4.3 some published data have been included, on *in vitro* Chl-a, for comparison with our results.

Table 4.3 Decay rate constants^{a)} of the three triplet sublevels of Chl-a at 4.2 K

System	$\lambda_f^{b)}$ (nm)	$\lambda_d^{c)}$ (nm)	k_x (s ⁻¹)	k_y (s ⁻¹)	k_z (s ⁻¹)	Method ^{d)}	Ref.
<i>Scenedesmus</i> C-6E	688	693	730± 80	1010± 150	410±30	MIRF	this work
"	688	693	530±250	970± 250	170±25	FF	this work
"	713	-	-	-	-	-	e)
CPI-I	684	684	520±150	3400±1000	120±40	MIRF	this work
	715	715	870±200	2250± 450	240±50	MIRF	this work
n-octane	- ^{f)}	- ^{f)}	661± 89	1255± 91	241±15	MIRF	[6]
ethanol	-	-	710±100	2710± 100	370±50	ESR ^{g)}	[5]
MTHF	(687) ^{h)}	-	620± 80	1120± 20	140±40	ESR ^{g)}	[5]

a) Uncorrected for effects of non-zero excitation intensity (see §4.4.1). Correction mainly affects k_x and k_y by an amount of <6%.

b) fluorescence maxima

c) fluorescence detection wavelengths

d) FF = fluorescence fading

MIRF = microwave induced response of fluorescence

e) S/N too low for kinetic experiment

f) Not quoted

g) Data obtained at 100 K

h) Chl-a·2H₂O [3].

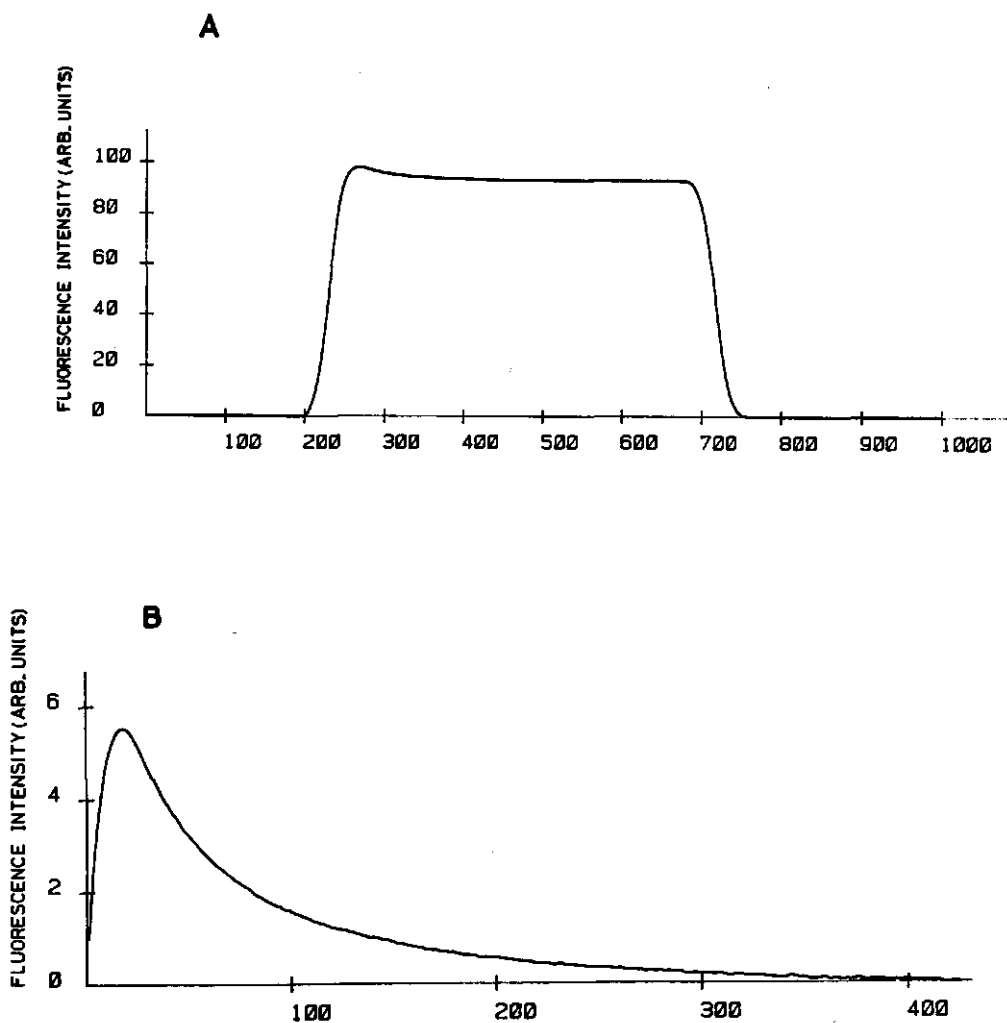


Figure 4.8 Fluorescence fading curves for *Scenedesmus* C-6E at 4.2 K, the response of luminescence to a rectangular excitation pulse. Timescale: 100 units corresponds to 4 ms. In Figure B the steady-state fraction (see Figure A) has been subtracted
Chopping frequency: 20 Hz. Excitation pulse width: 20 ms. Number of accumulated traces: 10^5 .

As an example of the results of an experiment using the FF method, Fig. 4.8 shows the FF curves obtained for *Scenedesmus* C-6E, where the precaution has been taken to diminish the excitation light intensity, to such extent, that the steady-state triplet population was $\leq 10\%$ of the population of the ground state, i.e.

$$\frac{I_f(\infty)}{I_f(0)} \geq 0.9 \text{ (see eqn (4.9))}.$$

Table 4.3 shows that significant differences occur only for k_y . To find information about effects on the other kinetic constants, more accurate measurements are needed. In §1.5 it was concluded that effects on kinetic constants by ligation to the ring V-keto group of Chl-a are expected to have a larger effect on k_x and k_y than on k_z . Here it appears that k_y is affected most.

On comparison of the data for CP-I and *S. C-6E*, a significant difference is seen for the k_y . The k_y of CP-I is in line with that of Chl-a in ethanol solution, while the k_y of *S. C-6E* agrees with that of Chl-a in n-octane. The fluorescence spectra of CP-I and *S. C-6E* algae (Fig. 1 of §3.2 and Fig. 4.5) show small differences in their fluorescence maxima.

4.5 DISCUSSION

The first question we want to address here is: where is the triplet detected in whole algal cells located within the photosynthetic system?

The fact that these triplets are only detected in the 715 nm fluorescence band in *A. nidulans* (726 nm in *S. obtusiusculus*), a wavelength region ascribed to PSI pigments, is a first indication, that these triplets are located in PSI. The CP-I complex, isolated from *A. nidulans* and found to have PSI activity, exhibits the same fluorescence band at 715 nm and triplet ODMR signals are found, when detecting in this band, with ZFS values and signs identical to those of the parent alga.

Also the behaviour of the two *Scenedesmus* mutants C-6E and # 8 confirm this assumption. In # 8 PSI is not active, and does not show any Chl-a triplet signals, whereas C6-E has no active PSII, but exhibits strong triplet signals.

For the question whether we see triplets of P700 or antenna pig-

ment Chl-a, we believe that our findings point to PSI antenna pigment, based on the following argument: Under the conditions of our experiment (low temperature, continuous illumination) P700 in CP-I complexes can be shown to be in the oxidized state (§4.2). Thus, the observed triplets cannot arise from P700. Strictly speaking, this argument can only be used, if the triplet detected in CP-I is the same as that found in whole algal cells, where we did not check the oxidation state of P700. It seems likely, however, that P700 is also oxidized in whole algae under our conditions in view of the similarity of the ODMR spectra at the same fluorescence wavelengths in both cases.

Furthermore, the following observations may be relevant, although they are certainly not completely understood: When the sample is preilluminated prior to freezing, in order to bring all P700 in oxidized state, no triplets are observed. The effect of addition of ferricyanide, which also oxidizes P700, is the same, while addition of dithionite and the combination of DCP/P/ascorbate/DCMU, which maintain P700 reduced, leads to observation of triplets. These observations cannot be reconciled with the effect of adding only DCMU, if one assumes, that the triplet state of P700 is observed. Also in this case P700 is oxidized, since DCMU prevents rereduction of $P700^+$ by electrons from PSII. Yet triplets are observed. Clearly the role of DCMU in the formation of triplets is still obscure.

We should also consider the possible role of carotenoids, abundantly available and known to be efficient triplet quenchers. An argument that carotenoids may play a role in our systems also, arises from the fact, that in *S. C-6E*, which is known to lack carotenoids, triplets are always observed in high yield, without any addition of DCMU.

In the CP-I complex prepared in TG buffer a large amount of carotenoid is still present, as judged from the absorption spectrum, and no triplets are observed, while in CP-I prepared in Pi buffer less carotenoid is present and triplets are detected (cf. the discussion in §4.2).

It is also striking, that the β -carotene, that is known to be associated with the RC, is present in both CP-I complexes, clearly has nothing to do with the presence of triplets in PSI, as detected by ODMR, again indicating that these triplets are located in the antennapigment system.

By comparison with *in vitro* data [3], the resonances of algae and the CP-I complex (see Table 4.1) can be assigned to triplet Chl-a, with ligands attached to it (see Table 4.4). The similarity of ZFS values for the various algae and the CP-I complex (see Table 4.1), indicates that we observe one and the same triplet in all systems.

Table 4.4 ZFS parameters as a function of fluorescence detection wavelength for Chl-a at 4.2 K

Species	I	II	III	IV
ligation ^{a)}	$\begin{array}{c} \\ \text{Chl} \end{array}$	$\begin{array}{c} \\ \text{Chl}- \end{array}$	$\begin{array}{c} \\ \text{Chl} \\ \end{array}$	$\begin{array}{c} \\ (\text{Chl})\text{Chl}- \\ \end{array}$
$\lambda_f^b)$ (nm)	669	684	688	715-725 ^{c)}
sign ODMR	-	-	+	+
decay constants k_x (s^{-1})	-	520 \pm 150	530 \pm 250	870 \pm 200
k_y (s^{-1})	-	3400 \pm 1000	970 \pm 250	2250 \pm 450
k_z (s^{-1})	-	120 \pm 40	170 \pm 25	240 \pm 50
$k_T^d)$ (s^{-1})	-	1350 \pm 200	560 \pm 120	1190 \pm 160
$D^e)$ (10^{-4} cm^{-1})	309	286 ^{f)}	282	280
$E^e)$ (10^{-4} cm^{-1})	42	38	38	40

a) Type of ligation of Chl-a in solution or *in vivo* systems. Vertical bars: Mg-ligands; horizontal bars: ring V-keto ligands. For species IV (Chl) means additional interaction with one or more other chlorophylls.

b) fluorescence wavelength

c) This wavelength varies over the indicated region for the wild type algae studied by us

d) mean decay rate constant of the triplet state

e) accuracy $\pm 5 \cdot 10^{-4}$ cm^{-1}

f) Although the ZFS values of species II-IV are equal within measuring error, in practice II and IV can be distinguished in spectra where both species occur. The difference in their ZFS values amounts to 20 MHz, i.e. $\sim 7 \cdot 10^{-4}$ cm^{-1} .

There is reason for caution in drawing this conclusion on the basis of ZFS values alone, however, since Chl-a species with very different fluorescence wavelengths have almost equal ZFS values (Table 4.1 and 4.4). The similarity of low-temperature fluorescence spectra of the investigated systems in the 680-725 nm region, on the other hand, also supports the assumption that the same species is observed.

Referring to Table 4.4, a remarkable discontinuity can be noted, if we compare the D values of species I-IV as a function of the fluorescence detection wavelength. Generally [11], a decrease of the S_1-S_0 energy gap correlates with a decrease in D. Species IV has a large red shift, which can only partly be explained by adding an additional ligand at the ring V-keto group of Species III (see discussion of Table 4.4 below).

There are two fundamentally different explanations for the deviating D value of the 715-725 nm species. First, we note that, if red shift to ~720 nm mainly arises through excitonic interaction between chlorophylls, this may not necessarily result in a decrease of the T_0-S_0 separation, and a decrease of D. Secondly, the triplet detected in the ~720 nm region may in effect correspond to a shorter fluorescence wavelength, such that energy transfer of this species to the 720 nm emitting collection of chlorophylls is allowed. This requires of course a finite overlap between the short wavelength emitting Chl-a species and the antenna pigment absorption. Also in this case, the D values of the 720 nm and the 684 nm species should be very similar (see Table 4.4).

It is uncertain if the appearance of a different triplet in S. C-6E treated with DCMU (Table 4.1b), is due to a photosynthetic pigment which is naturally present in the alga. The lack of carotenoid in this mutant may favour the photochemical formation of this new species, tentatively assigned to pheophytin-a, in view of its *in vitro* ZFS values (Table 4.1b). There are no published data justifying the assumption that pheophytin naturally occurs in PSI. It is conceivable however, that pheophytin-a present in PSII emits in a wavelength region permitting efficient energy transfer to the PSI antenna pigment. Although the *in vitro* emission maximum occurs at 675 nm [12], it may easily be shifted *in vivo* within reach of the antenna pigment absorption band, the geometrical distance between

both systems in the photosynthetic unit makes this possibility not very likely.

As a last remark to the results presented in §4.3, we note that no ODMR signals can be detected in the 684 nm region in *A. nidulans*, whereas the CP-I complex isolated from this alga does show these signals in the same region. As is evident from Fig. 4.6, the whole alga fluorescence spectrum contains maxima in the 685-695 region, some of which have been assigned to parts of the light harvesting pigment (LHP)[4], delivering its energy both to PSI and PSII. In the CP-I complex LHP is absent, so that part of the energy transfer chains in the 680-720 nm region is lacking, resulting in generation of triplets in the 684 nm as well as in the 720 nm species.

Tables 4.3 and 4.4 collect kinetic data which contain some structural information on the species observed by ODMR.

First of all we note that all constants in this Table can roughly be divided into two categories:

- (1) where a very fast value is found for k_y and
- (2) where k_y is roughly twice the value of k_x .

For *S. C-6E* from the FF method and Chl-a in MTHF (from ESR) we note close agreement between the values of λ_f and all kinetic constants. In the latter system, only ligation of the solvent to Mg is possible; at low temperature, Chl-a in an MTHF glass is biligated [5] to Mg. The fluorescence maximum of Chl-a·2H₂O (Mg) has been found at 687 nm [3], as compared to *S. C-6E* at 688 nm. The kinetic constants in *n*-octane, containing traces of water can also be ascribed to Chl-a·2H₂O. The kinetics of *S. C-6E* as determined by the FF method, are in fair agreement with those obtained by the microwave induced response in the fluorescence method.

By contrast, Chl-a *in vitro* dissolved in solid ethanol [5], has a characteristic high value of k_y . It is to be expected, that in neat ethanol at low temperature the Chl-a molecule is biligated at Mg as well as hydrogen-bonded at the ring V-keto group. As judged from the kinetic constants for CP-I, detected at 684 and 715 nm, both species are very likely hydrogen-bonded at ring V. Their difference is due to excitonic interaction in the singlet state and/or additional ligation of the 715-725 nm species at Mg. Both species observed *in vivo* therefore contain ring V hydrogen-bonds, confirming earlier Raman studies by Lutz [13].

The 688 nm species in *S. C-6E* apparently constitutes a different case, suggesting that in this species no or very weak hydrogen bonding to ring V occurs, possibly due to its hydrophobic environment. In other algae, no ODMR could be detected in this band, presumably as a result of rapid energy transfer.

On this basis we have constructed Table 4.4, assigning fluorescence-wavelengths, ZFS-, and kinetic parameters to various Chl-a species. A cautionary remark must be made with regard to ZFS and kinetic constants of the *in vivo* 715-725 nm species. It is possible that the set of values presented in Table 4.4 in fact reflects the properties of species II, observed through energy transfer to the 715-725 nm emission band (see e.g. [3]).

4.6 CONCLUSIONS

- The Chl-a triplet detected by ODMR in whole algae is located in the PSI antenna pigment.
- Based on very similar low temperature fluorescence spectra and triplet ZFS values, the Chl-a triplet in *A. nidulans* and its CP-I complex are probably identical.
- The amount of carotenoids in CP-I is very likely to determine the concentration of Chl-a triplets under otherwise identical conditions.
- In CP-I both Chl-a species detected at 684 and 715 nm are hydrogen-bonded at the ring V-keto group. The 684 species in addition is monoligated at Mg, whereas the 715 nm species, also detected in wild type algae contains one or two ligands to Mg.
- The ZFS values, kinetic constants and the positive sign of ODMR signals in CP-I and wild type algae is consistent with energy transfer from shallow traps, emitting below ~700 nm, to deeper traps, emitting at 710-730 nm.

4.7 REFERENCES

1. S.J. van der Bent, T.J. Schaafsma and J.C. Goedheer (1976). *Biochem.Biophys.Res.Comm.* 71: 1147-1152.
2. G.H. van Brakel, T.J. Schaafsma and J.J.S. van Rensen. *Isr.J. Chem.*, In Press, §3.3.4 of this Thesis.
3. R.P.H. Kooyman, T.J. Schaafsma and J.F. Kleibeuker (1977). *Photochem.Photobiol.* 26: 235-240.
4. J. Lavorel and A.-L. Etienne (1977). In *Primary Processes of Photosynthesis*, Ed. J. Barber, Elsevier/North-Holland Bio-medical Press, Amsterdam, 203-268.
5. J.F. Kleibeuker (1977). Thesis. Wageningen.
6. W.G. van Dorp, T.J. Schaafsma, M. Soma and J.H. van der Waals (1973). *Chem.Phys.Lett.* 21: 221-225.
7. W.G. van Dorp, W.H. Schoemaker, M. Soma and J.H. van der Waals (1975). *Mol.Phys.* 30: 1701-1721.
8. R. Avarmaa (1979). *Mol.Phys.* 37: 441-454.
9. R.H. Clarke and R.H. Hofeldt (1974). *J.Chem.Phys.* 61: 4582-4587.
10. S.J. van der Bent (1977). Thesis. Wageningen.
11. R.P.H. Kooyman (1980). Thesis. Wageningen.
12. T.J. Schaafsma, S.J. van der Bent and R.P.H. Kooyman (1979). In: *Magnetic Resonance and Related Phenomena*, Eds. E. Kundla et al., Proc. XXth Congress Ampere, Tallinn (1978). Springer Verlag, Heidelberg. p. 160.
13. M. Lutz, J.S. Brown and R. Rémy (1979). In: *Chlorophyll Organization and Energy Transfer in Photosynthesis*, CIBA Foundation Symposium 61 (1979). Excerpta Medica, Amsterdam, pp. 105-125.

5 THE EFFECT OF METAL IONS AND OXYGEN ON THE LOW TEMPERATURE TRIPLET YIELD OF CHLOROPHYLL-A IN ALGAE

5.1 INTRODUCTION

The next paragraph consists of a paper in press, to be published in the Proceedings of the Fifth International Congress on Photosynthesis, Ed. G.A. Akoyunoglou, International Science Services Balaban, Rehovot, Israel (1981) Vol. I. This Congress was held at Chalkidiki, Greece, sept. 1980. Its aim is to describe and discuss the effects of metal ions and oxygen, found in whole algal cells, on the triplet state of Chl.-a.

One of the questions to be answered in § 5.2 is, whether ODMR spectroscopy can provide data on the presence and location of paramagnetic species in the photosynthetic apparatus.

In general, effects can be expected to occur for any paramagnetic substance, present in the vicinity of the triplet. Several kinds of metal ions are known to be located near the chlorophyll-proteins within algal cells. Fe is present in e.g. Ferredoxin and cytochromes and Cu in plastocyanin and superoxide dismutase [1,2]. Oxygen is of course present, since it is formed by photosynthesis. Finally, P700, when forced in the oxidized $P700^+$ state, is also a paramagnetic species and may have an effect on triplets of Chl-a located in the nearby antenna pigment system.

For the work described in § 5.2 use has been made of algae cultured in the presence of various metal ion concentrations. Since it appeared that Cu had by far the largest effects on the triplets, algae have been cultured under controlled Cu supply. It is known, that algae, when the ion supply is deficient in Cu, can adapt to such a situation by forming Fe containing soluble cyt.c instead of plastocyanin [3,4]; cyt.c then serves as an electron donor to P700.

The first effect to be expected from metal ions is line-broadening of ODMR triplet spectra. The paramagnetic interaction of the metal ion with the electrons in the triplet state of Chl-a, is expected to perturb the local magnetic field at the Chl-a triplet. The

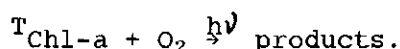
broadening of ODMR transitions is assumed to be caused by magnetic dipolar interaction between a Cu^{2+} $S=\frac{1}{2}$ spin and the Chl-a $S=1$ spin. The interaction energy is given by

$$E = \frac{(g\mu_B)^2}{4\pi\epsilon_0 c^2} \left[\frac{(\vec{S}_1 \cdot \vec{S}_2)}{r^3} - 3 \frac{(\vec{S}_1 \cdot \vec{r})(\vec{S}_2 \cdot \vec{r})}{r^5} \right] \quad (5.1)$$

where g is the g -factor of the free electron,
 μ_B is the electronic Bohr magneton,
 $\epsilon_0 = 10^{-9}/36\pi \text{ Farad} \cdot \text{m}^{-1}$,
 c is the velocity of light in $\text{m} \cdot \text{s}^{-1}$,
 \vec{S}_1, \vec{S}_2 are the spin-vectors of the Cu^{2+} $S=\frac{1}{2}$ spin and the Chl-a $S=1$ spin, expressed in units \hbar ,
 \vec{r} is the distance between the origins of both spin vectors.
The observed broadening in the presence of Cu^{2+} , w.r.t. the width in the absence of Cu^{2+} is ~ 10 MHz (see Table I of § 5.2). Inserting this number into (5.1) and the physical constants g, μ_B, ϵ_0 and c , and noting that $|\vec{S}_1| = \frac{1}{2}\hbar, |\vec{S}_2| = \hbar$, permits the calculation of r , which turns out to be 2.5-3 nm. This is a very reasonable figure in view of the distances and sizes for plastocyanin and the PSI complex (see Fig. 1.2 in Chapter 1).

The second main question, which ODMR might provide an answer to, is: what is the role of paramagnetic ions in the photochemical breakdown of Chl-a during illumination at low temperature and in the presence of oxygen?

For Chl-a and similar compounds, it is known that one possible pathway for this process occurs by an overall reaction



In addition to the effect on the ODMR linewidths, paramagnetic interaction is also expected to shorten the lifetime of the triplet state of Chl-a ('quenching'), and may thus protect Chl-a from photochemical damage. This effect has received ample attention *in vitro*, e.g. [5,6] and is further discussed in § 5.2 for Chl-a in algae.

The next question which arises is, whether the triplet detected by ODMR is identical to the triplet which participates in the photochemical breakdown of Chl-a. In § 5.2 we show, that this is probably

true, in view of the correspondence of the decay rates for photochemical breakdown and the disappearance of the triplet signal in ODMR, both under continuous illumination at low temperature.

The decay rate describing the disappearance of the Chl-a triplet under continuous illumination should not be confused with the decay rates observed as a response to a sudden increase or decrease of the exciting light or microwave intensity.

Finally, the role of oxygen is discussed in § 5.2: oxygen, being a paramagnetic species, is also expected to quench the triplet state of Chl-a and thus should exert a protective effect against photodamage of Chl-a. This is indeed observed, but here the situation is more complicated because of the fact that oxygen is also involved in the photochemical reactions of Chl-a itself.

The possible quenching by $P700^+$ has been discussed in § 4.2.

5.2 THE EFFECT OF METAL IONS AND OXYGEN ON THE LOW TEMPERATURE TRIPLET YIELD OF CHLOROPHYLL-A IN ALGAE

G.H. van Brakel^{a)}, J.J.S. van Rensen^{b)}, T.J. Schaafsma^{a)}

a) Dept. of Molecular Physics

b) Dept. of Plantphysiological Research

State Agricultural University, De Dreijen 6, 6703 BC WAGENINGEN;
the Netherlands

Abstract

The triplet state of Chl-a, as detected in whole algal cells of *Scenedesmus obtusiusculus* by use of Optically Detected Magnetic Resonance at 4.2 K, has a linewidth of 40 MHz. In copper deficient cells this linewidth reduces to 30 MHz. Copper influences the triplet by a mechanism of paramagnetic interaction.

During the ODMR experiment the fluorescence intensity of Chl-a at 718 nm decays irreversibly by photochemical reactions, and this decay contains three different rate constants. In copper deficient cells the decay of Chl-a is faster. Also the triplets detected by ODMR disappear with a rate constant comparable to that of the two fastest components. This indicates that the triplet state is involved in the photochemical breakdown of Chl-a.

Introduction

The triplet state of Chl-a can be detected in whole algal cells by use of Optically Detected Magnetic Resonance (ODMR) [1]. This triplet can be used as an internal probe in the cell.

To investigate the influence of metal ions, *Scenedesmus* cells are grown in media containing a variable amount of metal ions. It is found that only copper influences the triplet, together with oxygen. This effect can be observed as a line-narrowing in the ODMR spectra, measured in the absence of copper.

During the ODMR experiment the sample is illuminated with light of high intensity and this causes photochemical damage of Chl-a. When copper is absent the photochemical decay of Chl-a is much faster.

The photochemical decay at 715 nm appears to contain three components and two of them are much faster than the third. Only for the two fast decaying components the triplet state is detected.

This adds an argument to the evidence that the photochemical decay of Chl-a proceeds, at least partly, via the triplet state.

Materials and Methods

Normal cells of *Scenedesmus obtusiusculus* are cultured in a nitrate medium containing $6 \cdot 10^{-5}$ M of paramagnetic ions, mostly Fe and Mn. Copper deficient *Scenedesmus* is grown in the same medium, only the copper is left out. To make a copper deficient culture it is necessary to rinse all glassware thoroughly and to inoculate a few times over.

In order to decrease the total metal ion content of the cells, they are cultured in a medium containing no paramagnetic ions, except for 10^{-5} M Fe^{3+} . Of course the growth rate is then very slow.

Triplets are detected by ODMR: during continuous illumination of the cells at 4.2 K a steady state population of triplets builds up. Irradiation with microwaves of the frequency corresponding to transitions between the triplet sublevels, changes the total triplet population slightly, and this can be detected as a change of the fluorescence intensity. The signals are then time averaged for enhancement of the signal to noise ratio.

Full experimental details are given elsewhere [2,3]. Usually it is necessary to add DCMU (10^{-5} M) to the cells to find triplets.

Influence of Cu on triplet state of Chl-a

Triplets of Chl-a have been found in several blue-green and green algae [1], in the presence of DCMU. Because they are found at 715 nm (± 10 nm, depending on the organism) this triplet state is ascribed to photosystem I. In copper-deficient cells triplets can be detected without DCMU.

Presence of metal ions in the neighbourhood of Chl-a can cause line broadening by a mechanism of paramagnetic interaction, due to variance in the distance or in orientation of the spin of the metal

Table 1 Influence of metal ions on the linewidth of the triplet state of Chl-a.

	average linewidth (MHz)	standard deviation (MHz)
<i>in vivo</i>	37	10
<i>in vivo</i> Cu ²⁺ deficient cells	29	4
<i>in vivo</i> metal ion deficient cells	29	7
<i>in vitro</i> Chl-a in n-octane	40	7

ion with respect to the triplet. According to the magnitude of the line broadening effect these distances are in the range of 2-3 nm.

It appears that most of the effect can be attributed to Cu²⁺, present in the surrounding of Chl-a in plastocyanin and superoxide dismutase. It is known that in the absence of Cu *Scenedesmus* forms Fe containing soluble cyt. c, which then serves as an electron donor to P700 instead of plastocyanin [4]. It is very well possible that while plastocyanin is tightly membrane-bound, soluble cyt. c is more loosely bound and does not affect triplets.

Linewidths measured *in vitro* must be compared to *in vivo* measurements made in the absence of metal ions. *In vitro* samples are less homogeneous with respect to the triplet state of Chl-a than *in vivo* samples, because Chl-a is situated in specific sites in the photosynthetic membrane, while in a quickly frozen sample *in vitro* there is a whole range of sites.

The fact that in normal cells DCMU is needed for triplet detection is possibly connected with lifetime shortening of the triplet state by copper.

Influence of Cu on photochemical decay of Chl-a

Following the photochemical decay of Chl-a during a prolonged period of time at high intensity illumination revealed that Cu also had an influence on the decay rate.

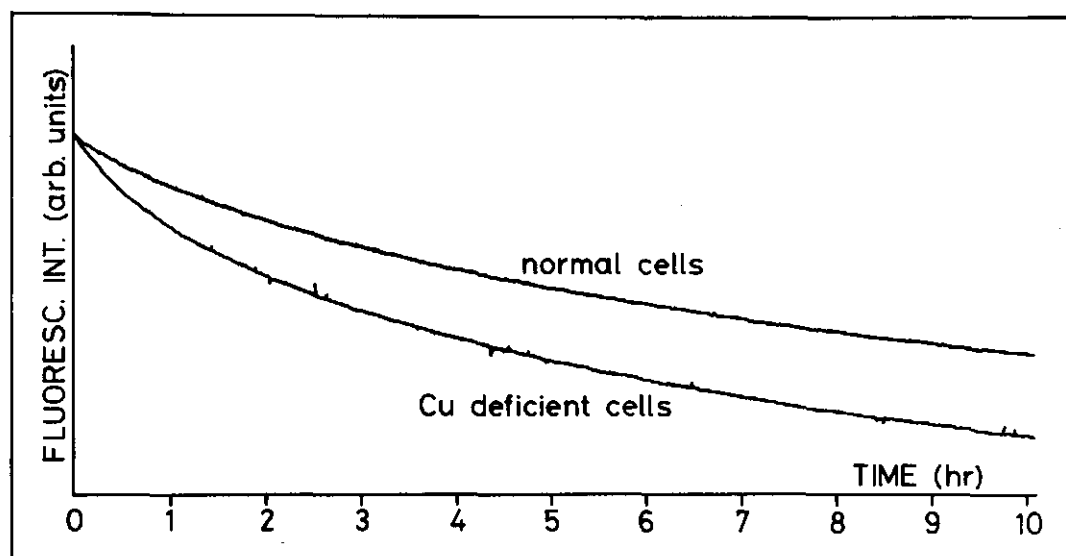


Figure 1 Photochemical decay of Chl-a.

Measured in *Scenedesmus obtusiusculus* at 715 nm. Light intensity 4000 Wm^{-2} . Temperature 4.2 K. Oxygen is removed from the samples.

It seems that presence of copper has a protective influence on Chl-a (Fig. 1). Also removal of oxygen slows down the breakdown of Chl-a, but less pronounced.

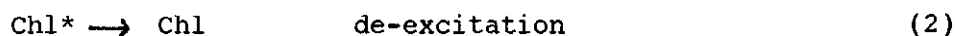
The photochemical breakdown measured in the fluorescence at 715 nm appears to contain three components (Table 2). The triplets also disappear with a half time of 2 hrs (± 2), comparable to the two fast decaying components in Table 2.

Table 2 Photochemical decay of Chl-a in whole cells of *Scenedesmus obtusiusculus*.

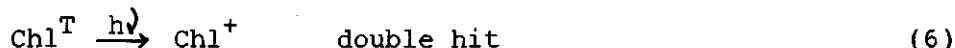
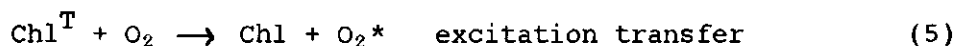
component	percentage of intensity	average lifetimes (h)	
		normal cells	Cu deficient cells
1	8 ± 2	1 ± 0.2	0.6 ± 0.1
2	27 ± 2	5 ± 0.5	4 ± 0.5
3	65 ± 2	49 ± 2	35 ± 2

Discussion

The mechanism of photo oxidation can be formulated according to the following scheme.



If Chl reaches the triplet state it may react via two different pathways:



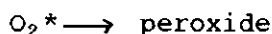
The excited oxygen can choose between a de-excitation reaction (e.g. chemoluminescence)



or it may perform damaging reactions to Chl-a, in two ways, by direct attack



or by first forming a peroxide which then attacks the Chl-a.



The reactions (8) and (9) have only a limited probability considering the temperature (4.2 K) and the fact that oxygen and Chl-a must be next neighbours, which will not occur often, even at the saturating concentration of oxygen ($\sim 2.5 \cdot 10^{-4}$ M). The double hit

process (6) seems much more likely, especially at high intensity illumination.

There are many possibilities for damaging reactions to Chl-a from (6), and the probability gains by the long lifetime of Chl^+ at this temperature.

The basic argument for triplet participation in the photochemical decay is the correspondence between the rate of disappearance of the triplet state and the rate of disappearance of the fast decaying species of Chl-a. This point has been put forward already by Chibisov [5], formulated in a different manner.

A few arguments can be added now. First the influence of copper is most likely on the triplet state of Chl-a. Copper, being a paramagnetic substance, shortens the lifetime of the triplet state, thus making a double hit process less likely.

The effect of oxygen is also protective for Chl-a and this seems rather surprising at first sight, considering reactions (8) and (9), but it has the same paramagnetic interaction with a triplet state.

Another argument is added by the fact that at moderate light intensity ($\sim 200 \text{ Wm}^{-2}$) Chl-a breakdown is extremely slow. This points again to a double hit process.

REFERENCES

1. S.J. van der Bent, T.J. Schaafsma and J.C. Goedheer (1976). Biochem.Biophys.Res.Comm. 71: 1147-1152.
2. S.J. van der Bent, P.A. de Jager and T.J. Schaafsma (1976). Rev. Sci.Instr. 47: 117-121.
3. J. Schmidt, D.A. Antheunis, J.H. van der Waals (1971). Mol.Phys. 22: 1-17.
4. P. Böger, Proc. Fourth Int. Congress Photosynthesis (1977). pp. 755-764.
5. A.K. Chibisov (1972). Dokl.Akad.Nauk.USSR 205: 142-145.

ACKNOWLEDGEMENT

We are indebted to J.B.M. Hudales, who has been tightly involved in the work described in this paragraph.

5.3 CONCLUSIONS

- Using ODMR, it has been shown, that Cu^{2+} ions are located at a distance $\sim 2.5\text{-}3$ nm from the Chl-a triplet detected in PSI of *Scenedesmus obtusiusculus*.
- The Cu^{2+} ion protects Chl-a from photochemical damage by illumination with blue light at low temperature, probably by quenching $^1\text{Chl-a}$.
- The Chl-a triplet observed by ODMR is very likely to be on the pathway of the photochemical damaging process.
- At low temperature, the net effect of oxygen is to protect Chl-a from photochemical damage, similar to that of Cu^{2+} , probably again by quenching $^1\text{Chl-a}$. This does not exclude a simultaneous participation of O_2 in the photochemical damage process.

5.4 REFERENCES

1. K. Asada, S. Kanematsu, S. Okaka and T. Hayakawa (1980). In: Chemical and Biochemical Aspects of Superoxide and Superoxide Dismutase. Eds. J.V. Bannister and H.A.O. Hill. Elsevier North Holland, Amsterdam. pp. 136-153.
2. K.J. Kunert and P. Böger (1975). Z.Naturforsch. 30c: 190-200.
3. P. Böger (1977). Proc. Fourth Int. Congr. Photosynthesis. pp. 755-764.
4. H. Bohner and P. Böger (1978). FEBS Lett 85: 337-339.
5. H. Linschitz and L. Pekkarinen (1960). J.Am.Chem.Soc. 82: 2411-2416.
6. P. Svejda, R.R. Anderson and A.H. Maki (1978). J.Am.Chem.Soc. 100: 7131-7138.

SUMMARY

The triplet state of chlorophyll-a (Chl-a) can be observed at 4K in intact algal cells using optically detected magnetic resonance (ODMR).

In this Thesis experiments are described, to determine, to which kind of physically distinguishable Chl-a molecules, involved in the process of photosynthesis in algae, the observed triplet state belongs. From the wavelength of the fluorescence (~ 715 - 725 nm in intact algal cells), where the Chl-a triplet is detected, it appears, that the triplet is located within photosystem I.

In the photosystem I containing chlorophyll-protein complex (CP-I), isolated from the blue-green alga *Anacystis nidulans*, the triplet state of Chl-a is also observed. This triplet has a number of properties in common with the triplet observed in intact cells: low temperature fluorescence spectra and triplet zero-field splitting parameters of the triplet detected in this spectral region, are identical for the alga and its complex.

For CP-I it is demonstrated by light minus dark absorption difference spectroscopy and ESR, that the reaction centers are in oxidized state under ODMR conditions. From this observation it is concluded, that the triplet is located in the antennapigment system in the intact algal cells, as well as in the chlorophyll-protein complex.

In the ODMR spectrum of intact cells the triplet signals of Chl-a appear with opposite sign compared to those of Chl-a *in vitro*, i.e. in intact cells the triplet is detected as an increase of fluorescence, while *in vitro* it is detected as a decrease.

Several models are conceivable to explain this sign reversal. The mechanism of energy transfer between parts of the pigment system is considered to be the most probable candidate for the cause of the observed sign reversal of both ODMR signals. As yet, it cannot be completely excluded, however, that the sign reversal is caused by altered kinetics as a result of hydrogen-bonding of amino acids of the surrounding protein to ring V keto- and/or ester groups of Chl-a.

The occurrence of the radical pair mechanism is unlikely, because the observed triplets are located in the antennapigment and not in reaction centers.

The theory of radiationless transitions is applied to Chl-a, using calculations of Petke and coworkers, of the energies and configurational composition of the ground and excited states of Chl-a. This offers an explanation, why only two of the expected three triplet signals are observed in the ODMR experiment. Furthermore, predicted effects of ligation and hydrogen-bonding to Chl-a

molecules on kinetics of Chl-a *in vivo* are in good agreement with the results from experiments on complexes and aggregates of Chl-a in solution.

Finally, the presence of paramagnetic metal ions, especially Cu^{2+} , in the vicinity of the triplet state of Chl-a *in vivo* causes a line-broadening of ODMR spectra as well as a slow-down of the rate of photochemical breakdown of Chl-a due to irradiation with blue light at low temperature. These observations indicate that the triplet state of Chl-a in algae is involved in this photochemical breakdown.

De triplettoestand van chlorofyl-a (Chl-a) kan bij 4K met behulp van optisch gedetecteerde magnetische resonantie (ODMR) waargenomen worden in intacte algencellen.

In dit proefschrift zijn experimenten beschreven, met de bedoeling om na te gaan van welke van de fysisch onderscheidbare Chl-a moleculen, die bij het fotosyntheseproces in algen betrokken zijn, de triplettoestand wordt waargenomen. Uit de golflengte van het fluorescentielicht ($\sim 715-725$ nm bij intacte algencellen), waarbij het Chl-a triplet gedetecteerd wordt, blijkt, dat het triplet binnen fotosysteem I gelocaliseerd moet zijn.

In het fotosysteem I bevattend chlorofyl-eiwit complex, geïsoleerd uit de blauwgroene alg *Anacystis nidulans*, wordt de triplettoestand van Chl-a eveneens waargenomen; dit triplet heeft een aantal eigenschappen, die identiek zijn aan die van het triplet in intacte cellen: er is overeenkomst in het fluorescentiespectrum bij lage temperatuur, terwijl bovendien de nulveldsplittingsparameters van het in deze band gedetecteerde triplet identiek zijn.

Voor dit chlorofyl-eiwit complex is d.m.v. verschilabsorptiemetingen en ESR aangetoond, dat het reactiecentrum zich in geoxideerde toestand bevindt onder de condities van het ODMR-experiment.

Dit leidt tot de conclusie, dat het waargenomen triplet, zowel in het chlorofyl-eiwit complex als in intacte algencellen, in het antennepigmentsysteem is gelocaliseerd.

Voor intacte cellen vertoont het ODMR spectrum de signalen, afkomstig van Chl-a met tegengesteld teken aan die van Chl-a in vitro, d.w.z. in intacte cellen wordt het triplet waargenomen als een toename van de fluorescentie, in vitro als een afname.

Er zijn verschillende modellen mogelijk, waarmee deze tekenomkeer kan worden verklaard. Het mechanisme van energieoverdracht tussen verschillende onderdelen van het pigmentsysteem wordt het meest waarschijnlijk geacht als oorzaak voor de waargenomen tekenomkeer van de beide ODMR signalen, met het behoud van relatieve intensiteit t.o.v. Chl-a in vitro. Het kan echter niet uitgesloten worden, dat de tekenomkeer een gevolg is van gewijzigde kinetiek ten gevolge van waterstofbinding van de aminozuren aan ring V keto- en estergroepen van Chl-a. Het optreden van het radikaal paar mechanisme is onwaarschijnlijk op grond van het feit, dat tripletten van antennepigmentmoleculen waargenomen worden, en niet van reactiecentra.

De theorie van stralingsloze overgangen is toegepast op Chl-a, gebruikmakend van berekeningen van Petke en medewerkers, van energieën en configurationele samenstelling van de grond- en aangeslagen toestanden van Chl-a. Hiermee kan worden verklaard waarom slechts twee van de drie te verwachten tripletsignalen waargenomen worden met behulp van ODMR. Tevens volgt uit de berekeningen een aantal voorspellingen over mogelijke effecten van ligandering en waterstofbinding van Chl-a moleculen, *in vivo*, die goed in overeenstemming blijken te zijn met experimenten, gedaan aan complexen en aggregaten van Chl-a in oplossing.

Tenslotte wordt een aantal effecten van de aanwezigheid van paramagnetische metaalionen, n.n. Cu^{2+} , op de triplettoestand van Chl-a besproken: de lijnwerking, die waargenomen wordt in tripletspectra en de vertraging van de fotochemische beschadiging van Chl-a, die de aanwezigheid van Cu^{2+} blijkt te veroorzaken. Deze verschijnselen vormen een sterke aanwijzing, dat de triplettoestand van Chl-a in algen een rol speelt bij de fotochemische afbraak van Chl-a.

CURRICULUM VITAE

Gerardus Hendrikus van Brakel is op 22 juli 1952 te Wageningen geboren. Na het behalen van het gymnasium diploma aan de Rijks-scholengemeenschap "Het Wageningsch Lyceum" te Wageningen, begon hij in 1971 met de studie Scheikunde aan de Rijksuniversiteit te Leiden. In mei 1974 werd het kandidaatsexamen Scheikunde en Wiskunde met Natuurkunde (S_4) afgelegd. Voor het hoofdvak van de doctoraalstudie werd op de vakgroep Theoretische Organische Chemie o.l.v. prof. dr. J.J.C. Mulder en dr. J.A. den Hollander een onderzoek verricht naar het CIDNP effect met behulp van NMR waargenomen aan gesubstitueerde dibenzoylperoxides. In februari 1978 werd het doctoraalexamen Scheikunde afgelegd met hoofdvak Theoretische Organische Chemie en bijvakken Experimentele Natuurkunde en Theoretische Natuurkunde.

Van 1 maart 1978 tot 1 september 1981 is hij medewerker geweest van de vakgroep Moleculaire Fysica van de Landbouwhogeschool te Wageningen, waar o.l.v. prof. dr. T.J. Schaafsma dit proefschrift bewerkt is, in een samenwerkingsverband met de vakgroep Plantenfysiologisch Onderzoek.

Vanaf 1 februari 1982 is hij in tijdelijke dienst van de Landbouwhogeschool te Wageningen en werkzaam in de vakgroep Moleculaire Fysica.